STEADY AND NONSTEADY POTENTIAL FLOW METHODS FOR AIRFOILS WITH SPOILERS

BY

GEOFFREY P. BROWN

B.E., University of Sydney, 1967

A THESIS SUBMITTED IN PARTIAL FULFILMENT OF
THE REQUIREMENTS FOR THE DEGREE OF
DOCTOR OF PHILOSOPHY

in the Department
of
Mechanical Engineering

We accept this thesis as conforming to the
required standard

THE UNIVERSITY OF BRITISH COLUMBIA

July, 1971

In presenting this thesis in partial fulfilment of the requirements for an advanced degree at the University of British Columbia, I agree that the Library shall make it freely available for reference and Study. I further agree that permission for extensive copying of this thesis for scholarly purposes may be granted by the Head of my Department or by his representatives. It is understood that copying or publication of this thesis for financial gain shall not be allowed without my written permission.

Department of MECH. ENG.

The University of British Columbia
Vancouver 8, Canada

Date 30 th SEPT 71

ABSTRACT

In part I a linearized cavity potential flow theory is developed to solve both the steady state airfoil spoiler problem and the transient loads on an airfoil during and after spoiler actuation. The theory is also applicable to the case of an airfoil with a spoiler and a flap. The theory uses conformal transformations to map that part of the airfoil exposed to the flow onto the upper half of a unit circle. The complete flow field about the airfoil maps into the upper half plane exterior to this unit circle.

Although no limitations are imposed in the paper upon the spoiler height, angle, or location, good agreement with experiment would not be expected in such a linearized theory for very large spoilers. Spoiler heights up to 10% of the airfoil chord are considered, and the theory shows good agreement with experiment.

A theory for the steady state airfoil spoiler problem for a solid airfoil, and an airfoil with a slotted flap is developed in part II. An exact potential free streamline theory using the surface singularity technique is used in this work. The wake is contained between two free streamlines. Following Jandali's technique (1), the wake flow is created by positioning sources on the airfoil surface in that region exposed to the wake. The actual flow in the wake region is ignored, and the base pressure is taken to be constant at the experimental value. The theory agrees well with the results obtained by Jandali.

TABLE OF CONTENTS

PART II

AN EXACT FREE STREAMLINE POTENTIAL FLOW THEORY FOR THE STEADY STATE AIRFOIL SPOILER AND SPOILER PLUS SLOTTED FLAP PROBLEM 82

LIST OF FIGURES

ACKNOWLEDGEMENTS

I would like to thank Dr. G.V. Parkinson for his able assistance during the course of this research and for his general guidance during my time in graduate school. I would also like to thank Dr. I.S. Gartshore for his suggestions during the early stages of this work and Dr. L. Mysak for his advice concerning the mathematics.

Special thanks go to the many from whom I borrowed reference books and to Mr. E. Abell who built the experimental equipment used.

This work was supported by the University of British Columbia, the National Research Council of Canada and the Defense Research Board of Canada.

LIST OF MAIN SYMBOLS-PART I

a - $\sqrt{\frac{\ell-c}{c}}$

a' - $\sqrt{\frac{1}{c}}$

$\vec{a}$ - acceleration vector

a_x - x-component of acceleration

a_y - y-component of acceleration

b - $a\sqrt{\frac{s+h}{\ell-s-h}}$

b' - $a'\sqrt{s+h}$

B_o - constant in cavity termination term

c - airfoil chord

c_ℓ - flap chord

C_o - constant in leading edge term

C_1' - constant from airfoil term

C_2' - constant from spoiler term

C_L - lift coefficient

C_{L_s} - quasi-steady lift coefficient

C_{L_f} - final lift coefficient

C_p - pressure coefficient

D_o - constant

E - $-F_c-F_t-F_s-F_f$

e - subscript indicating erection

F - complex acceleration function

F_i - $(i=1,2,3)$ complex functions of F_{in}

F_{in} - complex incidence function

F_c - complex camber function

F_f - complex flap function

F_s - complex spoiler function

F_t - complex thickness function

F_n - nonsteady complex function

h - spoiler height

I - actuation response function

i - $\sqrt{-1}$ in physical plane or its transforms

j - $\sqrt{-1}$ in phase plane or its transforms

J_n - nonsteady acceleration term Fourier series coefficient

K - cavitation number

k - μc

ℓ - cavity length

M_n - camber Fourier series coefficient

N_n - thickness Fourier series coefficient

P - static pressure

P_∞ - undisturbed free stream static pressure

P_c - pressure inside the cavity

p - static pressure perturbation

Q - frequency response function

$\vec{q}$ - velocity vector

q_c - magnitude of velocity on the cavity

R - real part of Q

S - imaginary part of Q

s - spoiler position

s' - distance moved in chords

t - time

U - free stream velocity

u - perturbation velocity in the x direction

v - perturbation velocity in the y direction

v_o - amplitude of velocity

V_o - amplitude of velocity

w - complex velocity

W - actuation response function

x, y- coordinate system in z-plane

z - complex variable describing airfoil plane

z' - complex variable describing z'-plane

α - angle of incidence

δ - spoiler angle to airfoil surface

ς - complex variable describing ς-plane

ς_∞ - point at infinity in ς-pane

η - flap angle

θ - angular measurement in ς-plane

θ_0 - angular position of leading edge in ς-plane

θ_1 - angular position of spoiler base in ς-plane

θ_2 - angular position of flap hinge point in ς-plane

μ - $\frac{\omega}{U}$

ν - complex variable describing ν-plane

ρ - density of flow

φ - acceleration potential

ψ - acceleration stream function

ω - frequency of blowing

LIST OF MAIN SYMBOLS-PART II

A_{ij} - element of matrix A

A^{T1}_{ik} - element of matrix A^{T1}

A^{T2}_{il} - element of matrix A^{T2}

B_{ij} - element of matrix B

B^{T1}_{ik} - element of matrix B^{T1}

B^{T2}_{il} - element of matrix B^{T2}

c - airfoil chord

C_{P_b} - base pressure coefficient

C_{P_i} - pressure coefficient at the ith control point

h - spoiler height

i - symbol representing ith element on the foil or flap

j - symbol representing jth element on the foil or flap

k - symbol representing kth element on the main foil

l - sumbol representing lth element on the flap

n - subscript indicating normal direction

N_1 - number of last element before the spoiler tip

N_2 - number of first element after the spoiler tip

N_3 - number of last element before the foil trailing edge

N_4 - number of first element after the foil trailing edge

N_5 - number of last element before the flap trailing edge

N_6 - number of first element after the flap trailing edge

s - spoiler position

T_i - velocity on the ith control point

t - subscript indicating tangential direction

V - velocity due to source s

α - angle of incidence

γ - circulation about the airfoil

δ - spoiler angle to airfoil surface (without subscript)

η - flap angle

λ - source strength

ϕ - velocity potential

σ_j - strength of the source on the jth element

SECTION 1

INTRODUCTION

Theoretical investigation of airfoil spoiler aerodynamics is an area of continuing importance. The transient loads of spoiler actuation and the spoiler plus flap combination have practical application in the recent interest in high lift devices. Spoilers are used for roll control at low speeds when actuated asymmetrically, or for lift and drag control if actuated symmetrically.

Experimental investigation shows that the flow in the region between a spoiler and the trailing edge is separated. Since no satisfactory method exists to predict the base pressure theoretically, a theoretical model will require at least one empirical parameter.

Some progress has been made in the attempt to solve the airfoil spoiler problem. Jandali (1) used an exact free streamline potential flow theory to solve for lift and pressure on a solid airfoil with a fixed normal spoiler. Both Jandali's 1- and 2-source models are calculated similarly, and since they depend on conformal mappings of the Theodorsen type, they cannot be used to solve the spoiler plus flap case. The 2-source model which gives good agreement with experiment requires both base pressure and zero lift angle input.

A linearized free streamline potential flow theory has been developed by Woods (2), who gave expressions to calculate incremental pressures, lift, drag and incremental pitching moment as a function of airfoil incidence, spoiler height, angle to the airfoil surface and chordwise position. Woods considers the airfoil thickness only in determining the spoiler angle, and drops it from the theory as a second order term. Barnes (3) used the results of wind tunnel experiments on two airfoils to devise an empirical modification to Woods'

for normal spoilers. Barnes used the boundary layer thickness on the basic airfoil to determine an effective spoiler height that gave him good agreement with experiment for normal spoilers. From this he was able to develop an empirical relationship that he states is applicable to most airfoils.

The theories presented so far have been free streamline separated potential flow theories. The linearized cavity potential flow theory presented in part I of the current work was developed by Parkin (4), who considered the hydrofoil case of separation from the leading edge. Fabula (5) extended this work to the general case of separation from a point on the upper surface, this case being applicable to a hydrofoil with blowing or a step on the upper surface. The current theory, presented in part I, extends this result to the airfoil problem, and relates the separation to a spoiler height and angle. The spoiler plus flap solution is also obtained. A new type of function with a singularity at the point corresponding to the leading edge has been used to solve for the thickness solution. This theory is developed in part I and applied to a 14% thick Clark Y airfoil. The theory for the airfoil spoiler problem is then extended to solve for the transient loads on an airfoil during and after spoiler actuation. The linearized theory of part I is mainly useful for the prediction of total forces and moments on the airfoil.

In part II of the current work the steady state spoiler problem is once again treated, this time using an entirely different technique. The exact surface singularity potential flow theory developed by Smith (6) is combined with the principles inherent in Jandali's theory(1). This type of theory is mainly useful for the prediction of surface pressure distribution. The solid airfoil with a spoiler, and the case of a spoiler plus a slotted flap, are treated. For the solid

airfoil case the theory is applied to a 14% thick Clark Y airfoil. For the spoiler plus slotted flap case the theory is applied to an NACA 23012 airfoil with a 25.66% slotted flap.

For the theories developed in both parts of the current work the spoiler height, location and angle are unrestricted. The linearized theory developed in part I is bounded in its agreement with experiment by the usual restrictions for perturbation theories.

PART I

A LINEARIZED CAVITY POTENTIAL FLOW THEORY FOR THE STEADY STATE AND TRANSIENT AIRFOIL SPOILER PROBLEM

SECTION 2

THE ACCELERATION POTENTIAL

Consider an irrotational flow of an incompressible inviscid fluid in which an airfoil of chord c is immersed. At points far from the airfoil the velocity field consists of a constant free stream velocity U in the positive x direction. Consider the airfoil to be positioned in the x-y coordinate system such that the leading edge is fixed at the origin. Suppose that there is a fully developed closed cavity of length ℓ, springing from an airfoil spoiler on the upper surface and from the trailing edge. If the undisturbed free stream static pressure is denoted by P_∞, and the constant pressure inside the cavity by P_c, a cavitation number for the flow, designated by K, is defined by the relationship:

$$K = \frac{P_\infty - P_c}{\frac{1}{2}\rho U^2},$$

where ρ is the density of the flow. This type of flow model, originally developed for cavity flows in liquids, is also useful for separated air flows, where the base pressure is constant in the wake just behind the generating body, and the base pressure coefficient, as usually defined, is

$$C_{P_b} = \frac{P_c - P_\infty}{\frac{1}{2}\rho U^2} = -K.$$

In the special case of steady flow the cavity surface velocity magnitude is a constant q_c. The steady-state Bernoulli equation can be used to relate q_c to the cavitation number, with the result that

$$q_c = U\sqrt{1+K}\,.$$

This quantity q_c is sometimes used as the fundamental reference speed in place of the more commonly used free stream velocity U. When the acceleration potential is used to solve the thin airfoil problem proposed, both systems reduce to the same linearized equations. In the usual linearized airfoil problem without cavity, U is the only characteristic velocity, and it is convenient to retain it here as the reference velocity. Thus at any point (x,y) in the nonsteady flow around the airfoil the velocity vector $\vec{q}$ can be expressed in terms of its x and y-components as

$$\vec{q}(x,y,t) = U\{(1+u),v\}\,.$$

The dimensionless quantities u(x,y,t) and v(x,y,t) are components of the small disturbance velocity in the x and y directions respectively. Both components u and v disappear at upstream infinity. Corresponding to these velocity perturbations, a small disturbance in the field of static pressure P(x,y,t) can be defined by putting

$$P(x,y,t) = P_\infty + p(x,y,t)\,.$$

This disturbance pressure also disappears at infinity.

To first order terms in the small perturbations, Euler's equations of motion may be written as

$$\frac{1}{U}\frac{\partial u}{\partial t} + \frac{\partial u}{\partial x} = a_x$$

and (1)

$$\frac{1}{U}\frac{\partial v}{\partial t} + \frac{\partial v}{\partial x} = a_y\,.$$

The acceleration components a_x and a_y of the acceleration vector $\vec{a}(x,y,t)$ can be expressed as the gradient of a scalar:

$$\vec{a}(x,y,t) = \{a_x, a_y\} = \nabla\varphi(x,y,t).$$

The scalar $\varphi(x,y,t)$ is the acceleration potential and its relationship with the perturbation pressure is

$$p = -\rho U^2\varphi + P_c - P_\infty ,$$

where φ has been defined to be zero on the cavity. In terms of the static pressure this becomes

$$P = -\rho U^2\varphi + P_c .$$

In an incompressible fluid the equation of continuity,

$$div\ \vec{q} = 0,$$

will also hold. If this equation is combined with equations (1), the divergence of a gradient being zero gives

$$\nabla^2\varphi = 0$$

at every instant. Hence φ is a harmonic functions, and a harmonic conjugate ψ can be defined by means of the Cauchy-Riemann equations as follows:

$$\frac{\partial\varphi}{\partial x} = \frac{\partial\psi}{\partial y} = a_x$$

and

$$\frac{\partial \varphi}{\partial y} = -\frac{\partial \psi}{\partial x} = a_y .$$

Introducing the complex variable,

$$z = x + iy ,$$

the complex acceleration potential which is an analytic function of z at every instant can be written as

$$F(z) = \varphi(x,y,t) + i\psi(x,y,t) .$$

The conjugate function $\psi(x,y,t)$ is the acceleration stream function. The analyticity of F guarantees that the complex acceleration,

$$\frac{dF}{dz} = a_x - ia_y$$

will also be an analytic function of z.

The pressure coefficient takes its customary definition:

$$C_p = \frac{P - P_\infty}{\frac{1}{2}\rho U^2} .$$

Introducing the acceleration potential this becomes

$$C_p = -2\varphi - K . \qquad (2)$$

Using the Euler and Cauchy-Riemann equations the x and y-components of perturbation velocity can be expressed by the linear first-order differential equations,

$$\frac{\partial u}{\partial t} + U\frac{\partial u}{\partial x} = U\frac{\partial \varphi}{\partial x}$$

and

$$\frac{\partial v}{\partial t} + U\frac{\partial v}{\partial x} = -U\frac{\partial \psi}{\partial x} \quad .$$

For the special case of steady flow these equations reduce to:

$$u = \varphi + \frac{K}{2} \tag{3}$$

and

$$v = -\psi \ , \tag{4}$$

where the conditions at infinity have been used to determine the constants of integration. Application of Bernoulli's equation between infinity and a point on the airfoil gives the linearized pressure coefficient on the airfoil as

$$C_p = -2u \ .$$

Substituting equation (3) into this result shows consistency with equation (2). Equations (3) and (4) are both consistent with the result obtained using the cavity velocity magnitude q_c as the fundamental reference velocity. It should be recognized however, that the velocity v in equation (4) has been nondimensionalized by reference velocity U rather than q_c.

SECTION 3

STEADY THEORY

3.1 Formulation of the Problem

The fully developed closed cavity flow model proposed for the solution to the airfoil spoiler problem has many features in common with the usual theory for thin airfoils. In fact, one can use the same techniques here that have proven so useful in solving the thin airfoil theory. In the present theory the cavity-foil system must be regarded as being a thin body, and for this reason the cavity termination is accompanied by a singularity. In practice the flow downstream of the airfoil is not a potential flow but a highly dissipative flow, and the presence of the singularity is an attempt to approximate this very complicated wake flow in the simplest analytical way. The important result of such a procedure is that in the neighbourhood of the airfoil, the flow appears to be well represented.

3.2 Transformations

The airfoil of chord c is located in the z-plane with the leading edge positioned at the origin. The undisturbed flow is in the positive x direction and the airfoil is inclined at a small angle α to this flow. The airfoil spoiler of height h is positioned at

$$x = s \ .$$

The spoiler angle to the chord line is denoted by δ. The airfoil configuration is shown in figure (1). The airfoil can also have a flap of chord c_η at an angle η to the chord line of the airfoil, not shown in figure (1). The physical representation of the airfoil in the z-plane is shown in figure (2). In order to apply the methods of thin

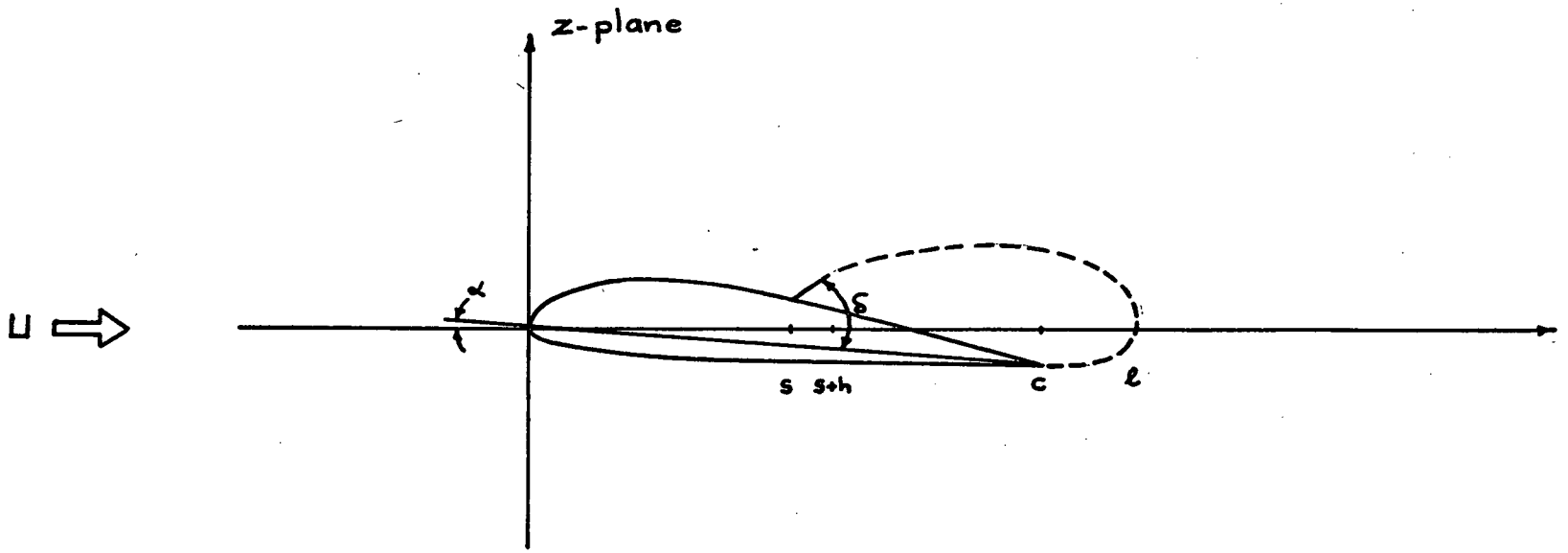

FIGURE (1): AIRFOIL IN Z-PLANE

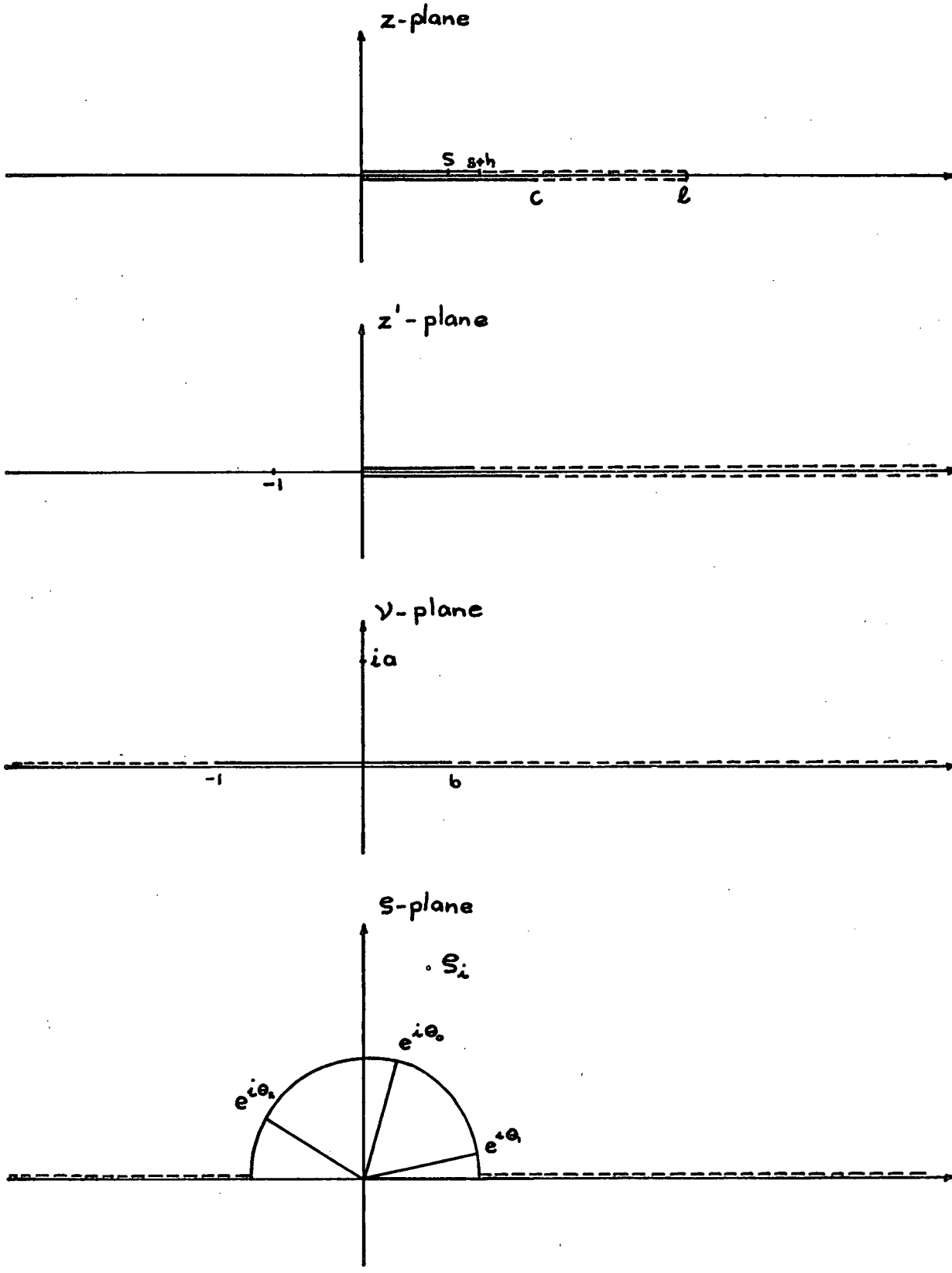

FIGURE (2): COMPLEX TRANSFORM PLANES

airfoil theory it is helpful to transform the z-plane into a more useful plane.

First consider the conformal transformation

$$z' = \frac{z}{\ell - z}$$

which maps the z-plane into the z'-plane. In the z'-plane the airfoil chord becomes equal to $\frac{c}{\ell - c}$ and the cavity termination point has been mapped to $z' = \infty$. The point at infinity has been mapped to the point $z' = -1$. The conformal transformation

$$\nu = a\sqrt{z'} \quad , \quad a = \sqrt{\frac{\ell - c}{c}}$$

maps the entire z'-plane into the upper half of the ν-plane. The foil occupies the slit $-1 \leq \nu \leq b$ on the real axis of the ν-plane. The point at infinity has been mapped to $+ia$. The cavity extends along $\nu > b$ and $\nu < -1$ on the real axis. The value of the constant b is

$$b = a\sqrt{\frac{s+h}{\ell - s - h}} \quad .$$

The foil is then mapped from the ν-plane on to the upper half of the unit circle in the ς-plane by means of the Joukowski transformation,

$$\nu = \frac{b+1}{4}\left(\varsigma + \frac{1}{\varsigma}\right) - \frac{1-b}{2} \quad .$$

The leading edge of the airfoil corresponds to the point $\varsigma = e^{i\theta_0}$, the spoiler base to the point $\varsigma = e^{i\theta_1}$, the flap hinge point to the point $\varsigma = e^{i\theta_2}$, the trailing edge to the point $\varsigma = -1$ and the spoiler tip to the point $\varsigma = 1$. The cavity extends along the real axis $\varsigma > 1$ and $\varsigma < -1$.

Using the mapping functions the angular locations of the critical points in the ζ-plane can be determined as

$$\theta_0 = \cos^{-1}\left(\frac{1-b}{1+b}\right) ,$$

$$\theta_1 = \cos^{-1}\left\{\frac{2}{1+b}\left[a\sqrt{\frac{s}{\ell-s}} + \frac{1-b}{2}\right]\right\}$$

and

$$\theta_2 = \cos^{-1}\left\{\frac{2}{1+b}\left[\frac{1-b}{2} - a\sqrt{\frac{c-c_n}{\ell-c+c_n}}\right]\right\}$$

where the inverse cosines are taken between 0 and π. The point at infinity in the ζ-plane is the field point ζ_i given by

$$\zeta_i = \frac{2}{1+b}\left[ia + \frac{1-b}{2}\right] + \sqrt{\left(\frac{2}{1+b}\right)^2\left[ia + \frac{1-b}{2}\right]^2 - 1} . \qquad (5)$$

The complex transform planes are shown in figure (2). The complex acceleration potentials in the various transform planes are invariant at corresponding points and so the accelerations differ only by the derivative of the mapping functions, and thus

$$\frac{dF}{d\zeta} = \frac{dF}{dz}\cdot\frac{dz}{d\zeta} .$$

3.3 Boundary Conditions

The steady state boundary conditions on the airfoil are as follows:

(i) $\varphi = \mathrm{Rl.F} = 0$ on the cavity, $\ell \geq x \geq (s+h)$, $y=0^+$ and $\ell \geq x \geq c$, $y=0^-$.

(ii) Kutta conditions, φ continuous, at the spoiler tip $x=(s+h)$, $y=0^+$ and at the trailing edge of the airfoil $x=c$, $y=0^-$.

(iii) Normal boundary condition of no flow through the airfoil surface. Hence if the airfoil surface is denoted by $[x,y(x)]$, the condition becomes, using equation (4)

$$v = -\psi = \frac{dy}{dx} .$$

(iv) The condition $F=-\frac{K}{2}$ for the point at infinity.

(v) The body cavity system must be equivalent to a closed body. Hence for a closed wake

$$\mathrm{Im}\oint w(z)\,dz = 0.$$

In the above boundary conditions $y=0^+$ refers to the upper surface of the slit and $y=0^-$ refers to the lower surface of the slit. In condition (v), $w(z)$ is the complex velocity and equations (3) and (4) combine to give

$$w(z) = F(z) + \frac{K}{2} .$$

Boundary condition (v) can then be rewritten

$$\mathrm{Im}\oint F(z)\,dz = 0 .$$

3.4 Mathematical Flow Model

Following the methods of thin airfoil theory we determine a set of functions in the ζ-plane that satisfy the boundary conditions

(i) through (v). The problem can be split into the determination of incidence, camber, thickness, spoiler and flap solutions and then superposed as in standard linearized theories. The next sections are then concerned with determining mathematical functions with the desired characteristics for these individual cases.

3.4.1 Incidence Case

Consider the complex function

$$F_1(\zeta) = i C_0 \left[\frac{1}{\zeta e^{i\theta_0} - 1} + \frac{1}{\zeta e^{-i\theta_0} - 1} \right] .$$

F_1 is purely imaginary on the cavity where ζ is real and $|\zeta| \geq 1$. This satisfies condition (i). On the unit circle $\zeta = e^{i\theta}$,

$$F_1(e^{i\theta}) = C_0 \left[\frac{\sin\theta}{\cos\theta_0 - \cos\theta} - i \right] .$$

At the spoiler tip and trailing edge $\theta \to 0, \pi$ respectively and F_1 is clearly continuous, hence satisfying condition (ii). A constant term

$$F_2(\zeta) = i D_0$$

does not violate conditions (i) or (ii) and is an acceptable function. It was previously decided that the cavity termination must be a singular point to account for the branching of the free streamlines at this point. In the ζ-plane this point is located at infinity so that the pole there is simply given by $i\zeta$. For the unit circle to remain a streamline a simple pole of opposite sign must be added to the inverse point of the unit circle. A complex function term giving the net contribution of the singularity at the cavity termination can

then be written as

$$F_3(\zeta) = i B_0(\zeta - \tfrac{1}{\zeta}) .$$

F_3 is purely imaginary on the cavity where ζ is real and hence satisfies condition (i). On the unit circle $\zeta = e^{i\theta}$,

$$F_3(e^{i\theta}) = -2 B_0 \sin\theta .$$

The function clearly satisfies the Kutta condition. It is to be remembered that boundary conditions (iii) through (v) are yet to be satisfied. The functions included in the incidence case are then,

$$F_{in}(\zeta) = i C_0\left[\frac{1}{\zeta e^{-i\theta_0} - 1} + \frac{1}{\zeta e^{-i\theta_0} - 1}\right] + i D_0 + i B_0(\zeta - \tfrac{1}{\zeta}) . \qquad (6)$$

On the foil the acceleration potential becomes

$$\varphi = C_0 \frac{\sin\theta}{\cos\theta_0 - \cos\theta} - 2 B_0 \sin\theta . \qquad (7)$$

3.4.2 Camber Case

Consider the complex function

$$F_c(\zeta) = -i \sum_1^\infty \frac{M_n}{\zeta^n} , \qquad (8)$$

where the M_n are real constants. This function is purely imaginary on the cavity where ζ is real and so satisfies condition (i). On the unit circle

$$F_c(e^{i\theta}) = -\sum_1^\infty M_n \sin n\theta - i\sum_1^\infty M_n \cos n\theta .$$

Once again the function clearly satisfies the Kutta conditions. Boundary condition (iii) can now be used to solve for the unknown M_n. For the camber case $\frac{dy_c}{dx}$ as a function of θ is a continuous curve that can be represented by its known Fourier cosine series as follows:

$$\frac{dy_c}{dx} = \frac{M_0}{2} + \sum_1^\infty M_n \cos n\theta , \qquad (9)$$

where

$$M_n = \frac{2}{\pi}\int_0^\pi \frac{dy_c}{dx}\cos n\theta \, d\theta .$$

The stream function condition then becomes

$$\psi = -\frac{M_0}{2} - \sum_1^\infty M_n \cos n\theta .$$

If the term $-\frac{M_0}{2}$ is included in the constant terms of the incidence case it is apparent that the camber function of equation (8) satisfies conditions (i), (ii) and (iii). Next it is to be demonstrated that the constant terms of the stream function also satisfy condition (iii). In the incidence case of a flat plate at angle of attack α,

$$\frac{dy}{dx} = -\alpha ,$$

and condition (iii) gives

$$\psi = \alpha .$$

Hence the constant parts of the stream function from the incidence case and from the camber case are as follows:

$$D_0 - C_0 = \alpha - \frac{M_0}{2}$$

or

$$D_0 = \alpha - \frac{M_0}{2} + C_0 \,. \tag{10}$$

Hence the camber function is

$$F_c(\zeta) = -i \sum_1^\infty \frac{M_n}{\zeta^n} \,,$$

and on the foil the acceleration potential becomes

$$\varphi_c = -\sum_1^\infty M_n \sin n\theta \,. \tag{11}$$

3.4.3 Thickness Case

For the thickness solution consider the complex function

$$F_t(\zeta) = \frac{i\zeta}{(\zeta - e^{i\theta_0})(\zeta - e^{-i\theta_0})} \sum_0^\infty \frac{N_n}{\zeta^n} \,, \tag{12}$$

where the N_n are real constants. On the cavity where ζ is real and $|\zeta| > 1$, this function is purely imaginary and therefore satisfies condition (i). On the unit circle

$$F_t(e^{i\theta}) = -\frac{1}{2(\cos\theta_0 - \cos\theta)} \sum_0^\infty N_n (\sin n\theta + i \cos n\theta) \,.$$

It can be seen that F_t also clearly satisfies condition (ii). The unknown N_n can be solved for identically as in the camber solution, through boundary condition (iii). In the thickness solution $\frac{dy_t}{dx}$ as a function of θ is a curved function with a discontinuity at the point corresponding to the leading edge of the airfoil. For the thickness function assumed to be applicable to the solution of this problem the following relation must be true:

$$\frac{dy_t}{dx} = \frac{\sum_0^\infty N_n \cos n\theta}{2(\cos\theta_0 - \cos\theta)} \quad .$$

It is apparent that this relation reduces to the solution of a Fourier series as in the camber solution. The unknown N_n are then given by

$$N_n = \frac{4}{\pi}\int_0^\pi \frac{dy_t}{dx}(\cos\theta_0 - \cos\theta)\cos n\theta \, d\theta \quad , \quad n \geq 1$$

and

$$N_0 = \frac{2}{\pi}\int_0^\pi \frac{dy_t}{dx}(\cos\theta_0 - \cos\theta)\, d\theta \quad .$$

The thickness complex function is then

$$F_t(\zeta) = \frac{i\zeta}{(\zeta - e^{i\theta_0})(\zeta - e^{-i\theta_0})} \sum_0^\infty \frac{N_n}{\zeta^n} \quad ,$$

and on the foil the acceleration potential is

$$\varphi_t = -\frac{\sum_1^\infty N_n \sin n\theta}{2(\cos\theta_0 - \cos\theta)} \quad . \qquad (13)$$

It was found necessary to use a thickness function that has a singularity at the point corresponding to the leading edge. An attempt to use a function identical to the camber case was not successful. It was found that the Fourier coefficients would not converge.

3.4.4 Spoiler Case

The base of the spoiler maps into the point $\zeta = e^{i\theta_1}$, in the ζ-plane. At points on the circle when ζ passes through $e^{i\theta_1}$, there is a step change in v, and therefore through equation (4), a step change in ψ. The logarithmic function is an analytic function which will provide such a jump. It is also required that the imaginary part of the function be constant over appropriate portions of the circle. Consider the function

$$\ln.\left\{\frac{\zeta - e^{i\theta_1}}{\zeta - e^{-i\theta_1}}\right\}$$

The imaginary part of this function in the required range of $\pi \geq \theta \geq 0$ is

$$\arg\left\{\frac{\zeta - e^{i\theta_1}}{\zeta - e^{-i\theta_1}}\right\} = \begin{cases} \theta_1 \text{ for } \pi > \theta > \theta_1 \\ (\theta_1 - \pi) \text{ for } \theta_1 > \theta > 0 \end{cases} .$$

If this function is combined with one of the same type as F_1 from the incidence case, the resulting function is

$$F_\zeta(\zeta) = \frac{\sin\delta}{\pi}\left[\frac{i\theta_1}{\zeta e^{i\theta_2} - 1} + \frac{i\theta_1}{\zeta e^{-i\theta_2} - 1} + \ln.\left\{\frac{\zeta - e^{i\theta_1}}{\zeta - e^{-i\theta_1}}\right\}\right] \qquad (14)$$

On the circle where $\zeta = e^{i\theta}$, this becomes

$$F_s(e^{i\theta}) = \frac{\sin\delta}{\pi}\left[\frac{\theta_1 \sin\theta}{\cos\theta_0 - \cos\theta} + \ln\left\{\frac{\sin\frac{|\theta-\theta_1|}{2}}{\sin\frac{\theta+\theta_1}{2}}\right\}\right] + \begin{cases} 0 & \text{for } \pi > \theta > \theta_1 \\ -i\sin\delta & \text{for } \theta_1 > \theta > 0. \end{cases}$$

Boundary condition (iii) then becomes

$$v = \begin{cases} 0 & \text{on the foil } (\pi > \theta > \theta_1) \\ \sin\delta & \text{on the spoiler } (\theta_1 > \theta > 0) \end{cases}.$$

The spoiler angle δ has not been restricted to a small angle and it is realised that this contravenes one of the basic assumptions of linearized theory. In most practical configurations the spoiler height is only a small percentage of the chord. It is therefore optimistically assumed that the linearized flow has not been too severely disturbed. Both Woods (2) and Barnes (3) have had some success with normal spoilers using linearized theories.

It now remains to demonstrate that the spoiler function F_s satisfies condition (i) and (ii). The first part of this function, having been drawn from the incidence case, has already been shown to satisfy the conditions. On the cavity in the ζ-plane where ζ is real and $|\zeta| > 1$, the logarithm term is purely imaginary and hence satisfies condition (i). In the equation for $F_s(e^{i\theta})$, it can be seen that $\varphi \to 0$ as $\theta \to 0, \pi$ and hence the function satisfies the Kutta conditions. The spoiler function is then

$$F_s(\zeta) = \frac{\sin\delta}{\pi}\left[\frac{i\theta_1}{\zeta e^{-i\theta_0} - 1} + \frac{i\theta_1}{\zeta e^{-i\theta_0} - 1} + \ln\left\{\frac{\zeta - e^{i\theta_1}}{\zeta - e^{-i\theta_1}}\right\}\right],$$

and the acceleration potential on the foil is

$$\varphi_s = \frac{\sin\delta}{\pi}\left[\frac{\theta_1 \sin\theta}{\cos\theta_0 - \cos\theta} + \ln\left\{\frac{\sin\frac{|\theta-\theta_1|}{2}}{\sin\frac{\theta+\theta_1}{2}}\right\}\right] . \qquad (15)$$

3.4.5 Flap Case

The flap hinge point in the ζ-plane corresponds to the point $\zeta = e^{i\theta_2}$. It can easily be recognized that this case is identical to the spoiler case, except that the flap is restricted to small angles. The velocity conditions (iii) on the surface for this case are

$$v = \begin{cases} 0 & \text{on the foil } (\theta_2 > \theta > 0) \\ -\eta & \text{on the flap } (\pi > \theta > \theta_2) \end{cases} .$$

The complex function for the flap case is then

$$F_f(\zeta) = \frac{\eta}{\pi}\left[\frac{i(\theta_2-\pi)}{\zeta e^{i\theta_0} - 1} + \frac{i(\theta_2-\pi)}{\zeta e^{-i\theta_0} - 1} + \ln\left\{\frac{\zeta - e^{i\theta_2}}{\zeta - e^{-i\theta_2}}\right\}\right] , \qquad (16)$$

and on the foil the acceleration potential is

$$\varphi_f = \frac{\eta}{\pi}\left[\frac{(\theta_2-\pi)\sin\theta}{\cos\theta_0 - \cos\theta} + \ln\left\{\frac{\sin\frac{|\theta-\theta_2|}{2}}{\sin\frac{\theta+\theta_2}{2}}\right\}\right] . \qquad (17)$$

It has been shown in the spoiler case that these functions making up F_f satisfy the boundary conditions (i) and (ii).

3.5 Method of Solution

The functions developed in the previous paragraphs to solve the individual cases of incidence, camber, thickness, spoiler and flap solutions were shown to satisfy boundary conditions (i) through (iii). It remains then that boundary conditions (iv) and (v) be

satisfied. Condition (iv), the condition at infinity can be expressed as

$$F_{in}(\zeta_\infty) + F_c(\zeta_\infty) + F_t(\zeta_\infty) + F_s(\zeta_\infty) + F_f(\zeta_\infty) = -\frac{K}{2} \qquad (18)$$

where ζ_∞, the point at infinity in the ζ-plane, is given by equation (5). The last four terms on the left hand side of equation (18) are known functions; the unknown constants are contained in $F_{in}(\zeta_\infty)$. The equation can then be written as

$$F_{in}(\zeta_\infty) = E - \frac{K}{2} \qquad (19)$$

where

$$E = -F_c(\zeta_\infty) - F_t(\zeta_\infty) - F_s(\zeta_\infty) - F_f(\zeta_\infty),$$

and using equations (10) and (6), $F_{in}(\zeta_\infty)$ can be written as

$$F_{in}(\zeta_\infty) = iC_0\left[\frac{1}{\zeta_\infty e^{i\Theta_{-1}}} + \frac{1}{\zeta_\infty e^{-i\Theta_{-1}}} + 1\right] + i(\alpha - \tfrac{M_0}{2}) + iB_0(\zeta_\infty - \frac{1}{\zeta_\infty}).$$

In this equation put

$$\lambda_1 = i\left[\frac{1}{\zeta_\infty e^{i\Theta_{-1}}} + \frac{1}{\zeta_\infty e^{-i\Theta_{-1}}} + 1\right]$$

and

$$\lambda_2 = i(\zeta_\infty - \frac{1}{\zeta_\infty}).$$

Equation (19) can then be expressed as

$$C_0\lambda_1 + B_0\lambda_2 = E - i(\alpha - \tfrac{M_0}{2}) - \tfrac{K}{2} .$$

The real and imaginary parts of this equation furnish two equations in the two unknowns C_0 and B_0. The values of these constants are

$$B_0 = \frac{Rl.\lambda_1[Im.E - (\alpha - \frac{M_0}{2}) - Im.\lambda_1 Rl.E + \frac{K}{2} Im.\lambda_1}{Rl.\lambda_1 Im\lambda_2 - Im.\lambda_1 Rl.\lambda_2} \qquad (20)$$

and

$$C_0 = \frac{Rl.E - B_0 Rl.\lambda_2 - \frac{K}{2}}{Rl.\lambda_1} . \qquad (21)$$

All the function constants have been determined. The remaining unknowns are the cavity number K and the cavity length ℓ. There is not currently a theory that will correctly predict the base pressure, and at least this parameter will be an empirical input. It turns out however, that this is the only empirical input needed since the cavity length ℓ can be related to K through boundary condition (v). Condition (v) physically means that, if the body cavity system is to be a closed body, then the sum of the sources inside a contour including the body-cavity system must be zero. Mathematically it was found that condition (v) could be expressed as

$$Im.\oint F(z)dz = 0 .$$

From the mapping functions, points in the ζ-plane are related to the z-plane by

$$\zeta = \frac{2}{1+b}\left[a\sqrt{\frac{z}{\ell - z}} + \frac{1-b}{2}\right] + \sqrt{\left(\frac{2}{1+b}\right)^2\left[a\sqrt{\frac{z}{\ell - z}} + \frac{1-b}{2}\right]^2 - 1} . \qquad (22)$$

Since any contour of integration is suitable, one can be chosen such that $|z| \gg \ell$. The integral can then be solved using a Laurent expansion. For $|z| \gg \ell$ equation (22) becomes

$$\varsigma = a_0 + \frac{\ell a_1}{z} + \ldots\ldots ,$$

where

$$a_0 = \frac{1-b}{1+b} + \frac{2ia}{1+b} + \sqrt{\left[\frac{1-b}{1+b} + \frac{2ia}{1+b}\right]^2 - 1}$$

and

$$a_1 = \frac{2a}{1+b}\left[1 + \frac{\frac{1-b}{1+b} + \frac{2ia}{1+b}}{\sqrt{\left[\frac{1-b}{1+b} + \frac{2ia}{1+b}\right]^2 - 1}}\right] .$$

The coefficients of $\frac{1}{z}$ in the following terms are given:

$$(\varsigma - \tfrac{1}{\varsigma}) \;:\; \ell a_1 (1 + \tfrac{1}{a_0^2})$$

$$\left[\frac{1}{\varsigma e^{i\theta_0} - 1} + \frac{1}{\varsigma e^{-i\theta_0} - 1}\right] \;:\; -\ell a_1 \left[\frac{e^{i\theta_0}}{(a_0 e^{i\theta_0} - 1)^2} + \frac{e^{-i\theta_0}}{(a_0 e^{-i\theta_0} - 1)^2}\right]$$

$$\ln\left\{\frac{\varsigma - e^{i\theta_1}}{\varsigma - e^{-i\theta_1}}\right\} \;:\; \ell a_1 \left[\frac{1}{(a_0 - e^{i\theta_1})} - \frac{1}{(a_0 - e^{-i\theta_1})}\right]$$

$$\ln\left\{\frac{\varsigma - e^{i\theta_2}}{\varsigma - e^{-i\theta_2}}\right\} \;:\; \ell a_1 \left[\frac{1}{(a_0 - e^{i\theta_2})} - \frac{1}{(a_0 - e^{-i\theta_2})}\right]$$

$$\frac{1}{\varsigma^n} \;:\; -\frac{n \ell a_1}{a_0^{n+1}}$$

$$\frac{\varsigma}{\varsigma^n (\varsigma - e^{i\theta_0})(\varsigma - e^{-i\theta_0})} \;:\; \frac{\ell a_1 \left[\frac{1-n}{a_0} - \frac{e^{i\theta_0}}{a_0 e^{i\theta_0} - 1} - \frac{e^{-i\theta_0}}{a_0 e^{-i\theta_0} - 1}\right]}{a_0^{n-1} (a_0 e^{i\theta_0} - 1)(a_0 e^{-i\theta_0} - 1)} .$$

Although the solution appears straight forward, such is not the case and an iterative solution is necessary. The angles in the ζ-plane, θ_0, θ_1 and θ_2, the points corresponding to the leading edge, the spoiler base and the flap hinge point on the unit circle respectively, are complex functions of ℓ. The coefficient of $\frac{1}{z}$ can be written as

$$iB_0\ell a_1\left(1+\frac{1}{a_0^2}\right) - i\left[C_0 + \frac{\theta_1 \sin\delta}{\pi} + \frac{(\theta_2-\pi)\eta}{\pi}\right]\ell a_1\left[\frac{e^{i\theta_0}}{(a_0e^{i\theta_0}-1)^2} + \frac{e^{-i\theta_0}}{(a_0e^{-i\theta_0}-1)^2}\right]$$

$$+ \frac{\sin\delta}{\pi}\ell a_1\left[\frac{1}{(a_0-e^{i\theta_1})} - \frac{1}{(a_0-e^{-i\theta_1})}\right] + \frac{\eta}{\pi}\ell a_1\left[\frac{1}{(a_0-e^{i\theta_2})} - \frac{1}{(a_0-e^{-i\theta_2})}\right]$$

$$+ i\ell a_1\sum_1^\infty \frac{nM_n}{a_0^{n+1}} + i\ell a_1\sum_0^\infty N_n \frac{\left[\frac{1-n}{a_0} - \frac{e^{i\theta_0}}{(a_0e^{i\theta_0}-1)} - \frac{e^{-i\theta_0}}{(a_0e^{-i\theta_0}-1)}\right]}{a_0^{n-1}(a_0e^{i\theta_0}-1)(a_0e^{-i\theta_0}-1)} .$$

From equation (20) and (21) B_0 and C_0 can be written as

$$B_0 = \frac{Rl.\lambda_1[Im.E - (\alpha - \frac{M_0}{2})] - Im.\lambda_1 Rl.E}{Rl.\lambda_1 Im.\lambda_2 - Im.\lambda_1 Rl.\lambda_2} + \frac{K}{2}\frac{Im.\lambda_1}{Rl.\lambda_1 Im.\lambda_2 - Im.\lambda_1 Rl.\lambda_2}$$

and

$$C_0 = \frac{Rl.\lambda_2[Im.E - (\alpha - \frac{M_0}{2})] - Im.\lambda_2 Rl.E}{Rl.\lambda_2 Im.\lambda_1 - Im.\lambda_2 Rl.\lambda_1} + \frac{K}{2}\frac{Im.\lambda_2}{Rl.\lambda_2 Im.\lambda_1 - Im.\lambda_2 Rl.\lambda_1}$$

Now

$$Im.\oint F(z)dz = 2\pi\, Rl.\{\text{coefficient of } \tfrac{1}{z}\},$$

and hence the closure condition becomes

$$Rl.\{\text{coefficient of } \tfrac{1}{z}\} = 0 .$$

Putting the values of B_0 and C_0 in the above expression for the coefficient of $\frac{1}{z}$ gives

$$K = 2\,\mathrm{Rl.}\Big\{ \ell a_1 \Big(i\Big(1+\tfrac{1}{a_0^2}\Big)\Big[\frac{\mathrm{Rl.}\lambda_1[\mathrm{Im.}E-(\alpha-\frac{M_0}{2})]-\mathrm{Im.}\lambda_1\,\mathrm{Rl.}E}{\mathrm{Rl.}\lambda_1\mathrm{Im.}\lambda_2-\mathrm{Im}\lambda_1\,\mathrm{Rl.}\lambda_2}\Big]$$

$$-i\Big[\frac{e^{i\theta_0}}{(a_0e^{i\theta_0}-1)^2}+\frac{e^{-i\theta_0}}{(a_0e^{-i\theta_0}-1)^2}\Big]\Big[\frac{\mathrm{Rl.}\lambda_2[\mathrm{Im.}E-(\alpha-\frac{M_0}{2})]-\mathrm{Im.}\lambda_2\,\mathrm{Rl.}E}{\mathrm{Rl.}\lambda_2\mathrm{Im.}\lambda_1-\mathrm{Im.}\lambda_2\,\mathrm{Rl.}\lambda_1}+\frac{\theta_1\sin\delta}{\pi}+\frac{(\theta_2-\pi)\eta}{\pi}\Big]$$

$$+\frac{\sin\delta}{\pi}\Big[\frac{1}{(a_0-e^{i\theta_1})}-\frac{1}{(a_0-e^{-i\theta_1})}\Big]+\frac{\eta}{\pi}\Big[\frac{1}{(a_0-e^{i\theta_2})}-\frac{1}{(a_0-e^{-i\theta_2})}\Big]$$

$$+i\sum_{1}^{\infty}\frac{nM_n}{a_0^{n+1}}+i\sum_{0}^{\infty}N_n\frac{\Big[\frac{1-n}{a_0}-\frac{e^{i\theta_0}}{(a_0e^{i\theta_0}-1)}-\frac{e^{-i\theta_0}}{(a_0e^{-i\theta_0}-1)}\Big]}{a_0^{n-1}(a_0e^{i\theta_0}-1)(a_0e^{-i\theta_0}-1)}\Big)\Big\}$$

$$\Big/\,\mathrm{Rl.}\Big\{\ell a_1\Big(i\frac{\mathrm{Im.}\lambda_2}{\mathrm{Rl.}\lambda_2\mathrm{Im.}\lambda_1-\mathrm{Im.}\lambda_2\mathrm{Rl.}\lambda_1}\Big[\frac{e^{i\theta_0}}{(a_0e^{i\theta_0}-1)^2}+\frac{e^{-i\theta_0}}{(a_0e^{-i\theta_0}-1)^2}\Big]$$

$$-i\frac{\mathrm{Im.}\lambda_1}{\mathrm{Rl.}\lambda_1\mathrm{Im.}\lambda_2-\mathrm{Im.}\lambda_1\mathrm{Rl.}\lambda_2}\Big(1+\tfrac{1}{a_0^2}\Big)\Big)\Big\}\,. \qquad (23)$$

Hence with K given from experiment the correct value of the cavity length ℓ can be determined by plotting a graph of K v's ℓ, or by iteratively changing the value of ℓ in equation (23). The required real parts of this equation could be expressed by algebraically splitting each term into its real and imaginary parts. However it is desirable to retain the concise form of equation (23).

This completes the problem formulation for the steady theory. It remains to determine the pressure and lift coefficients. Using equation (2) and collecting the values of acceleration potential from equations (7), (11), (13), (15) and (17), the pressure coefficient, as a function of angular position on the unit circle in the ζ-plane, can be written as

$$C_p = -2\varphi - K\,,$$

where

$$\varphi = \left[C_0 + \frac{\eta(\theta_2-\pi)}{\pi} + \frac{\theta_1 \sin\delta}{\pi}\right]\frac{\sin\theta}{\cos\theta_0-\cos\theta} - 2B_0\sin\theta \qquad (24)$$

$$+ \frac{\sin\delta}{\pi}\ln.\left\{\frac{\sin\frac{|\theta-\theta_1|}{2}}{\sin\frac{\theta+\theta_1}{2}}\right\} + \frac{\eta}{\pi}\ln.\left\{\frac{\sin\frac{|\theta-\theta_2|}{2}}{\sin\frac{\theta+\theta_2}{2}}\right\}$$

$$- \sum_1^\infty M_n \sin n\theta - \frac{\sum_1^\infty N_n \sin n\theta}{2(\cos\theta_0-\cos\theta)}$$

Consideration of the transformations leads to the result that on the airfoil angular points on the unit circle in the ζ-plane, and points on the airfoil in the z-plane are related by

$$x = \frac{\frac{\ell}{a^2}\left[\frac{b+1}{2}\cos\theta - \frac{1-b}{2}\right]^2}{1+\frac{1}{a^2}\left[\frac{b+1}{2}\cos\theta - \frac{1-b}{2}\right]^2} \qquad (25)$$

It follows immediately that equations (2), (24) and (25) are used to relate the pressure coefficient to points on the airfoil.

The lift coefficient can be determined by the use of the Blasius equation,

$$D - iL = i\frac{\rho U^2}{2}\oint_\gamma w^2(z)\,dz\,, \qquad (26)$$

where the contour γ encloses the body and cavity system. To the first order in the dimensionless perturbation velocities

$$w^2(z) = 1 + 2(u - iv)$$

and equation (26) can be written as

$$D - iL = i\rho U^2\oint_\gamma (u - iv)\,dz\,. \qquad (27)$$

Using equations (3) and (4) and nondimensionalizing the lift and drag, equation (27) can be expressed as

$$C_D - i C_L = \frac{2i}{c}\oint_{\gamma} F(z)\,dz . \tag{28}$$

$F(z)$ can be expanded in a Laurent series for a contour γ such that $|z| \gg \ell$. Equation (28) then allows the lift coefficient to be written as

$$C_L = \frac{4\pi}{c}\,\mathrm{Im.}\{\text{coefficient of } \tfrac{1}{z}\}, \tag{29}$$

and the total drag coefficient on the body cavity system as

$$C_D = -\frac{4\pi}{c}\,\mathrm{Rl.}\{\text{coefficient of } \tfrac{1}{z}\} . \tag{30}$$

The $\mathrm{Rl}\{\mathrm{coeff}(\frac{1}{z})\}$ was shown to be zero in the consideration of the closure condition and the drag coefficient is zero as expected in such a potential theory. The drag on the airfoil can still be worked out theoretically. The drag on the airfoil is balanced equally by the force on the singularity at the cavity termination point. In determining the drag on the airfoil this cavity termination point only need be considered. The drag predicted is unrealistically high due to the theory being unable to model the separation bubble in-front of the spoiler evident in the real flow. The drag theory therefore will not be pursued further.

Using the results just determined for the cavity closure condition the lift coefficient can be written as

$$C_L = \frac{4\pi}{c}\,\mathrm{Im.}\Big\{ i B_0 \ell a_1 (1+\tfrac{1}{a_0^2}) - i\Big[C_0 + \frac{\theta_1 \sin\delta}{\pi} + \frac{(\theta_2-\pi)\eta}{\pi}\Big]\ell a_1\Big[\frac{e^{i\theta_0}}{(a_0 e^{i\theta_0}-1)^2} + \frac{e^{-i\theta_0}}{(a_0 e^{-i\theta_0}-1)^2}\Big]$$

$$+ \frac{\sin\delta}{\pi}\ell a_1\Big[\frac{1}{(a_0 - e^{i\theta_1})} - \frac{1}{(a_0 - e^{-i\theta_1})}\Big] + \frac{\eta}{\pi}\ell a_1\Big[\frac{1}{(a_0 - e^{i\theta_2})} - \frac{1}{(a_0 - e^{-i\theta_2})}\Big]$$

$$+ i l a_1 \sum_{1}^{\infty} \frac{n M_n}{a_0^{n+1}} + i l a_1 \sum_{0}^{\infty} N_n \frac{\left[\frac{1-n}{a_0} - \frac{e^{i\Theta_0}}{(a_0 e^{i\Theta_0} - 1)} - \frac{e^{-i\Theta_0}}{(a_0 e^{-i\Theta_0} - 1)} \right]}{a_0^{n-1} (a_0 e^{i\Theta_0} - 1)(a_0 e^{-i\Theta_0} - 1)} \Bigg\}. \qquad (31)$$

The Blasius equation for the pitching moment could equally be applied to determine the pitching moment coefficient of the airfoil.

SECTION 4

NONSTEADY THEORY

4.1 Formulation of the Problem

The nonsteady problem to be considered is the case of spoiler actuation on a fixed airfoil in initially steady flow. Nonsteady airfoil motions with fixed spoiler angles have not been considered. Such cases are a much simpler application of this theory and they have many features in common with existing results as given by Parkin (4).

The following theory is developed for the case of zero cavitation number. The reasons behind this merit careful consideration. First consider an airfoil without a spoiler in steady flow. If a spoiler is actuated on the upper surface, the flow is going to be disturbed. Even a detailed experimental tabulation of how the cavity number varies with the variables of time and spoiler angle will not enable a solution to be formulated. It must be remembered that the cavity length is related to the cavity number due to the fact that there can be no drag on the body-cavity system. It will be recalled that this was expressed by boundary condition (v) of the steady state. Hence, knowing the cavity number as a function of time, the cavity length can be calculated. Since the transformations of section (3.2) depend upon cavity length, the mapping function will change as cavity number changes with time. Modification to the current theory would be necessary to effect a solution in such a situation. The only solutions would appear to be, to assume that as soon as the spoiler starts to move the cavity number assumes its final steady state value, or assume that the cavity number is at all times zero. The first solution has obvious limitations and the second solution al-

though not physically attainable does have merit. The average pressure on the rear part of the upper surface of an airfoil in most configurations is very close to zero. Hence during the initial part of the spoiler actuation the cavitation number is close to zero. The zero cavitation number solution is comparatively simpler mathematically and its complete linearity permits easy comparisons to existing nonsteady thin airfoil theory problems such as change of angle of attack. At zero cavitation number the flow resembles a Helmholtz flow with the cavity behind the body extending to infinity. In this case the cavity pressure is equal to the undisturbed free stream static pressure. The foil is positioned as described in section (3.2). The airfoil configuration is shown in figure (3).

In solving this problem once again linear airfoil techniques are employed. The first problem for which a solution is required is the unit step spoiler actuation. To achieve this solution a case that is not physically attainable must be considered. The step boundary condition on the spoiler is a step in the y-component of velocity given by $v=\sin\delta$ over that portion of the x-axis that corresponds to the spoiler. Such a step change in velocity can be achieved by solving for the case of $v=v_0e^{j\omega t}$ over this region and then integrating over all frequencies. Looking more closely at this problem of a sinusoidal velocity however it can be seen that it is not physically possible. Over the negative portion of the velocity cycle when physically the portion of the x-axis corresponding to the spoiler has a suction on it, the airfoil could not possibly support a cavity. There are however, no mathematical limitations and the cavity is just considered to exist. This point is easier to understand if the sinusoidal velocity is considered to be a disturbance on the existing steady state solution for some spoiler angle. In such a case the

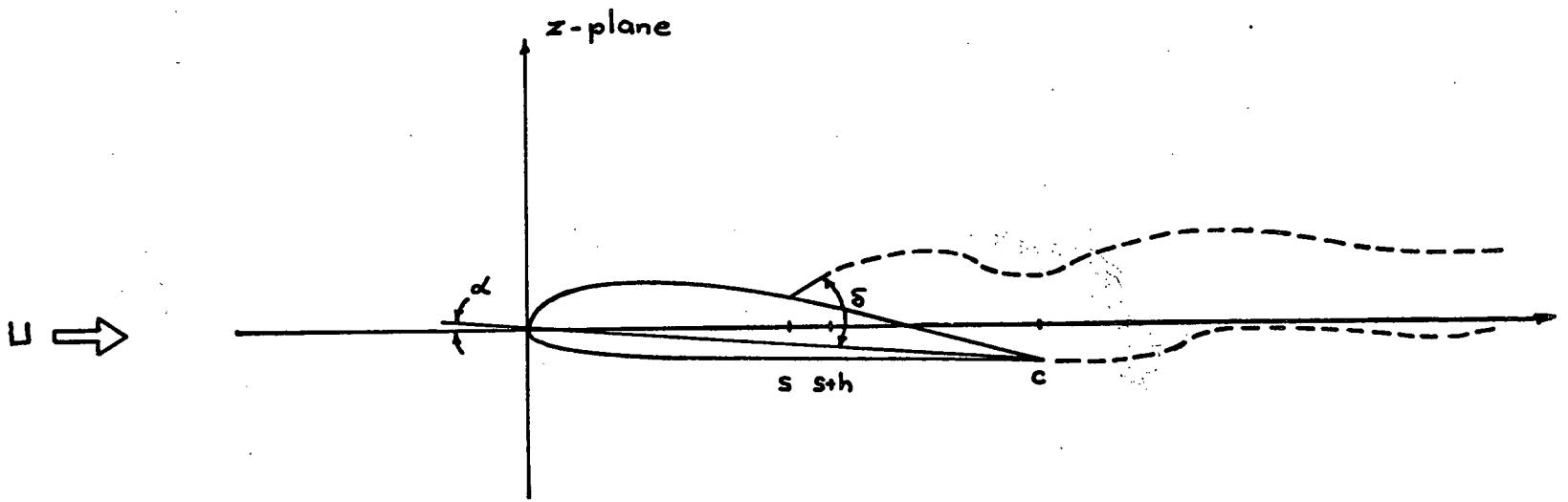

FIGURE (3): AIRFOIL IN THE Z'-PLANE

cavity does already exist. This case of a sinusoidal velocity over the spoiler region henceforth will be referred to as blowing theory.

4.2 Blowing Theory

In considering this problem only the flat plate solution of zero incidence is considered. This section is the equivalent of the spoiler case in the steady solution. The remaining existing steady state solutions of incidence, camber, thickness, and flap for K=0 are fully additive to this nonsteady solution.

4.2.1 Boundary Condition

The boundary conditions for this nonsteady blowing problem are as follows:

(i) $\varphi=0$ on the cavity, $x\geq(s+h)$, $y=0^+$ and $x\geq c$, $y=0^-$.

(ii) Kutta conditions, φ continuous, at the spoiler tip $x=(s+h)$, $y=0^+$ and at the trailing edge of the airfoil $x=c$, $y=0^-$.

(iii) $v=\begin{cases}0 & \text{on the foil } 0\leq x\leq s,\ y=0^+ \text{ and } 0\leq x\leq c,\ y=0^-.\\ v_0 e^{j\omega t} & \text{on the spoiler } s\leq x\leq(s+h),\ y=0^+.\end{cases}$

(iv) $F=0$ for the point at infinity, $z=-\infty$.

(v) $\mathrm{Im}\frac{dF}{dz}\begin{cases}=0 & \text{on the foil } 0\leq x\leq s,\ y=0^+ \text{ and } 0\leq x\leq c,\ y=0^-.\\ =-j\mu v_0 e^{j\omega t} & \text{on the spoiler } s\leq x\leq(s+h),\ y=0^+.\end{cases}$

In the above boundary conditions

$$\mu=\frac{\omega}{U}.$$

4.2.2 Transformations

The physical plane for this case is the z-plane of figure (2) with $\ell=\infty$. The transformations are obtained from the steady state transformations given in section (3.2), with the z'-plane omitted. The transformations are

$$\nu = a'\sqrt{z} \quad , \quad a' = \sqrt{\frac{1}{c}}$$

and

$$\nu = \frac{b'+1}{4}\left(\varsigma + \frac{1}{\varsigma}\right) - \frac{1-b'}{2} \quad , \quad b' = a'\sqrt{s+h}\,.$$

These transformations are shown in figure (2). Points on the airfoil in the z-plane are related to the corresponding points on the ς-plane by the relation:

$$\frac{x}{c} = \left(\frac{b'+1}{2}\right)^2 \left[\cos\theta - \cos\theta_0\right]^2 . \qquad (32)$$

4.2.3 Method of Solution

Using boundary condition (v) and the definition of the acceleration stream function from section (1), the stream function can be written as

$$\frac{\partial \psi}{\partial x} \begin{cases} = 0 & \text{on the foil} \\ = -j\mu v_0 e^{j\omega t} & \text{on the spoiler.} \end{cases}$$

Integration of this equation gives

$$\psi \begin{cases} = C_2 e^{j\omega t} & \text{on the foil} \\ = -j\mu v_0 e^{j\omega t} x + \hat{C}_1 e^{j\omega t} & \text{on the spoiler,} \end{cases}$$

where the 'constants' of integration have been assumed to be harmonize function of t. Substitution of x from equation (32) into these relations enables ψ to be expressed as

$$\psi \begin{cases} = C_2 e^{j\omega t} & \text{on the foil} \\ = -j\mu v_0 e^{j\omega t}\left[\left(\frac{b'+1}{2}\right)^2 \frac{1}{2}\cos 2\theta - \left(\frac{1-b'^2}{2}\right)\cos\theta\right] + C_1 e^{j\omega t} & \text{on the spoiler} \end{cases} \tag{33}$$

where $C_1 = \hat{C}_1 - j\mu v_0 \left(\frac{b'+1}{2}\right)^2 \left(\frac{1}{2} + \cos^2\theta_0\right)$. The solution to the problem closely follows the techniques of the steady state problem. Complex functions must be determined to satisfy the boundary conditions developed. The constant terms of equation (33) can be satisfied by functions given in the spoiler case solution as follows:

$$-\frac{C_1}{\pi}\left[\frac{i\theta_1}{\zeta e^{i\theta_0} - 1} + \frac{i\theta_1}{\zeta e^{-i\theta_0} - 1} + \ln\left\{\frac{\zeta - e^{i\theta_1}}{\zeta - e^{-i\theta_1}}\right\}\right] e^{j\omega t}$$

$$+\frac{C_2}{\pi}\left[\frac{i(\theta_1 - \pi)}{\zeta e^{i\theta_0} - 1} + \frac{i(\theta_1 - \pi)}{\zeta e^{-i\theta_0} - 1} + \ln\left\{\frac{\zeta - e^{i\theta_1}}{\zeta - e^{-i\theta_1}}\right\}\right] e^{j\omega t} \tag{34}$$

The part of equation (33) that is a function of θ is similar to a camber type problem and once again a Fourier series complex function is required. Suppose the function of θ in equations (33) is expressed as

$$f(\theta) \begin{cases} = \left(\frac{b'+1}{2}\right)^2 \frac{1}{2}\cos 2\theta - \left(\frac{1-b'^2}{2}\right)\cos\theta & \theta_1 \geq \theta \geq 0 \\ = 0 & \pi \geq \theta \geq \theta_1 \end{cases}$$

A Fourier cosine series can be determined as follows:

$$\sum_1^\infty J_n \cos n\theta = f(\theta) ,$$

where

$$J_n = \frac{2}{\pi}\int_0^\pi f(\theta)\cos n\theta \, d\theta .$$

Since this Fourier cosine series has to be the imaginary part of any function determined, it follows that the required complex function can be written as

$$-j\mu V_\infty e^{j\omega t} i \sum_1^\infty \frac{J_n}{\zeta^n}.$$

Hence combining expression (34) with this function allows the total nonsteady complex function to be written as

$$\begin{aligned} F_n(\zeta) = & -j\mu V_\infty e^{j\omega t} i \sum_1^\infty \frac{J_n}{\zeta^n} \\ & - \frac{C_1}{\pi} e^{j\omega t} \left[\frac{i\theta_1}{\zeta e^{i\theta_2} - 1} + \frac{i\theta_1}{\zeta e^{-i\theta_2} - 1} + \ln. \left\{ \frac{\zeta - e^{i\theta_1}}{\zeta - e^{-i\theta_1}} \right\} \right] \\ & + \frac{C_2}{\pi} e^{j\omega t} \left[\frac{i(\theta_1 - \pi)}{\zeta e^{i\theta_2} - 1} + \frac{i(\theta_1 - \pi)}{\zeta e^{-i\theta_2} - 1} + \ln. \left\{ \frac{\zeta - e^{i\theta_1}}{\zeta - e^{-i\theta_1}} \right\} \right] \end{aligned} \qquad (35)$$

It remains to demonstrate that these functions satisfy all the boundary conditions. Conditions (i) and (ii) are identical conditions to the steady state solution and since the functions are of the steady state type these conditions are fully satisfied. Through the mapping functions it can be shown that $|\zeta|$ approaches infinity as $|z|$ approaches infinity. Hence the complex functions in equation (35) disappear at infinity and condition (iv) is satisfied. Boundary condition (v) was used to determine the nonsteady complex functions and is inherently satisfied. The velocity boundary condition (iii) now must be satisfied.

Using the definition of the stream function from section (1), equation (1) can be written as

$$\frac{dV_\infty}{dx} + j\mu V_\infty = -\frac{\partial \psi_\infty}{\partial x}, \qquad (36)$$

where the nonsteady flow quantities have been written as $\varphi = \varphi_0 e^{j\omega t}$ $\psi = \psi_0 e^{j\omega t}$ and $v = V_0 e^{j\omega t}$. In equation (35) these values enable the nonsteady complex function to be expressed as

$$F_n(\zeta) = [\varphi_0(\zeta) + i\psi_0(\zeta)] e^{j\omega t}. \tag{37}$$

Since V_0, the velocity amplitude about the x-axis of a given point in the flow field, must vanish at infinity, the integral of equation (36) can be written as

$$V_0 = -e^{-j\mu x} \int_{-\infty}^{x} \frac{\partial \psi}{\partial x} e^{j\mu \xi} d\xi \tag{38}$$

where x refers to any point on the foil or spoiler region and ξ is a dummy variable of integration. At points on the foil $V_0 = 0$ and at points on the spoiler region $V_0 = v_0$. Consideration of the leading edge and the spoiler base in equation (38) will result in two equations in the two unknowns C_1 and C_2. It should be noted that consideration of any general points results in the same equations, but mathematical simplicity makes the leading edge and the spoiler base the desired choice. The equations are

$$0 = \int_{-\infty}^{0} \frac{\partial \psi_0}{\partial x} e^{j\mu s} ds$$

and

$$v_0 = -e^{-j\mu s} \int_{-\infty}^{s} \frac{\partial \psi_0}{\partial x} e^{j\mu s} ds$$

Integrating these equations by parts and changing the variable of integration gives

$$0 = -e^{j\mu\xi}\psi_0\Big|_{-\infty}^{0} + j\mu\int_0^{\infty} e^{-j\mu\xi'}\psi_0(-\xi')\,d\xi'$$

and (39)

$$v_0 e^{j\mu s} = -e^{j\mu\xi}\psi_0\Big|_{-\infty}^{s} + j\mu\int_0^{\infty} e^{-j\mu\xi'}\psi_0(-\xi')\,d\xi' + j\mu\int_0^{s} e^{j\mu\xi}\psi_0\,d\xi$$

where ξ has been replaced by $-\xi'$. Substituting the value of ψ_0 from equation (37) into the first of equations (39) results in the equation

$$\frac{C_2}{\pi}\left[j\mu\int_0^{\infty} e^{-j\mu\xi'}T_3\,d\xi' - \pi\right] - \frac{C_1}{\pi}j\mu\int_0^{\infty} e^{-j\mu\xi'}T_2\,d\xi' + \mu^2 v_0\int_0^{\infty} e^{-j\mu\xi'}T_1\,d\xi' = 0.$$

Substituting ψ_0 into the second of equations (39) gives

$$\frac{C_2}{\pi}\left[\pi e^{j\mu s} - \pi + j\mu\int_0^{\infty} e^{-j\mu\xi'}T_3\,d\xi'\right] - \frac{C_1}{\pi}\left[\pi e^{j\mu s} + j\mu\int_0^{\infty} e^{-j\mu\xi'}T_2\,d\xi'\right]$$

$$+\mu^2 v_0\int_0^{\infty} e^{-j\mu\xi'}T_1\,d\xi' + j\mu v_0 e^{j\mu s}\left\{\frac{1}{2}\left(\frac{b'+1}{2}\right)^2\cos 2\theta_1 - \left(\frac{1-b'^2}{2}\right)\cos\theta_1\right\} - v_0 e^{j\mu s} = 0.$$

In the above equations

$$T_1 = \mathrm{RI.}\sum_1^{\infty}\frac{J_n}{\left[\cos\theta_0 + \frac{2j}{1+b'}\sqrt{\xi'} + \sqrt{\left\{\cos\theta_0 + \frac{2j}{1+b'}\sqrt{\xi'}\right\}^2 - 1}\right]^n}$$

$$T_2 = \mathrm{RI}\left\{\theta_1\left[\frac{\sqrt{\left\{\cos\theta_0 + \frac{2j}{1+b'}\sqrt{\xi'}\right\}^2 - 1}}{\frac{2j}{1+b'}\sqrt{\xi'}} - 1\right]\right\} + \arg\left\{\frac{\cos\theta_0 + \frac{2j}{1+b'}\sqrt{\xi'} + \sqrt{\left\{\cos\theta_0 + \frac{2j}{1+b'}\sqrt{\xi'}\right\}^2 - 1} - e^{j\theta_1}}{\cos\theta_0 + \frac{2j}{1+b'}\sqrt{\xi'} + \sqrt{\left\{\cos\theta_0 + \frac{2j}{1+b'}\sqrt{\xi'}\right\}^2 - 1} - e^{-j\theta_1}}\right\}$$

and

$$T_3 = \mathrm{RI.}\left\{(\theta_1 - \pi)\left[\frac{\sqrt{\left\{\cos\theta_0 + \frac{2j}{1+b'}\sqrt{\xi'}\right\}^2 - 1}}{\frac{2j}{1+b'}\sqrt{\xi'}} - 1\right]\right\} + \arg\left\{\frac{\cos\theta_0 + \frac{2j}{1+b'}\sqrt{\xi'} + \sqrt{\left\{\cos\theta_0 + \frac{2j}{1+b'}\sqrt{\xi'}\right\}^2 - 1} - e^{j\theta_1}}{\cos\theta_0 + \frac{2j}{1+b'}\sqrt{\xi'} + \sqrt{\left\{\cos\theta_0 + \frac{2j}{1+b'}\sqrt{\xi'}\right\}^2 - 1} - e^{-j\theta_1}}\right\}$$

The solution to the two simultaneous equations for C_1 and C_2 is

$$C_1 = -v_0 C_1'$$

and

$$C_2 = v_0 C_2'$$

The values of C_1' and C_2' are

$$C_1' = \frac{\left[j\mu\int_0^\infty e^{-j\mu\xi'} T_3\, d\xi' - \pi\right]\left[j\mu\left\{\frac{1}{2}\left(\frac{b'+1}{2}\right)^2\cos 2\theta_1 - \left(\frac{1-b'^2}{2}\right)\cos\theta_1\right\} - 1\right] - \mu^2\pi\int_0^\infty e^{-j\mu\xi'} T_1\, d\xi'}{\pi\left\{1 + j\mu\int_0^\infty e^{-j\mu\xi'} T_4\, d\xi'\right\}}$$

and (40)

$$C_2' = \frac{\pi\mu^2\int_0^\infty e^{-j\mu\xi'} T_1\, d\xi' + j\mu C_1'\int_0^\infty e^{-j\mu\xi'} T_2\, d\xi'}{\pi - j\mu\int_0^\infty e^{-j\mu\xi'} T_3\, d\xi'} ,$$

where

$$T_4 = \mathrm{RL}\left[\frac{\sqrt{\left\{\cos\theta_0 + \frac{2\lambda}{1+b'}\sqrt{\xi'}\right\}^2 - 1}}{\frac{2\lambda}{1+b'}\sqrt{\xi'}} - 1\right] .$$

It can be seen that C_1' and C_2' are very complicated expressions that cannot be solved analytically. The numerical solution of C_1' and C_2' as a function of μ involves large numbers of calculations and necessitates the use of a computer. In solving the expressions for C_1' and C_2', ξ' obviously cannot be extended to infinity. Fortunately this does not limit the solution. A closer look at the integrands of the expressions in equations (40) helps to demonstrate this point. These integrands all approach zero as ξ' approaches infinity. It is not this fact however, that facilitates the solution of these integrals.

It is found that when ξ' is greater than a few chords, the integrands are very slowly varying functions of ξ'. The important aspect of the integrals then becomes the fact that the integrand must be truncated at the end of a complete cycle. This means that $\mu\xi'$ has to be an exact even multiple of π. Using this technique it is found that 10 chords gives a high degree of accuracy. The value will actually fluctuate around 10 chords as $\mu\xi'$ is kept as an exact even multiple of π. In the integrals involving T_2, T_3, and T_4 the integrand is infinite at the lower limit. Care must be taken in numerically determining the Cauchy Principal value of these integrals.

From equation (37) the acceleration potential φ_0 for points on the foil can be written as

$$\varphi_0 = [C_2' + C_1']V_0 \ln\left\{\frac{\sin\frac{|\theta-\theta_1|}{2}}{\sin\frac{\theta+\theta_1}{2}}\right\} + [C_2'(\theta_1-\pi) + C_1'\theta_1]V_0\frac{\sin\theta}{\cos\theta_0-\cos\theta} - j\mu V_0\sum_1^\infty J_n \sin n\theta. \quad (41)$$

Using equation (2) and integrating the pressure, the lift coefficient can be written as

$$C_L = -\frac{2}{c}\int_0^\pi \varphi\frac{dx}{d\theta}\,d\theta .$$

Substituting the expression for x from equation (32) gives

$$C_{L_0} = 2\left(\frac{b'+1}{2}\right)^2\int_0^\pi \varphi_0 \sin 2\theta\, d\theta - (1-b^2)\int_0^\pi \varphi_0 \sin\theta\, d\theta ,$$

where C_{L_0} is the amplitude of the unsteady lift coefficient, and $C_L = C_{L_0}e^{j\omega t}$. Putting the expression for φ_0 in this equation and integrating gives

$$C_{L_0} = V_0[C_1'D_1 + C_2'D_2 - j\mu D_3]$$

where

$$D_1 = \pi\left\{\left(\frac{b'+1}{2}\right)^2[2\theta_1\cos 2\theta_0 - \sin 2\theta_1] + (1-b^2)[\sin\theta_1 - \theta_1\cos\theta_0]\right\},$$

$$D_2 = \pi\left\{\left(\frac{b'+1}{2}\right)^2\left[2(\theta_1-\pi)\cos 2\theta_0 - \sin 2\theta_1\right] + (1-b'^2)\left[\sin\theta_1 - (\theta_1-\pi)\cos\theta_0\right]\right\}$$

and

$$D_3 = \tfrac{1}{2}\left(\frac{b'+1}{2}\right)^4\left[\theta_1 + \tfrac{1}{4}\sin 4\theta_1\right] - \tfrac{3}{4}\left(\frac{b'+1}{2}\right)^2(1-b'^2)\left[\sin\theta_1 + \tfrac{1}{3}\sin 3\theta_1\right] + \tfrac{1}{4}(1-b'^2)^2\left[\theta_1 + \tfrac{1}{2}\sin 2\theta_1\right].$$

Suppose the quasi-steady lift coefficient C_{L_S} is defined to be the value of the unsteady lift coefficient for $\mu \to 0$, then,

$$C_{L_S} = v_0 D_1 e^{j\omega t},$$

since

$$C_1' = 1 \quad \text{and} \quad C_2' = 0 \quad \text{for } \mu \to 0.$$

The ratio of the nonsteady lift coefficient to the quasi-steady lift coefficient can be written as

$$\frac{C_L}{C_{L_S}} = Q(\mu) - j\mu\frac{D_3}{D_1}, \tag{42}$$

where

$$Q(\mu) = C_1' + C_2'\frac{D_2}{D_1}.$$

The lift coefficient is then expressed as

$$C_L = v_0 D_1 e^{j\omega t}\left[Q(\mu) - j\mu\frac{D_3}{D_1}\right].$$

This lift coefficient must now be used to determine the unit step spoiler actuation problem.

4.3 Unit Step Actuation

The complete linearity of the present system for K=0 makes it possible to use the methods of superposition to obtain the transient solution to the spoiler actuation problem. The second term of equation (42) represents the contribution of the apparent mass term and will be discarded since it has no contribution to the solution. Before proceeding with the problem, a closer look at $Q(\mu)$ is warranted. The numerical solution of Q has limitations for large values of μ. Fortunately such large values of μ have little effect on the solution to the problem. $Q(\mu)$ is shown in section (6) for different spoiler positions and sizes. It can be seen that as μ gets larger, Q tends to the imaginary axis and the rate of change of the real part of Q with μ is very small. This contributes to the solution converging rapidly as μ increases. A further discussion of this point will be given after the solution has been developed. A further point to notice is that as μ approaches infinity, Q becomes asymptotic to the imaginary axis. This means that the real part of the lift approaches zero as μ approaches infinity. Physically it can be argued that the blowing and sucking cycles occur so rapidly that the wake circulation cancels the lift more effectively for these shorter wavelengths.

Equation (42) can be written as

$$C_L = v D_1 Q(\mu), \tag{43}$$

where $v = v_0 e^{j\omega t}$ and the apparent mass term has been dropped. The velocity boundary condition on the spoiler region for the unit step spoiler actuation problem is as follows:

$$v = \begin{cases} 0, & t<0 \\ \sin\delta, & t\geq 0. \end{cases}$$

This can be expressed as $\sin\delta 1(t)$. If v_o is put equal to $\frac{\sin\delta}{2\pi j\omega}$ and equation (43) is integrated over all frequencies, the transient lift coefficient becomes

$$C_L = \sin\delta\, D_1 \cdot \frac{1}{2\pi j}\int_{-\infty}^{\infty} \frac{e^{j\omega t}}{\omega} Q(\omega)\, d\omega.$$

Suppose

$$Ut = s'c$$

where s' is the distance moved in chords, then this equation can be written as

$$C_L = C_{L_f} I(s'), \tag{44}$$

where C_{L_f} is the final steady state value of the lift coefficient and

$$I(s') = \frac{1}{2\pi j}\int_{-\infty}^{\infty} \frac{e^{jks'}}{k} Q(k)\, dk. \tag{45}$$

The frequency parameter k is given by

$$k = \mu c.$$

The technique for solving this integral is given by Bisplinghoff (8). Suppose

$$Q(k) = R(k) + jS(k)$$

where R and S are both real functions of k. The integral of equation (45) becomes

$$I(s') = \frac{2}{\pi}\int_{0}^{\infty} \frac{R(k)\sin ks'}{k}\, dk. \tag{46}$$

R is only known numerically and this integral must also be solved numerically. It will be recalled that as μ and hence k, increases in size, R(k) and the rate of change of R(k) approach zero. This and the k factor in the denominator make the integrand very rapidly approach zero. Once again it is advantageous to integrate over a length corresponding to an even multiple of π. It is not necessary to take k any greater than 25 to give very good accuracy for this integral. The solutions to this problem are given graphically for different airfoil configurations in section (6).

4.4 Finite Time Actuation

In practical applications the spoiler actuation takes a finite period of time. Once again the complete linearity of the zero cavity number solution allows this problem to be easily solved. The unit step integral in equation (46) is entirely independent of the spoiler angle. This means that nonsteady spoiler actuation solutions can be superposed. For example, suppose at t=0 the spoiler angle jumps $\Delta\delta$ and after $t=\Delta t$ the spoiler angle again jumps $\Delta\delta$. At $t=\Delta t$ the distance travelled, $\Delta s'$, is $U\Delta t$ and the total spoiler angle is $2\Delta\delta$. After time $t=t_e=N\Delta t$, during which time the foil has travelled $s'=s'_e=N\Delta s'$, the spoiler angle has risen to its erection angle

$$\delta=(N+1)\Delta\delta$$

Using equation (44) and summing up each small step gives

$$C_L = D_1 \sin\Delta\delta\left\{I_1[N\Delta s'] + I_2[(N-1)\Delta s'] + \ldots\ldots + I_{N+1}[0]\right\}.$$

After time $t>t_e$, during which time the foil has travelled a distance $(s'-s'_e)$ with its spoiler fully erected, the lift coefficient is

$$C_L = D_1 \sin\Delta\delta\left\{I_1(s') + I_2(s' - \frac{s'_e}{N}) + I_3(s' - 2\frac{s_e}{N}) + \ldots\ldots + I_{N+1}(s' - s'_e)\right\}.$$

Now $\Delta\delta \ll 1$ and $\sin\Delta\delta$ can be replaced by

$$\Delta\delta = \frac{\delta}{N+1} \quad .$$

This gives the lift coefficient

$$C_L = C_{L_f} W(s')$$

where

$$W(s') = \frac{1}{N+1}\left\{I_1(s') + I_2(s' - \frac{s'_e}{N}) + \ldots\ldots + I_{N+1}(s' - s'_e)\right\}.$$

Strictly speaking in this solution C_{L_f} should equal $D_1\delta$ and not $D_1\sin\delta$. However since it is the response function $W(s')$ that is the important part of this solution it is allowable, for conformity purposes, to write the solution as given in equation (44). Once N is chosen, the solution is a function of the total distance travelled and the distance travelled during spoiler erection. Typically N=20 shows very good results. This solution for different airfoil configurations is also shown graphically in section (6).

SECTION 5

EXPERIMENTS

Experimental measurements for lift, drag and pitching moment were taken for the 14% thick Clark Y airfoil, shown graphically in figure (4). The airfoil was constructed of wood and had a 14 inch chord. Each end of the airfoil had 1/8 inch steel plates attached to allow spanwise spoilers of heights 5% and 10% chord to be mounted at spoiler angles of 15, 30, 45, 60, 75, and 90 degrees to the airfoil surface at varying positions on the airfoil. Measurements were taken for spoiler positions of 50 and 70% chord.

The airfoil was mounted at the mid-chord position on a six-component strain gauge balance system. The lift, drag and pitching moment were measured over a wide range of incidence. The gap between the spoiler and the airfoil surface was sealed with masking tape for each configuration. The base pressure in the wake region was measured by taping a thin tube to the airfoil in the wake region. This tube was connected to an alcohol manometer together with a tube leading to a static probe measuring the upstream undisturbed static pressure. The test Reynolds number was 4×10^5.

Identical measurements were taken on a 14% thick Clark Y airfoil with a 32.5% flap. This airfoil and flap combination is shown graphically in figure (5). For these measurements the airfoil was mounted at the $\frac{1}{4}$-chord point. The gap on the lower surface between the main foil and the flap was sealed with masking tape.

All measurements were made in the low speed wind tunnel of the Mechanical Engineering Department of the University of British Columbia. This tunnel has a test section of 3 ft. by $2\frac{1}{4}$ ft. over a length of 8 2/3 ft. The tunnel produces a very uniform flow, with a

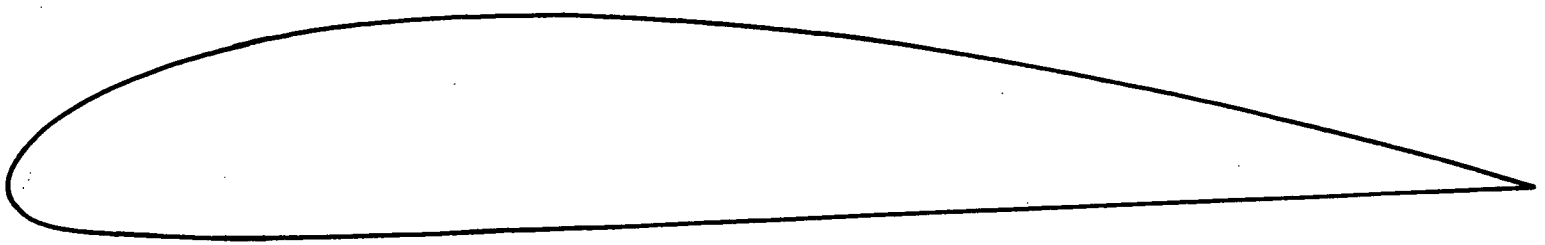

FIGURE (4): 14% THICK CLARK Y AIRFOIL

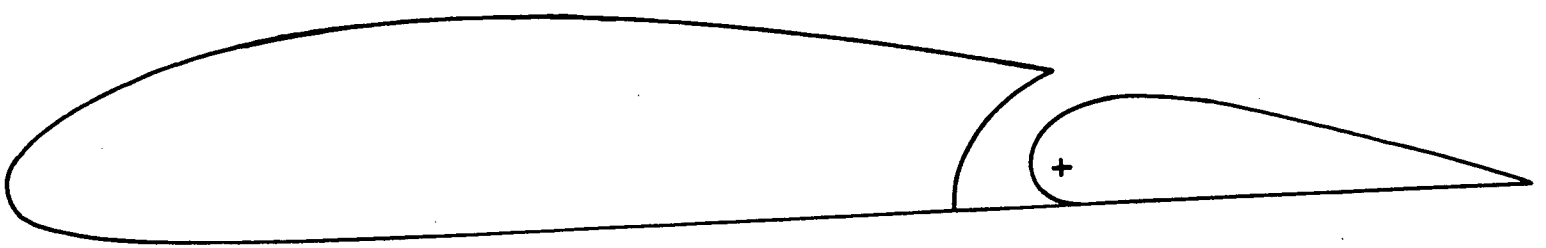

FIGURE (5): 14% THICK CLARK Y AIRFOIL WITH 32.5% FLAP

turbulence level of less than 0.1% over a wind speed range of 0-150 fps.

The wind tunnel wall correction technique employed was the same as that employed by Jandali (1). This method uses the corrections established by Pope and Harper (9), with a wake blockage term of $\frac{1}{4}(c/H)C_D$ instead of $\frac{1}{2}(c/H)C_D$. Jandali found that measurements on airfoils of varying chord lengths collapsed more suitably using these corrections. There exists some controversy over the techniques employed for correcting the wake pressure coefficient. Bluff body and stalled airfoil techniques such as those presented by Maskell (10) are not strictly applicable. To overcome this problem, base pressure measurements were taken over a range of incidences on airfoils of chords 9, 14, 19 and 24 inches for normal spoilers of 5% and 10% heights located at both the 50% and 70% chord positions. These measurements were plotted and interpolated back to zero chord (or infinite stream). The base pressure coefficient for the remaining spoiler angles, for which measurements were taken on the 14 inch chord airfoil, were then corrected in the same respective ratio. It is realized that, as the spoiler angle changes, the wake characteristics also change slightly. This in turn would affect the correction ratios slightly. This technique does however, give reasonably realistic results and was used in the absence of a better technique.

At low airfoil incidences and small spoiler angles the possibility of flow reattachment occurs. In such a case the theories developed in sections (3) and (4) are not applicable. To ensure that measurements were not taken for such cases tufts of cotton were attached to the airfoil surface in the wake region. Observation of these tufts in all airfoil configurations was carefully carried out. The lower surface of the Clark Y airfoil is flat, and this base is used as a reference for incidence rather than the usual chord line.

SECTION 6

RESULTS AND COMPARISONS

The first part of this section shows the results from the steady linearized cavity flow theory developed in section (3). The lift coefficients over a wide range of incidence, obtained for normal spoilers, are compared to those obtained theoretically by Woods (2) and Jandali (1). The theoretical lift coefficients as functions of incidence for several spoiler angles, including the normal spoilers, are compared with experiment. Comparisons between theory and experiment are also presented showing the variation of lift coefficient with spoiler angle for a given airfoil incidence. Examples of the pressure coefficient predicted by the linearized theory complete the steady state results presented.

The latter part of this section contains the results from the unsteady linearized cavity flow theory developed in section (4) to solve the spoiler actuation problem. In the blowing case theoretical results are given showing the variation with frequency of the ratio of lift coefficient to quasi-steady lift coefficient. The ratio of lift coefficient to final lift coefficient as a function of distance moved in chords is presented theoretically for the unit step and finite time spoiler actuation problems.

6.1 Steady Theory

In figure (6) the experimental lift coefficient and the lift coefficient calculated using standard linearized techniques are plotted as a function of incidence for the 14% thick Clark Y airfoil. As is expected the agreement around the zero lift angle of incidence is good, the agreement becoming worse as the incidence increases. Around the zero lift incidence the vorticity dissipation in the boundary

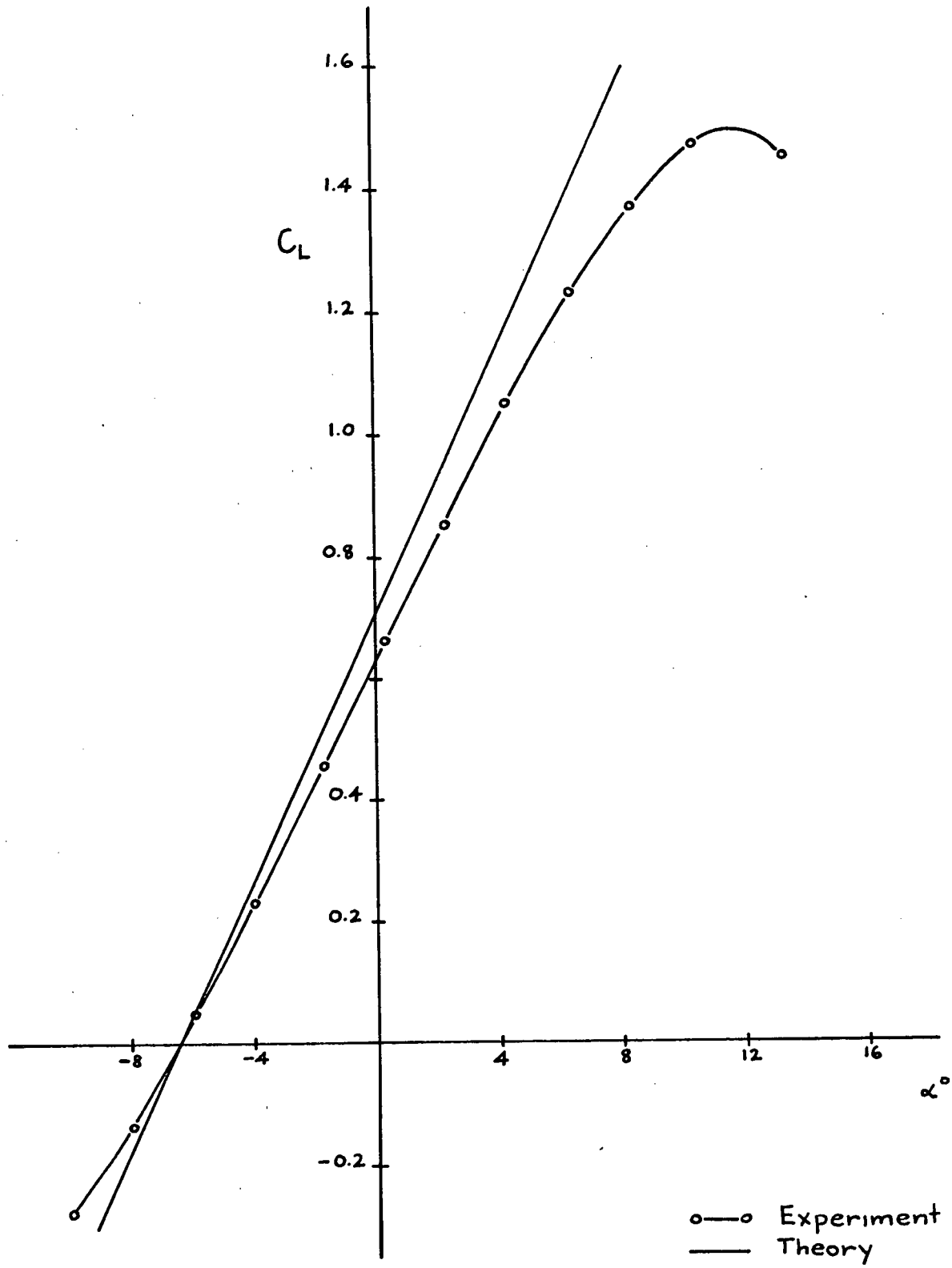

FIGURE (6): LIFT COEFFICIENT FOR BASIC CLARK Y AIRFOIL

layer is at a minimum and a close comparison between theory and experiment is expected.

First lift coefficients over a range of incidence from the present theory will be compared to the results of other theories, and to experimental results, for the case of a normal spoiler. All spoiler heights and positions are given as a percentage of the airfoil chord.

In figure (7) and (8) the lift coefficients for the three theories and the experimental lift coefficients are shown for a 10% normal spoiler at the 50 and 70% positions respectively. The corresponding comparisons for a 5% normal spoiler are shown in figures (9) and (10). These figures show the agreement between the theory and experiment is quite good. The agreement with experiment shown by Jandali's theory is very good, but it will be recalled the additional condition of no lift incidence is required as an input into this theory. In the calculation of Woods' theory the empirical equation for C_{p_o} suggested by Barnes (3) was used. Although Woods' theory shows reasonable agreement with experiment, it does not seem to predict the correct lift curve slope. For the experimental base pressure applicable in these cases, the cavity length is quite short. This has the tendency of making the solution more highly dependent on the accuracy of the base pressure coefficient. The camber and thickness solutions which constitute a considerable portion of the lift coefficient, are dependent to a very small extent on the cavity number. They have a very small effect on the determination of the cavity length, and enter primarily through satisfying the condition at infinity. This fact reduces the solution dependence on the cavity length and hence the cavity number. The contribution of the thickness solution increases negatively from zero as the spoiler moves ahead

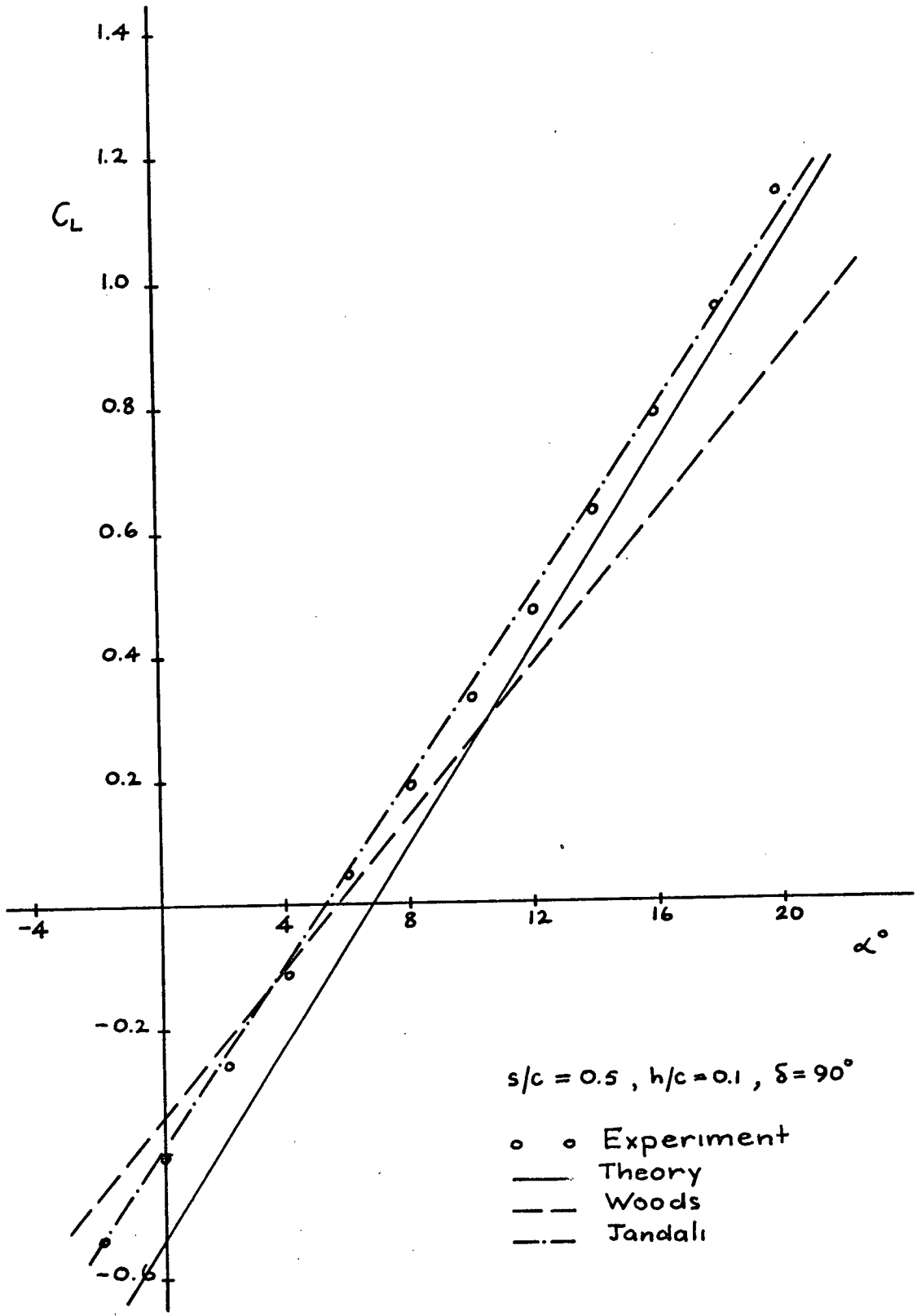

FIGURE (7): LIFT COEFFICIENT FOR CLARK Y AIRFOIL WITH SPOILER

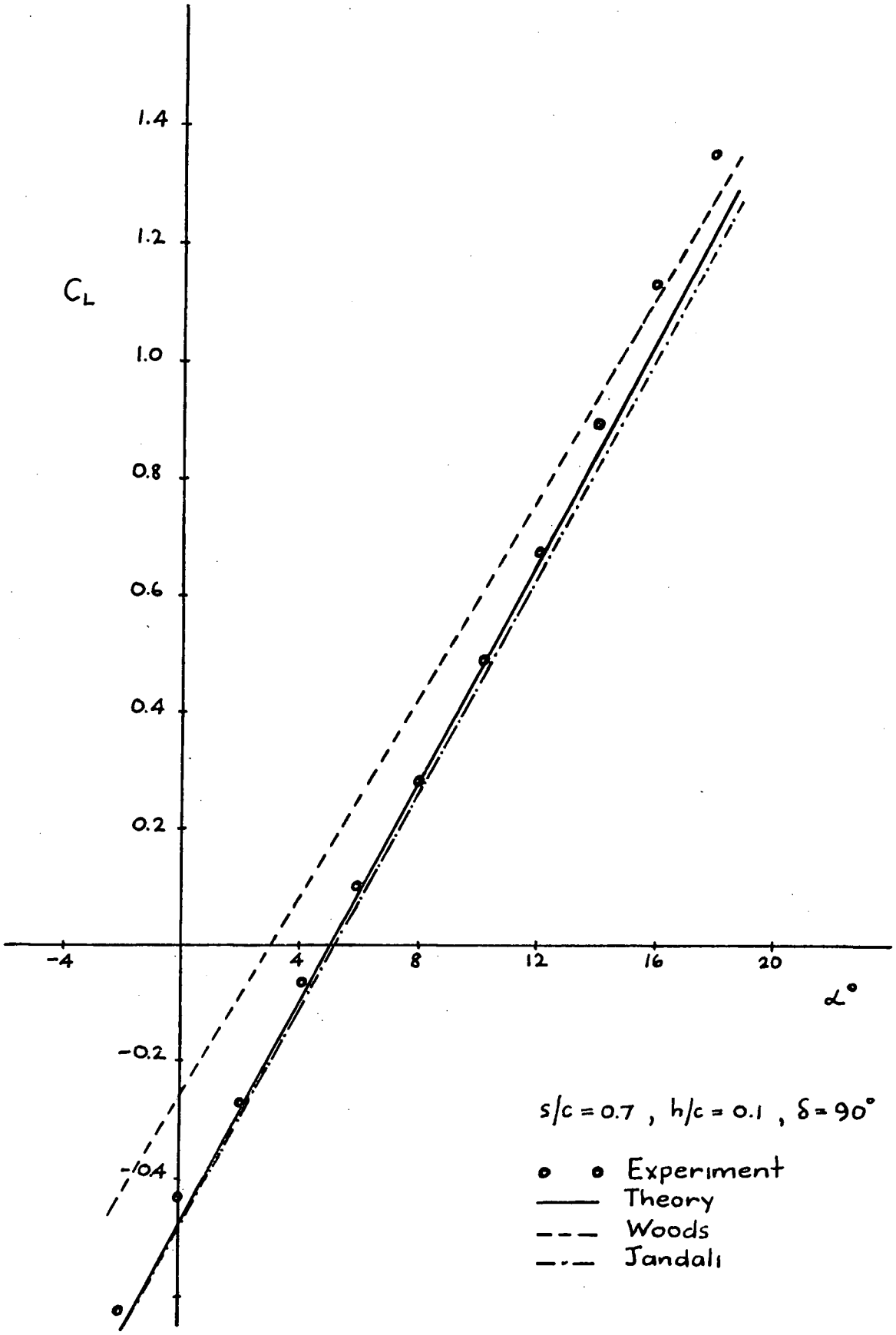

FIGURE (8): LIFT COEFFICIENT FOR CLARK Y AIRFOIL WITH SPOILER

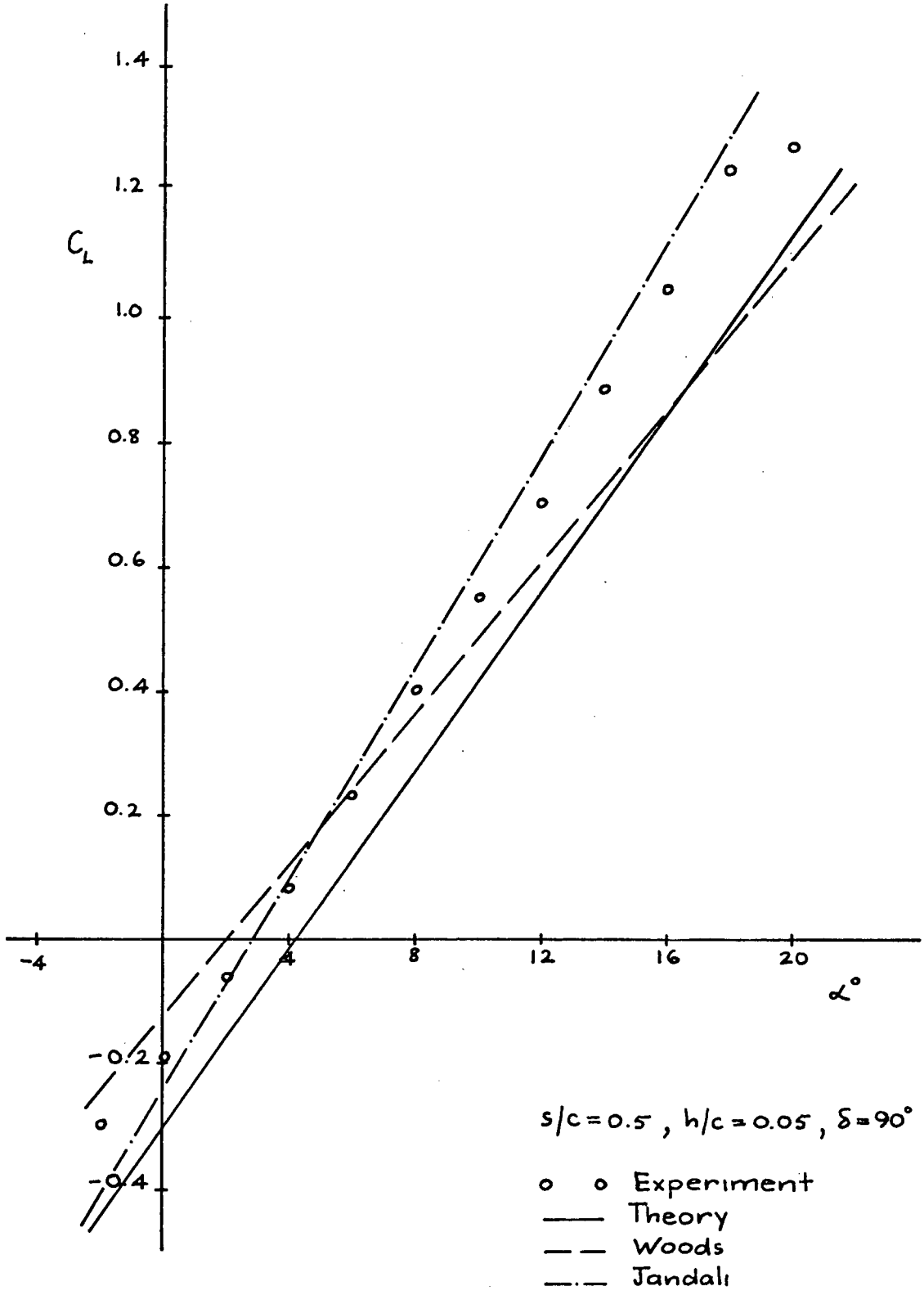

FIGURE (9): LIFT COEFFICIENT FOR CLARK Y AIRFOIL WITH SPOILER

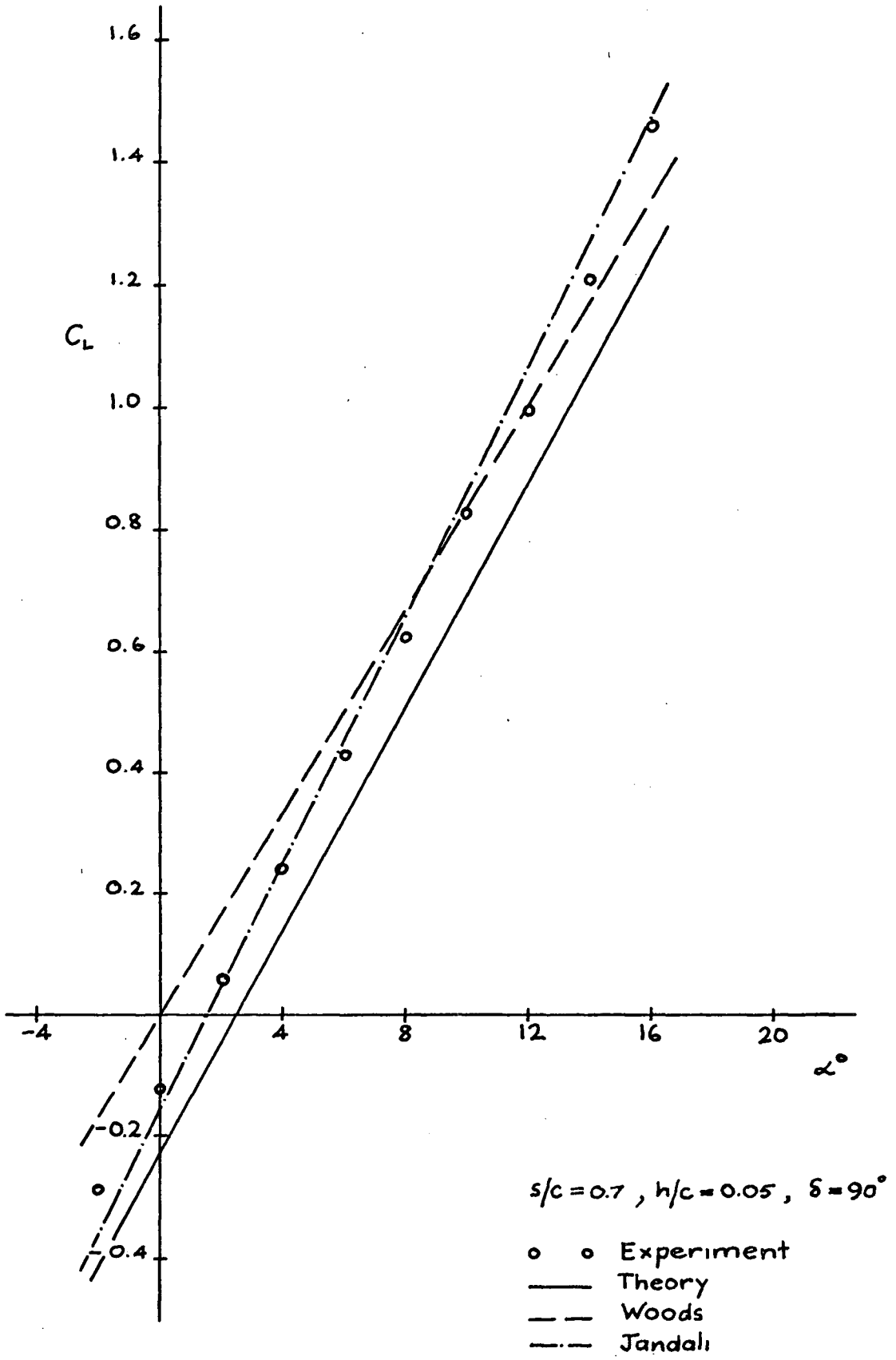

FIGURE (10): LIFT COEFFICIENT FOR CLARK Y AIRFOIL WITH SPOILER

from the trailing edge. The contribution of the camber solution decreases from a maximum as the spoiler moves forward. For the cases presented of 50 and 70% spoiler positions, the thickness contributions is the same order of magnitude as the camber contribution. In Woods' theory the thickness term is discarded as a second order term.

Comparisons between theoretical and experimental results will now be considered for spoiler angles other than 90 degrees. In figures (11) and (12) the comparisons are shown for a spoiler of angle 45 degrees positioned at the 50% chord point, the spoiler heights being 10% and 5% respectively. Figures (13) and (14) show a comparison of theoretical and experimental lift coefficients for spoilers located at the 70% chord point with a spoiler angle of 60 degrees and spoiler heights of 10% and 5% respectively. Figures (15) and (16) show the corresponding comparisons for a spoiler angle of 30 degrees.

These results will now be presented for a fixed airfoil incidence, the spoiler angle being the variable against which the lift coefficient is plotted. The spoiler is located at the 70% chord point. Figure (17) is a comparison in lift coefficients between theory and experiment at an airfoil incidence of 6 degrees, and a spoiler height of 10%. Figure (18) shows a corresponding comparison at an airfoil incidence of 6 degrees and a spoiler height of 5%. As expected the lift coefficient decreases as the spoiler angle increases. The agreement between theory and experiment is once again quite good. It should be recalled that this graph of lift coefficient verses spoiler angle cannot be extrapolated back to zero spoiler angle, since the theory is only applicable as long as the cavity exists, and in such a case the cavity physically could not exist.

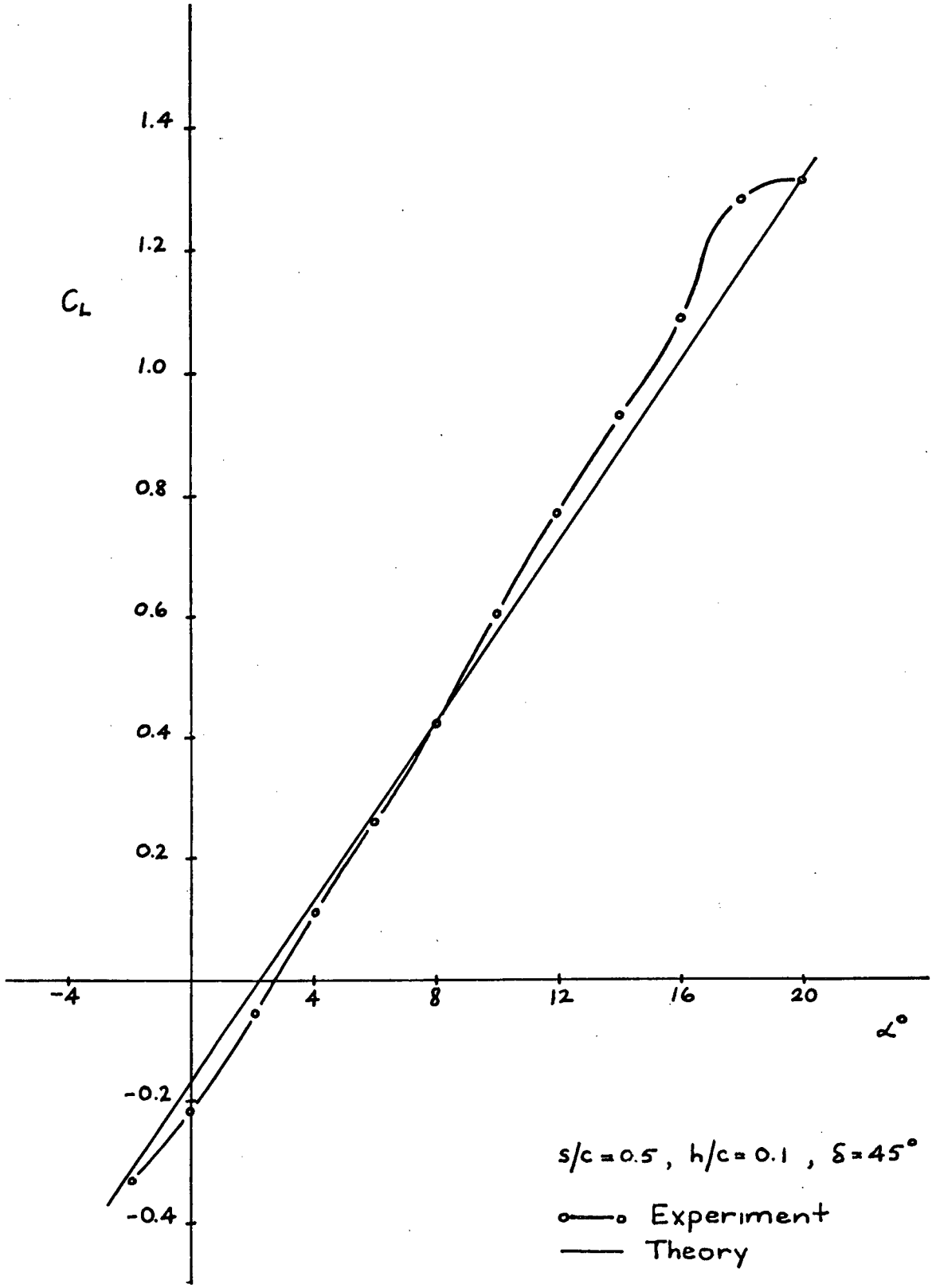

FIGURE (11): LIFT COEFFICIENT FOR CLARK Y AIRFOIL WITH SPOILER

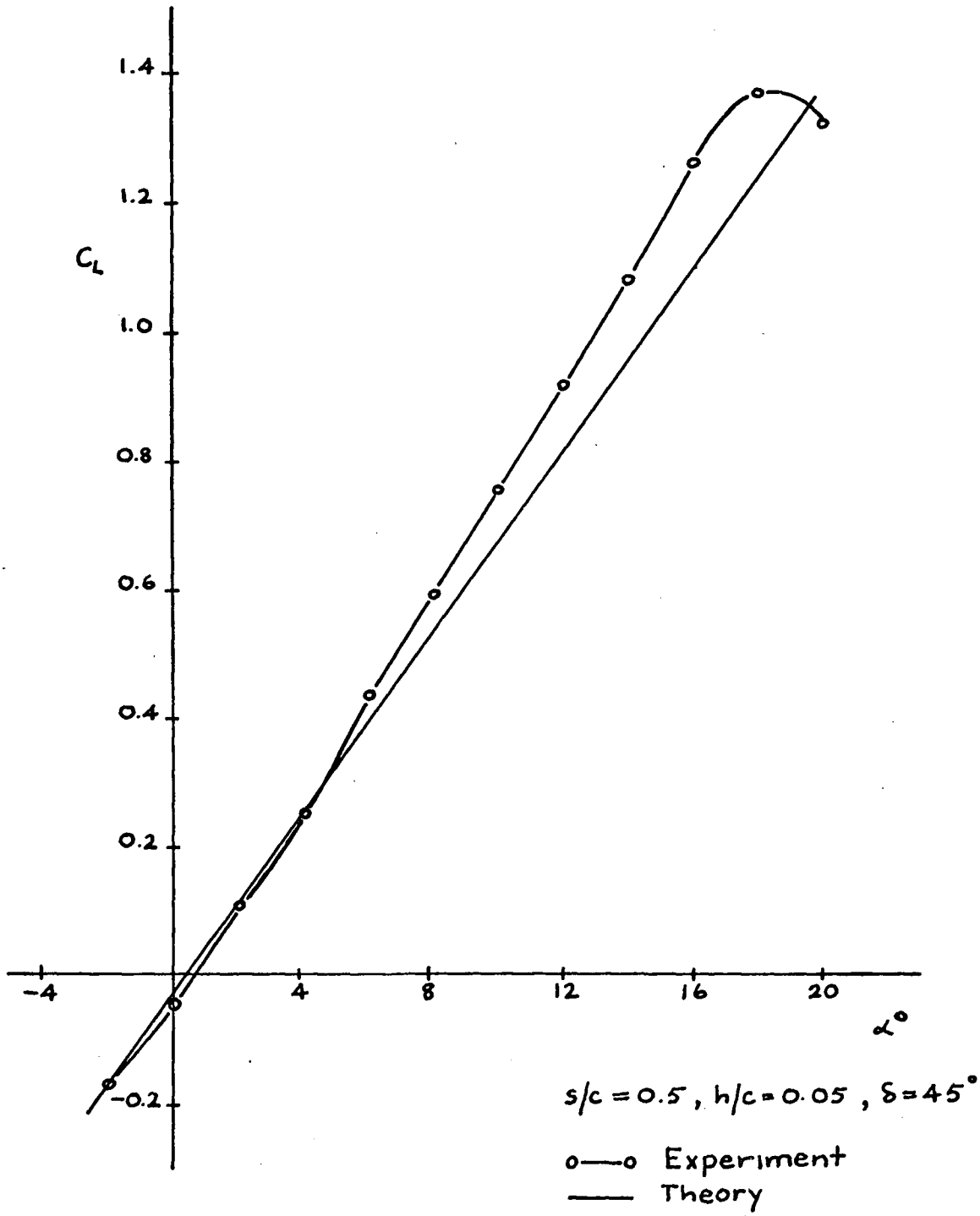

FIGURE (12): LIFT COEFFICIENT FOR CLARK Y AIRFOIL WITH SPOILER

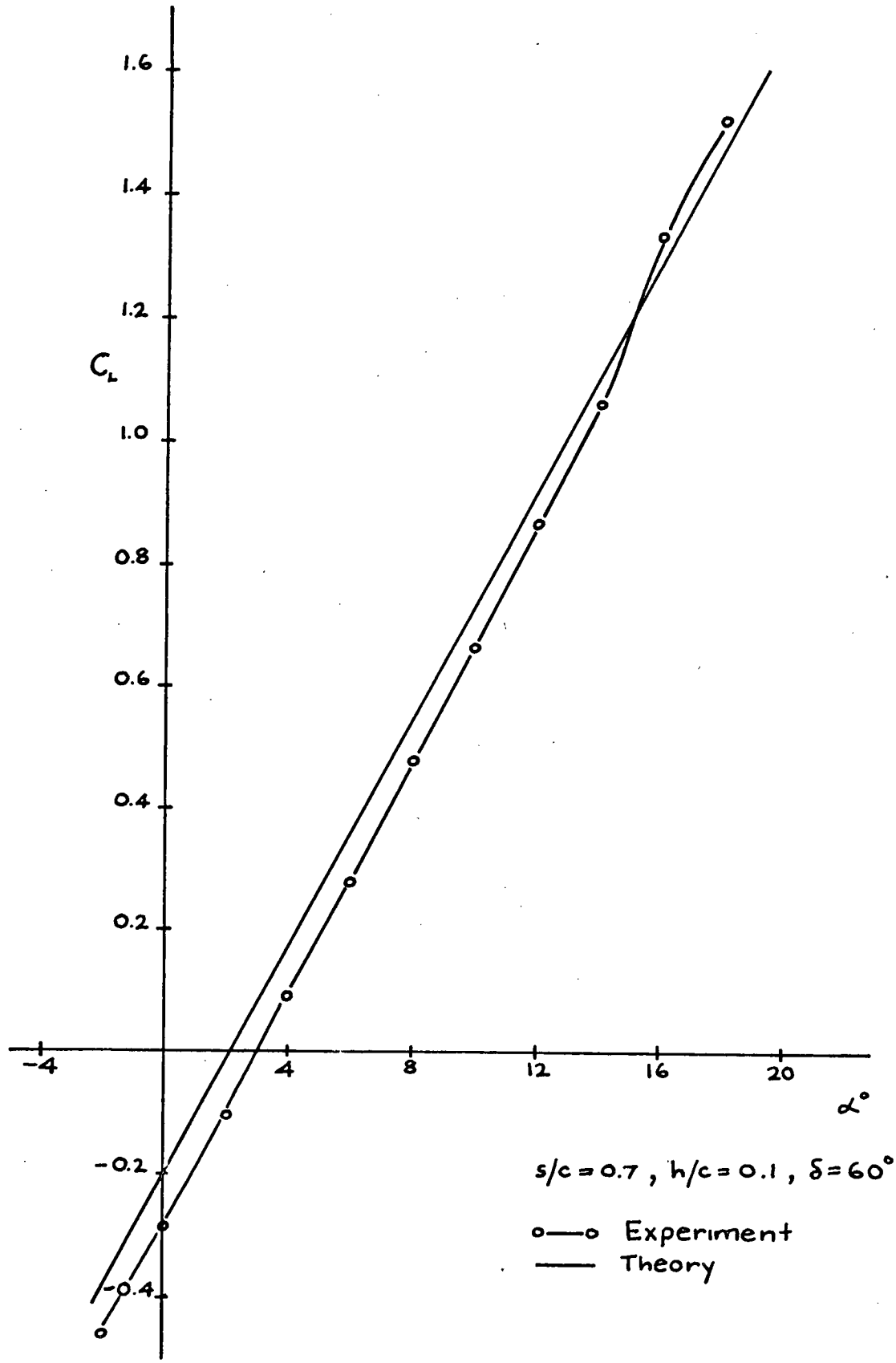

FIGURE (13): LIFT COEFFICIENT FOR CLARK Y AIRFOIL WITH SPOILER

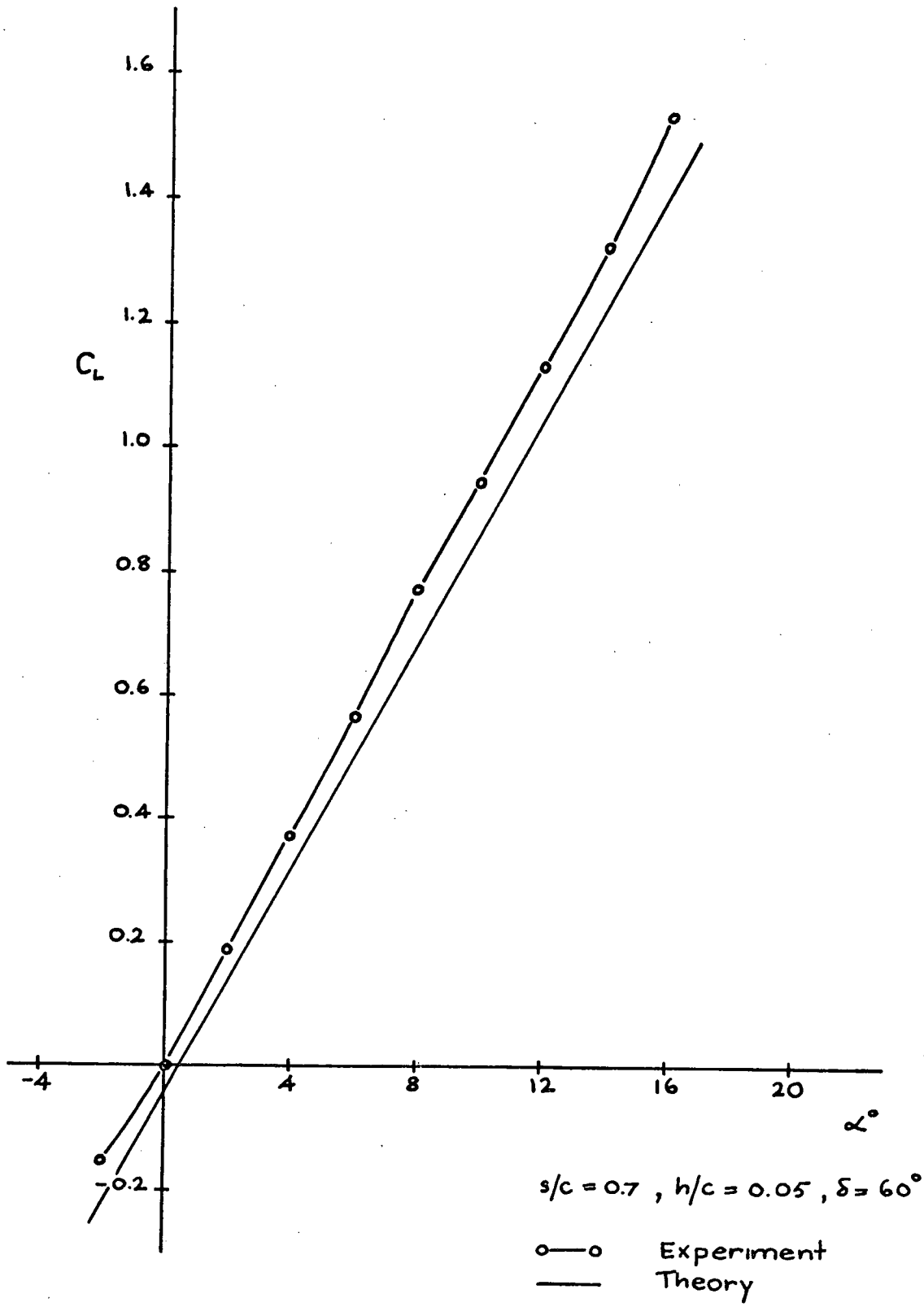

FIGURE (14): LIFT COEFFICIENT FOR CLARK Y AIRFOIL WITH SPOILER

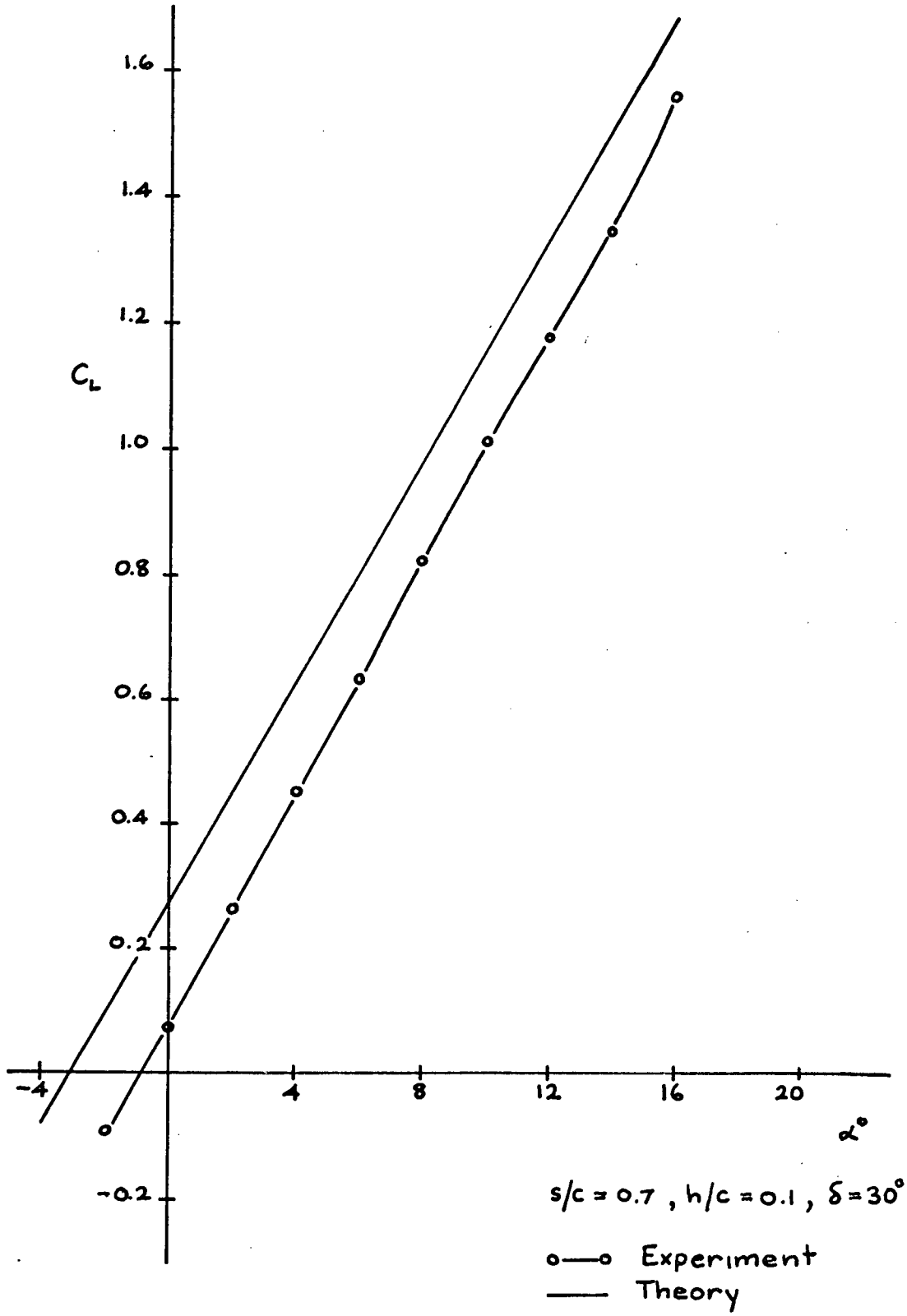

FIGURE (15): LIFT COEFFICIENT FOR CLARK Y AIRFOIL WITH SPOILER

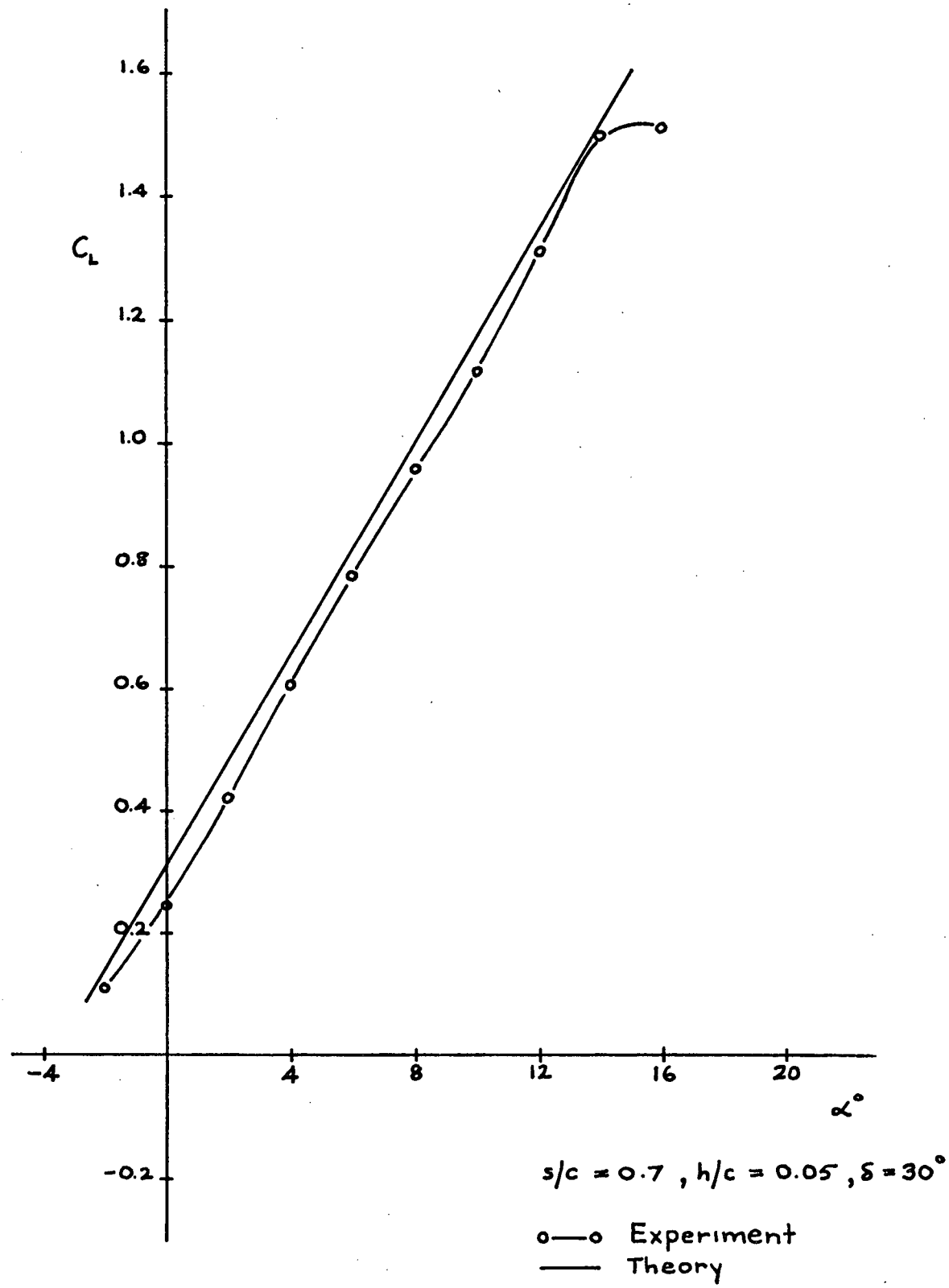

FIGURE (16): LIFT COEFFICIENT FOR CLARK Y AIRFOIL WITH SPOILER

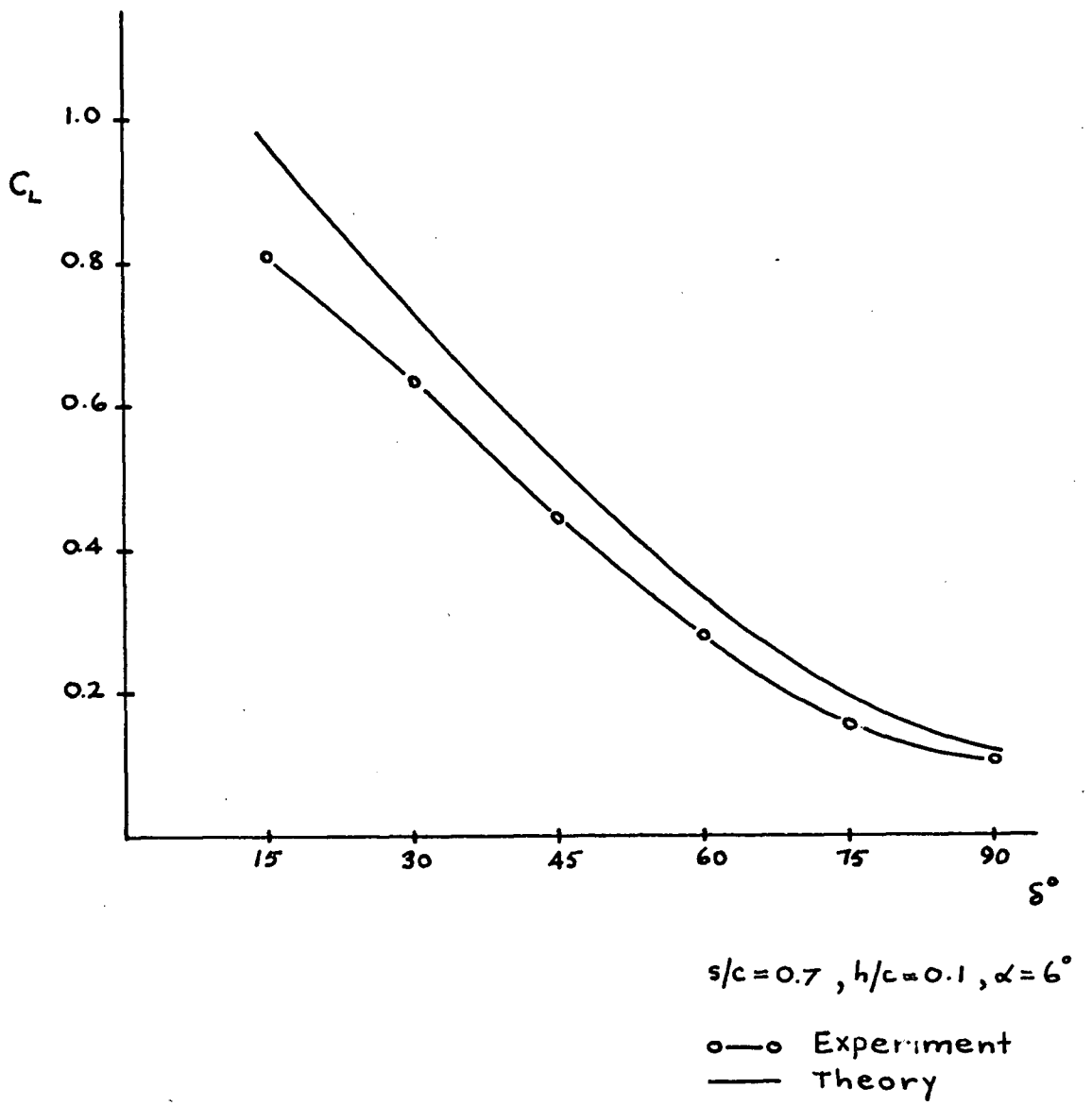

FIGURE (17): LIFT COEFFICIENT FOR CLARK Y AIRFOIL WITH SPOILER

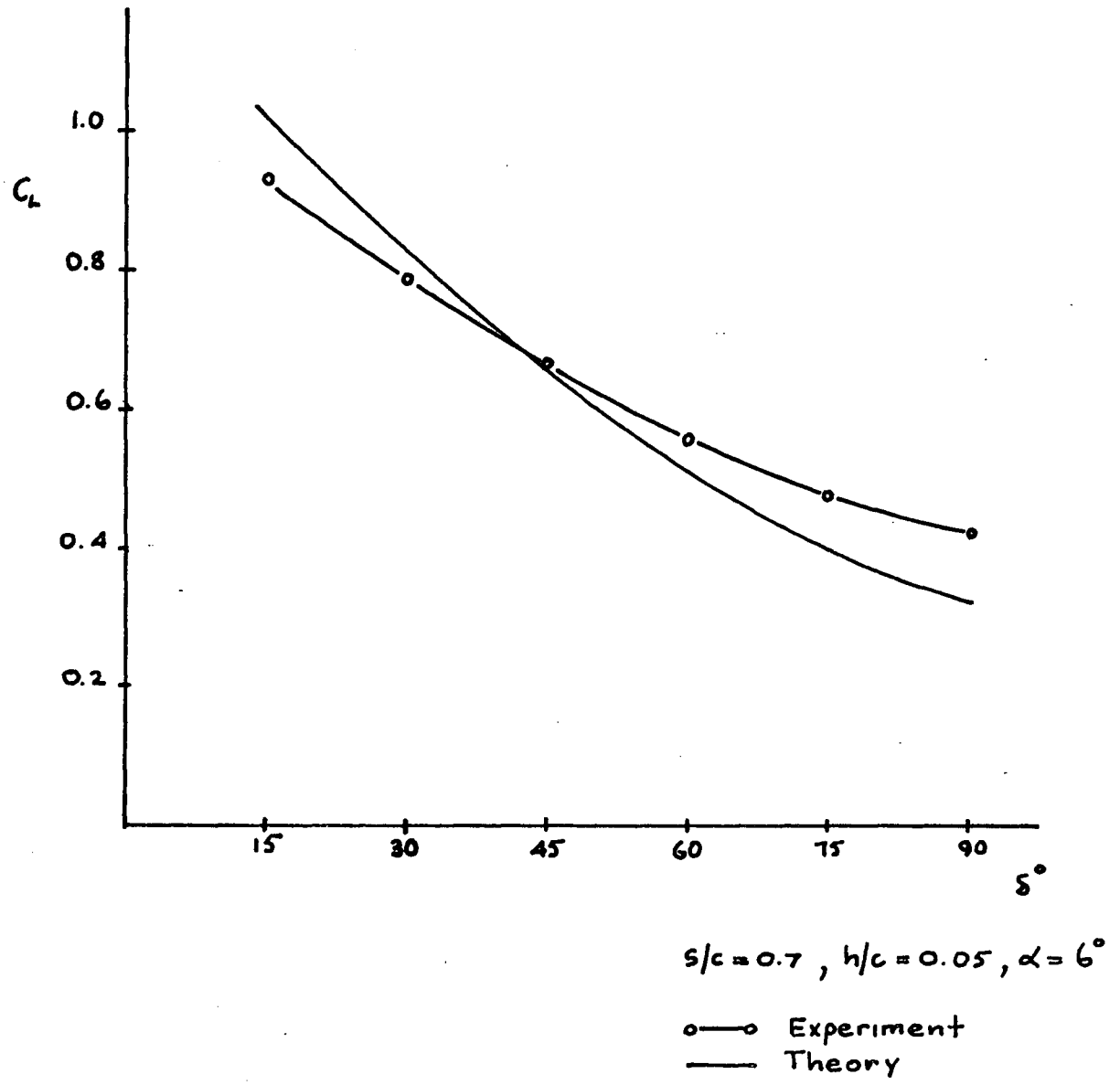

FIGURE (18): LIFT COEFFICIENT FOR CLARK Y AIRFOIL WITH SPOILER

Comparisons for the airfoil with spoiler and flap between the theoretical and experimental lift coefficients for a 10% normal spoiler at the 70% chord point will now be given for different flap angles. Figure (19) shows the comparison for a flap angle of 15 degrees, and figure (20) is a comparison for a flap angle of 30 degrees. This result is consistent with simple linear flap theory, the theory over predicting the lift as the flap angle gets large.

To complete the results presented for the steady state solution, some examples of the theoretical pressure coefficient distribution for normal spoilers will be given. Figure (21) shows the theoretical pressure coefficient distribution for a 10% spoiler located at the 70% chord position with an airfoil incidence of 12 degrees. The theoretical pressure coefficient distribution for a 5% spoiler located at the 50% chord point for an airfoil incidence of 10 degrees, is given in figure (22). For comparison the results given by Jandali (1) are shown on these graphs for the same airfoil configurations. The singularities in the pressure distributions are inherent in linearized techniques, and the distributions give basically qualitative information.

6.2 Nonsteady Theory

In the consideration of the nonsteady solutions it will be recalled that the solution is independent of the spoiler angle and that the cavity must already exist. This fact means that the thickness, camber, incidence, and flap solutions are not going to change during further spoiler actuation and their steady state solutions are fully additive to the nonsteady spoiler solution. It is proposed therefore to present only the results to the nonsteady spoiler solution.

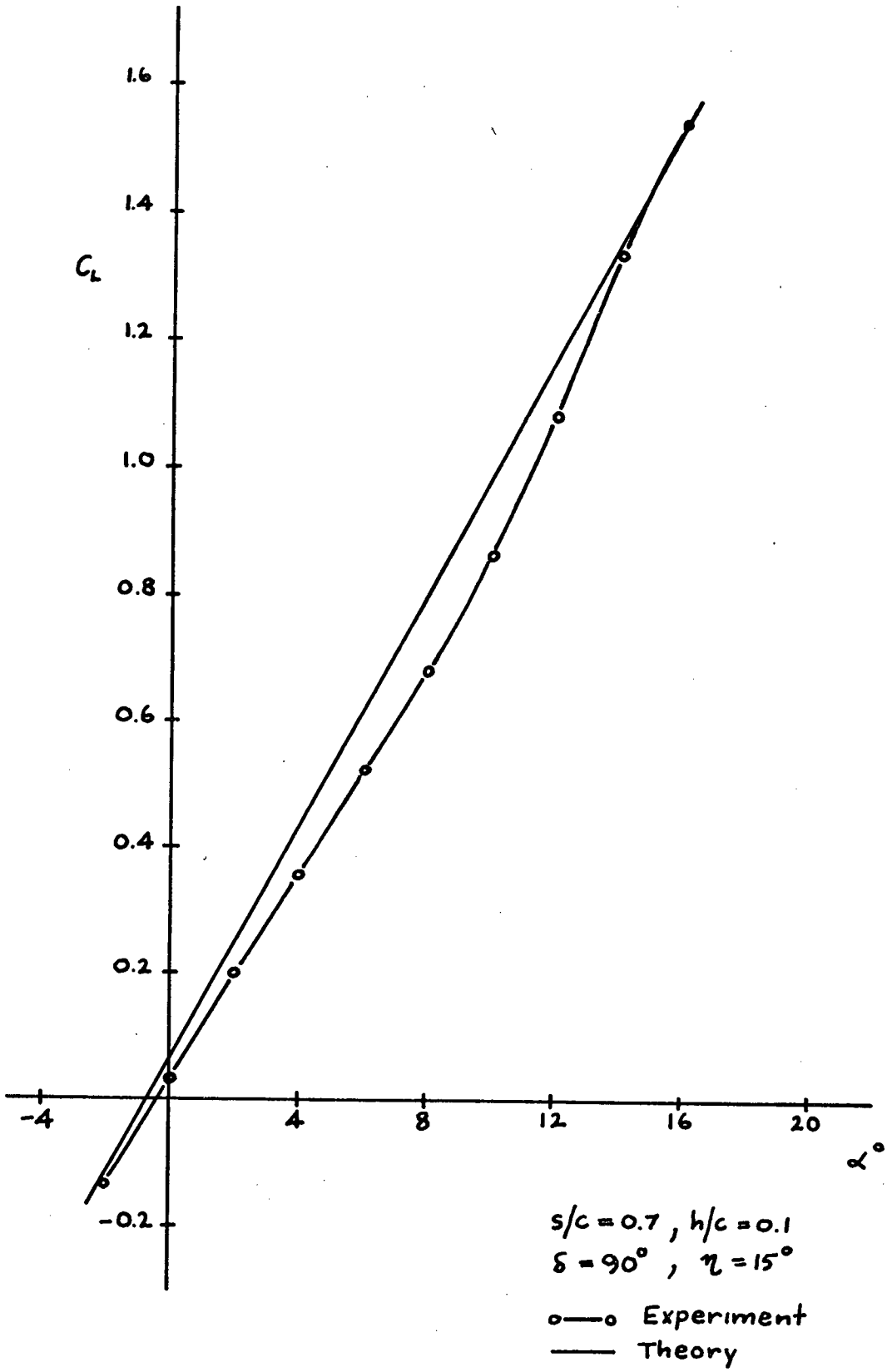

FIGURE (19): LIFT COEFFICIENT FOR CLARK Y AIRFOIL WITH SPOILER AND FLAP

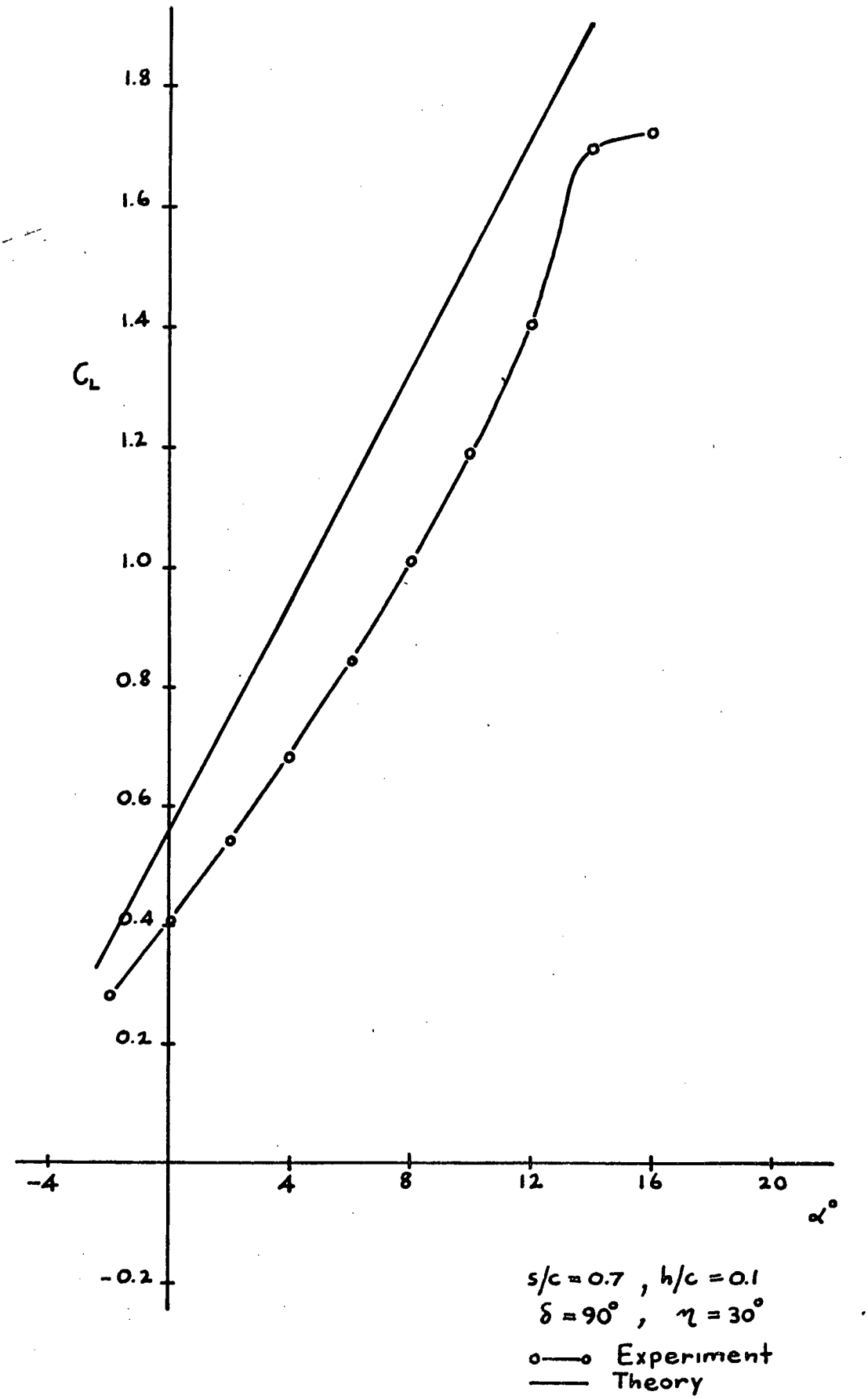

FIGURE (20): LIFT COEFFICIENT FOR CLARK Y AIRFOIL WITH SPOILER AND FLAP

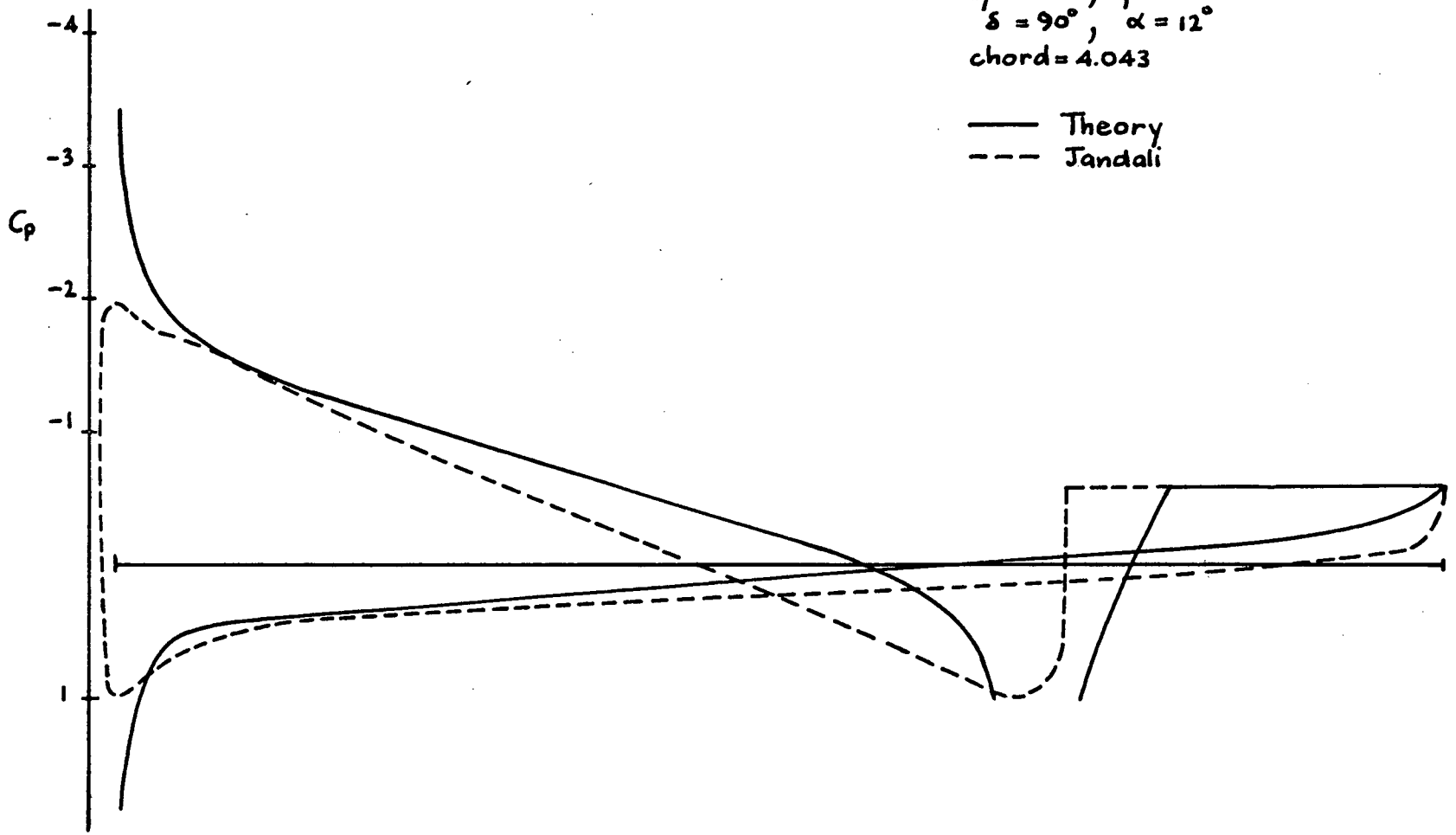

FIGURE (21): PRESSURE DISTRIBUTION FOR CLARK Y AIRFOIL WITH SPOILER

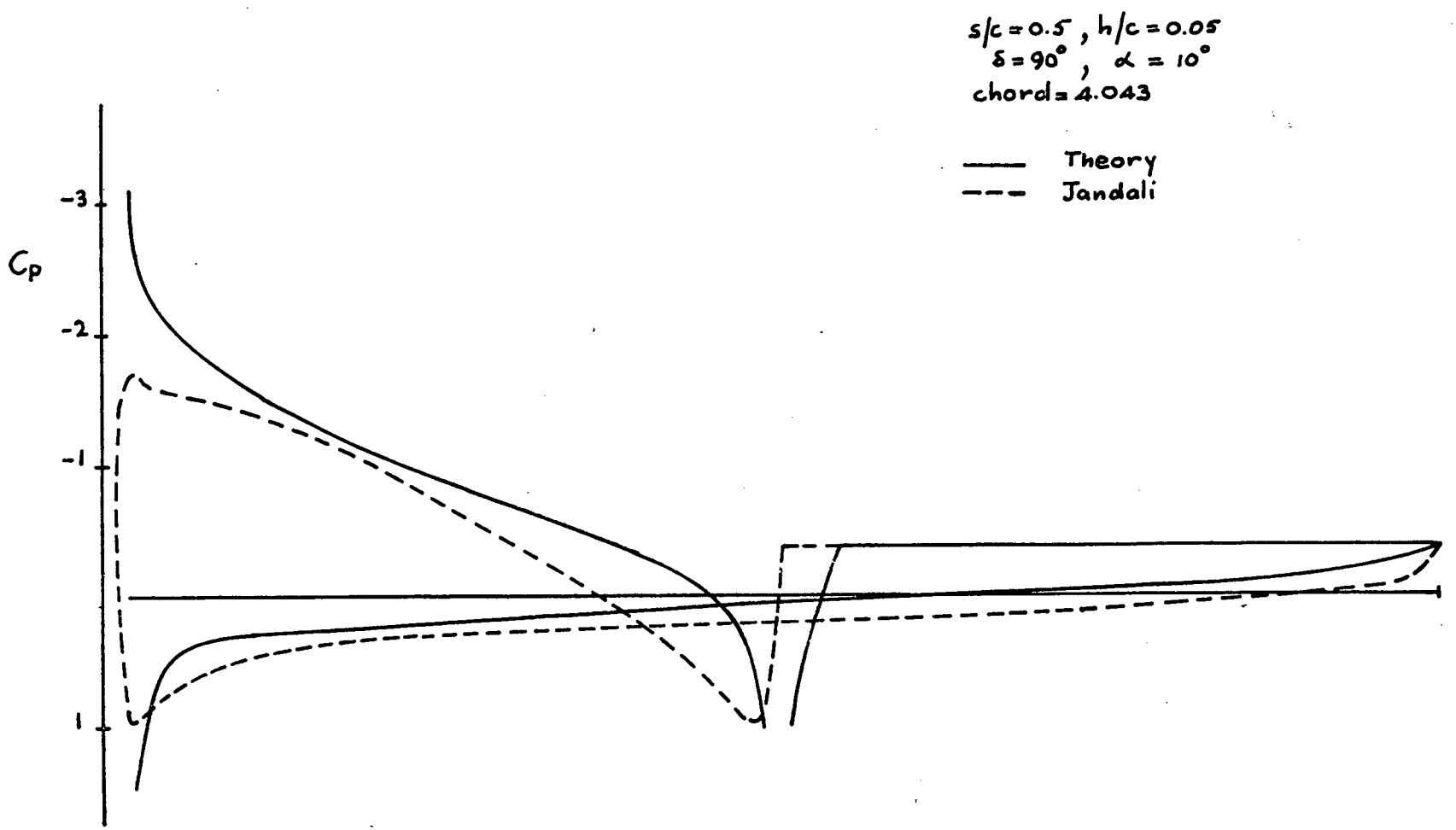

FIGURE (22): PRESSURE DISTRIBUTION FOR CLARK Y AIRFOIL WITH SPOILER

Although they are of little physical importance and are primarily an intermediate result, some blowing case solutions will be presented. It will be recalled from equation (42) that the ratio of lift coefficient to quasi-steady lift coefficient was expressed as a function of μ, the frequency of blowing. Figure (23) gives this ratio for a spoiler region length of 10% positioned at the 70% chord point. Figure (24) gives this ratio for a spoiler region length of 5% positioned at the 50% chord point. It can be seen that these plots asymptotically approach the imaginary axis, the real part of the lift coefficient approaching zero. It may be reasonable to argue physically that the blowing and sucking cycles occur so quickly as the frequency gets large, that the net affect approaches zero.

The unit step spoiler actuation problem will be considered next. The results for the spoiler actuation problems are reported as the ratio of the instantaneous lift coefficient over the final steady state lift coefficient, as a function of the distance moved in chords. Since the spoiler actuation problems are independent of spoiler angle, the solution becomes a function of spoiler position and height only. Figure (25) is the solution for a 10% and a 5% spoiler at the 70% chord point.

The use of linearized theory allowed the superposition of the unit step solutions into the finite time spoiler actuation problem. This again makes the solution independent of spoiler angle. These results are also reported as the ratio of the instantaneous lift coefficient to the final steady state lift coefficient as a function of distance moved in chords. The unit step spoiler actuation solution is included with the finite time solutions for purposes of comparison. Theoretical results are given for actuation distances of 5, 10 and 15 chords. In figures (26) and (27) the theoretical solutions

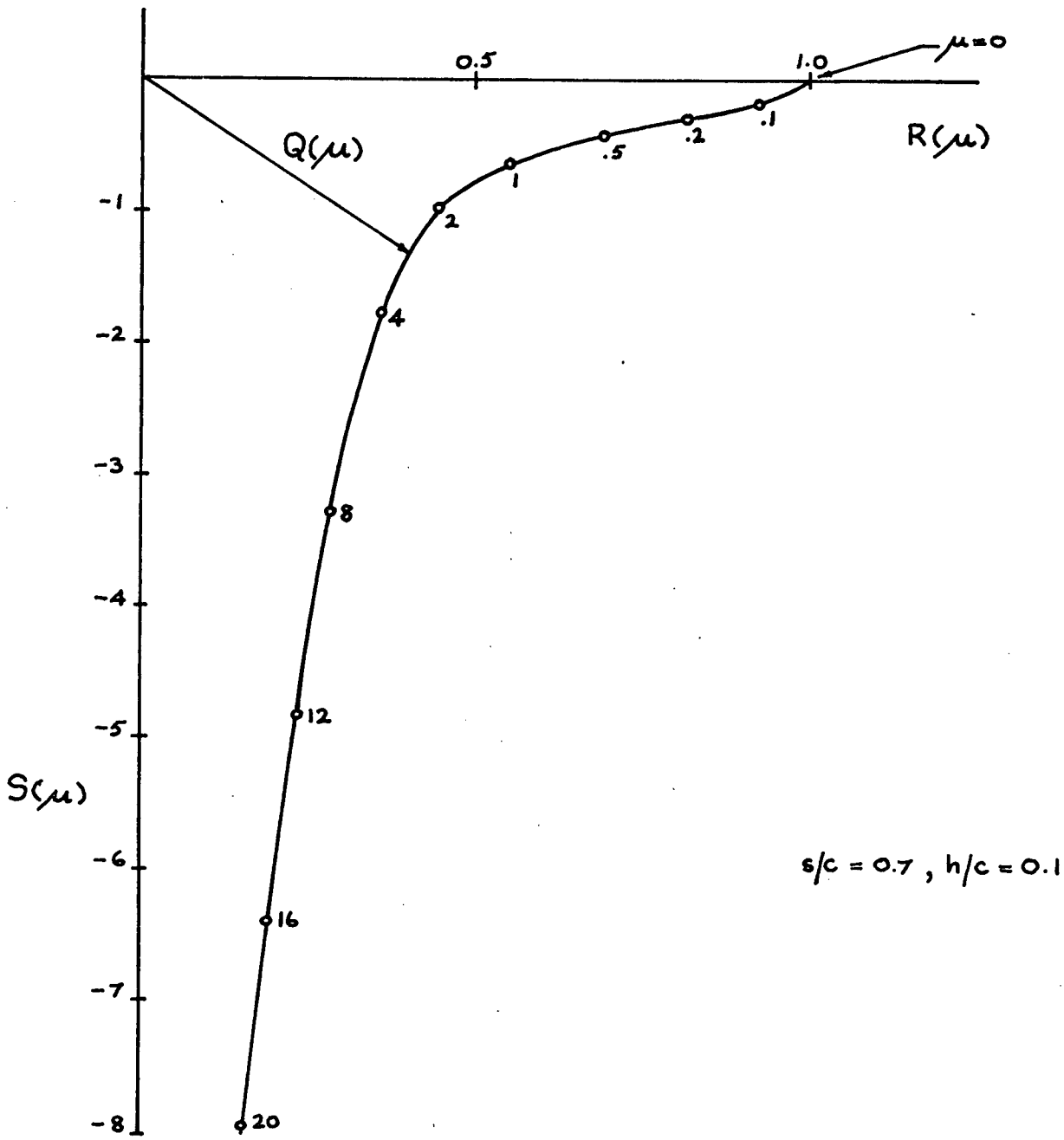

FIGURE (23): BLOWING THEORY SOLUTION

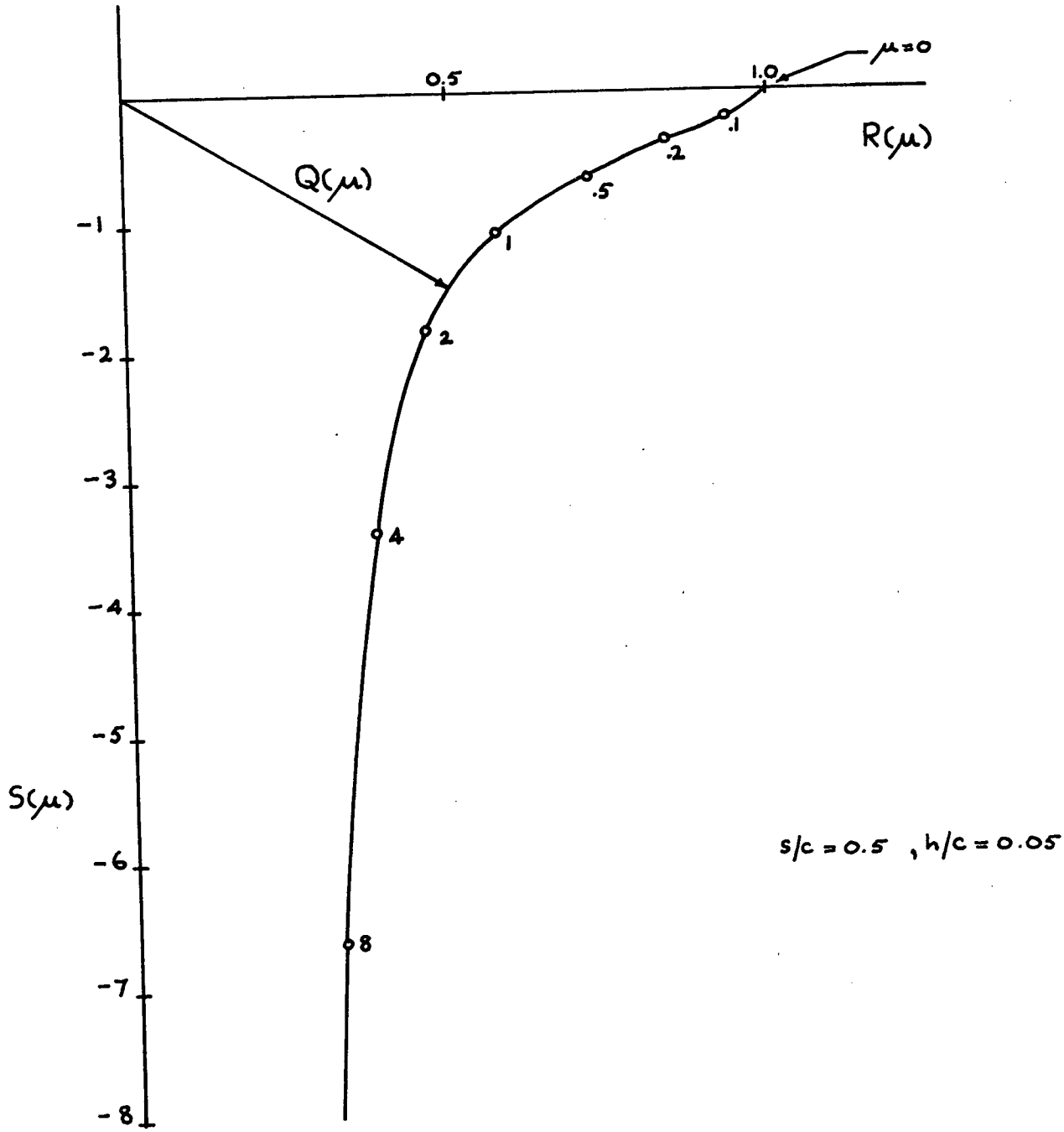

FIGURE (24): BLOWING THEORY SOLUTION

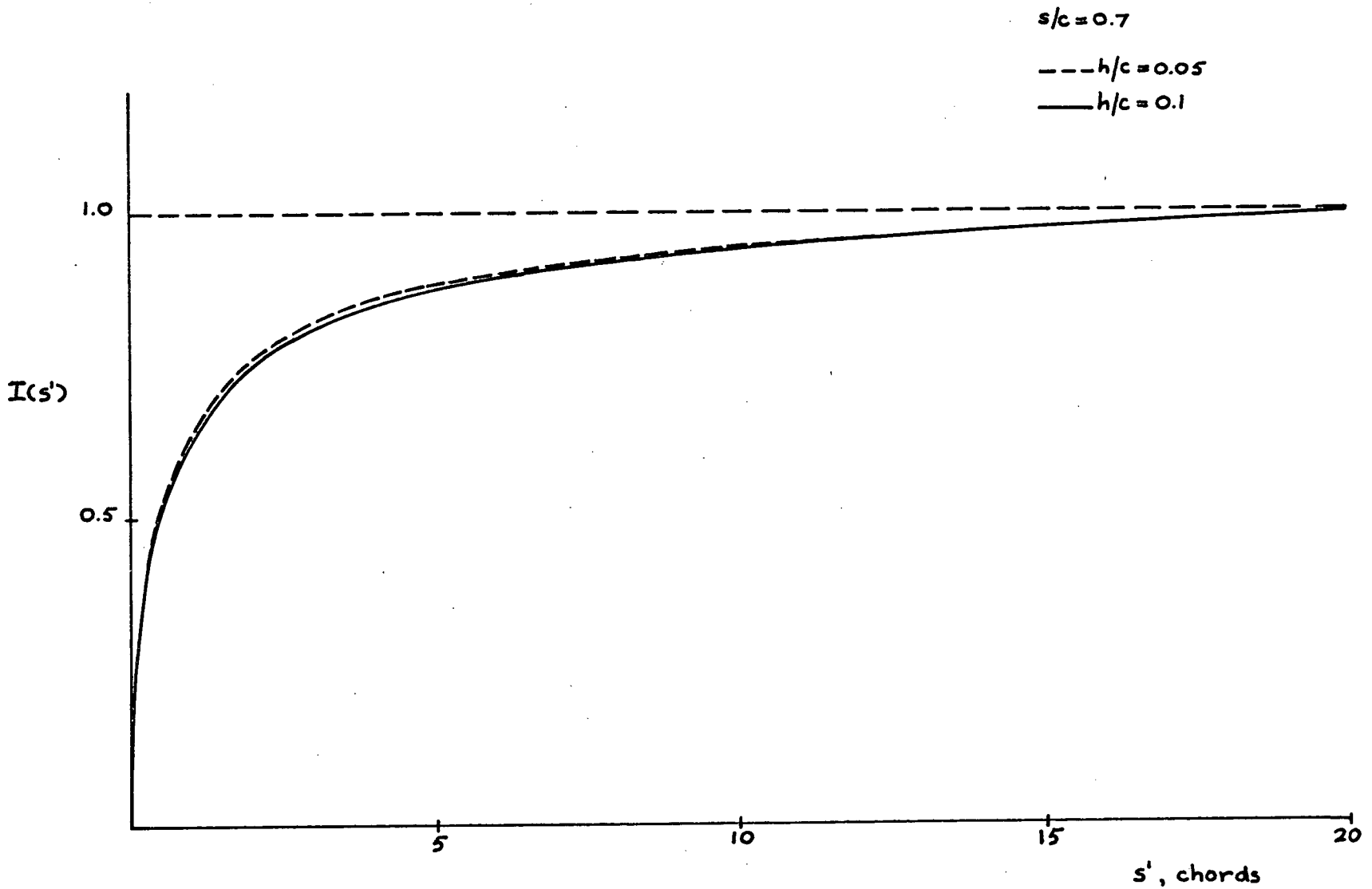

FIGURE (25): UNIT STEP SPOILER ACTUATION SOLUTION

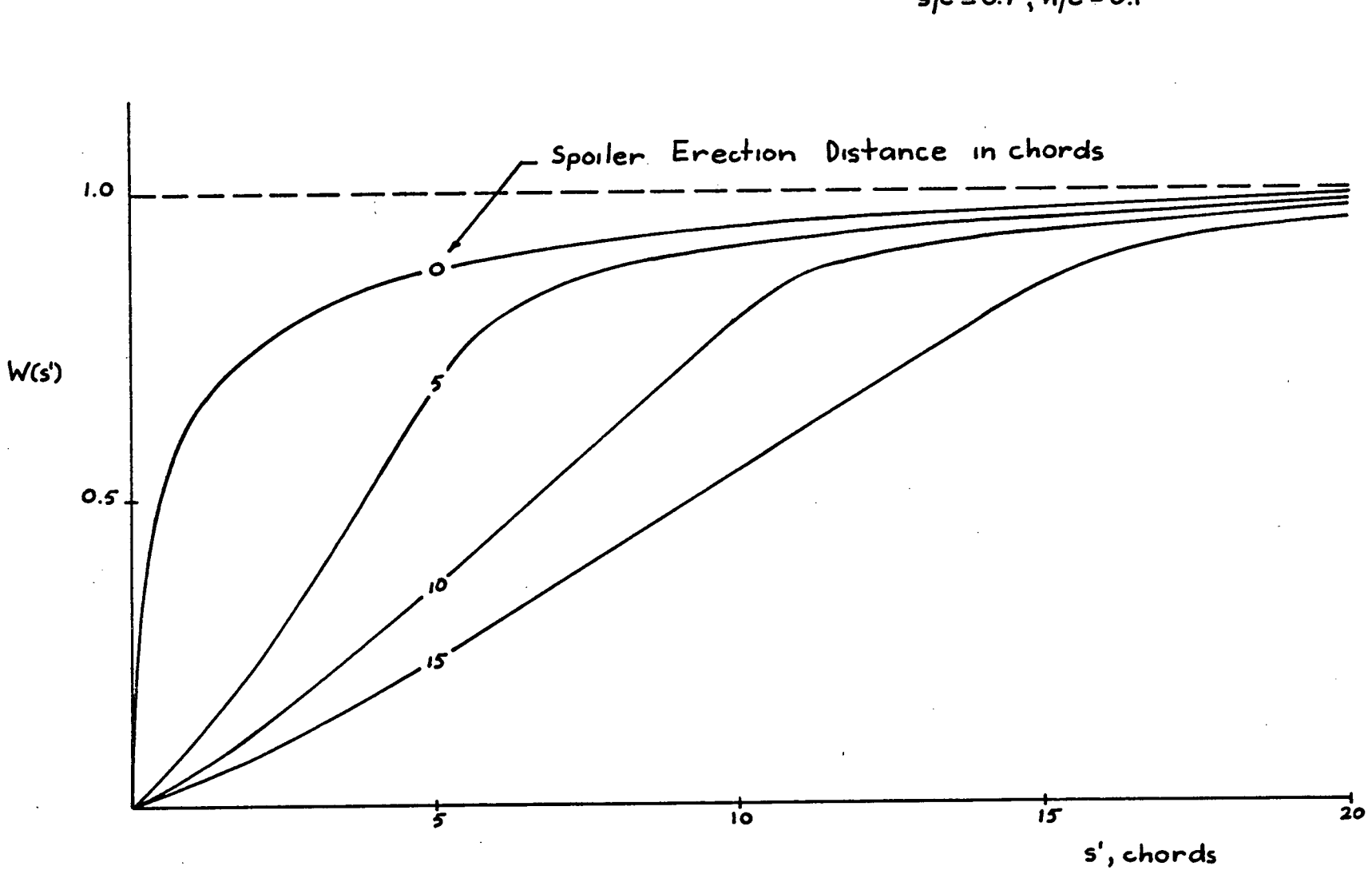

FIGURE (26): UNIT STEP AND FINITE TIME SPOILER ACTUATION SOLUTIONS

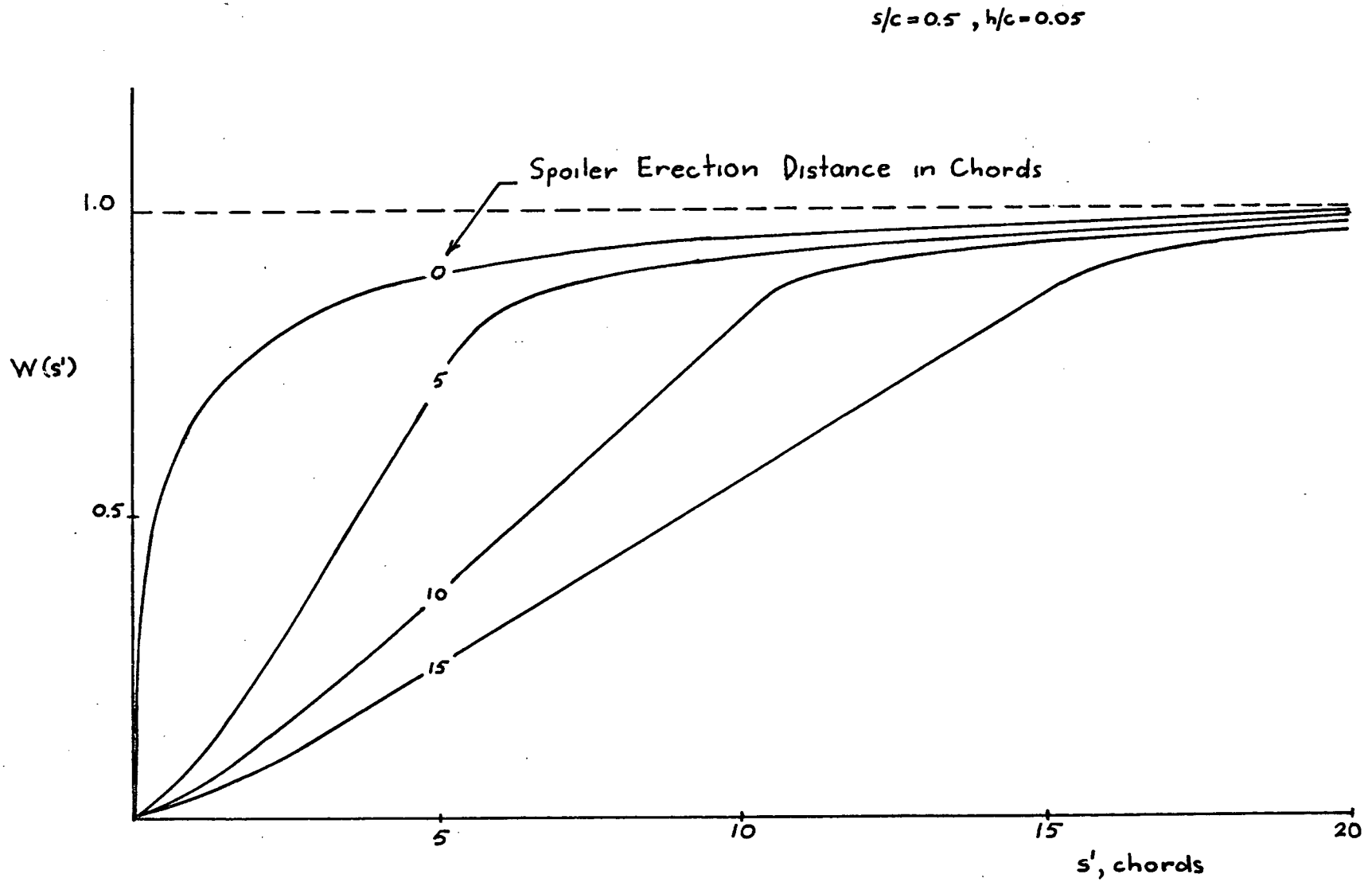

FIGURE (27): UNIT STEP AND FINITE TIME SPOILER ACTUATION SOLUTIONS

are given for 10% spoiler at the 70% chord point and a 5% spoiler at the 50% chord point. In figure (28) the distance travelled for the lift coefficient to fall to 90% of its final steady state value is plotted against spoiler position for both 5% and 10% spoilers with varying erection distances.

Figure (29) shows the distance travelled for the lift coefficient to fall to 90% of its steady state value as a function of erection distance for both 5% and 10% spoilers at various spoiler positions. As the spoiler erection time increases the nonsteady solution asymptotically approaches the quasi-steady solution. For very slow spoiler actuation rates only the quasi-steady solution is necessary. However for faster rates of actuation a full nonsteady analysis is necessary.

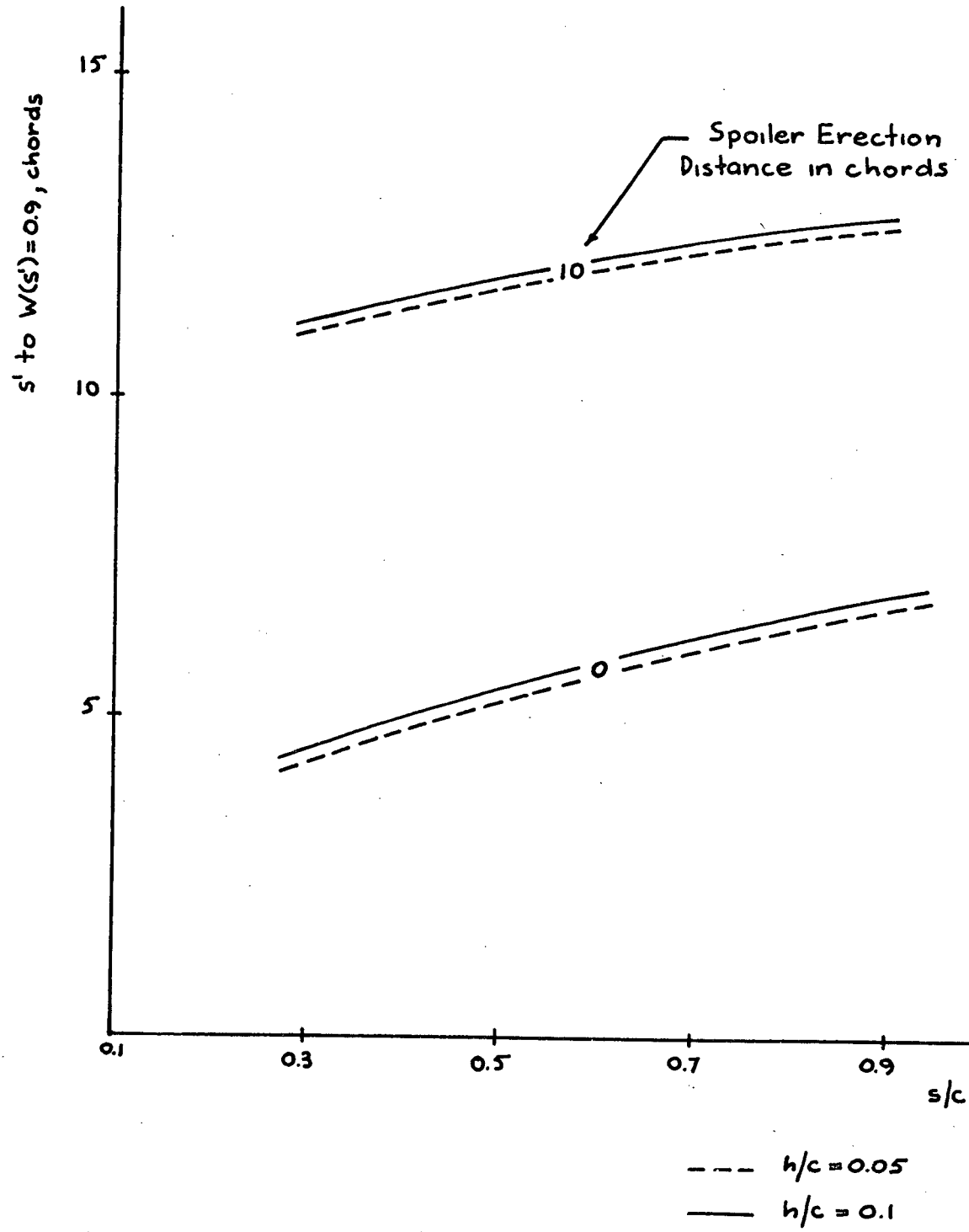

FIGURE (28): UNIT STEP AND FINITE TIME SPOILER ACTUATION SOLUTIONS

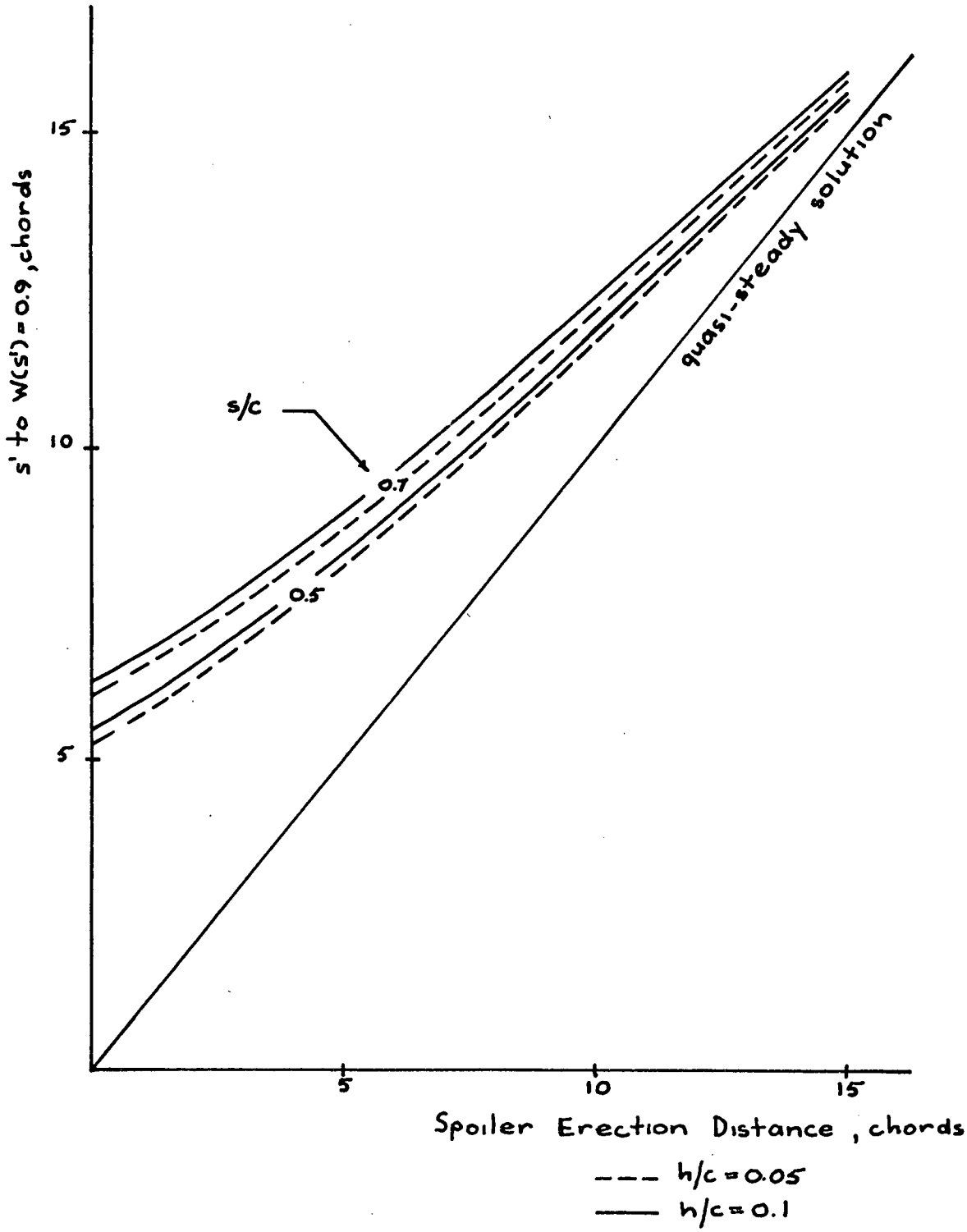

FIGURE (29): UNIT STEP AND FINITE TIME SPOILER ACTUATION SOLUTIONS

PART II

AN EXACT FREE STREAMLINE POTENTIAL FLOW THEORY FOR THE STEADY STATE AIRFOIL SPOILER AND SPOILER PLUS SLOTTED FLAP PROBLEMS

SECTION 7

SOLID AIRFOIL WITH A SPOILER

7.1 Surface Singularity Theory

The surface singularity technique employed in the following problems was developed recently by A.M.O. Smith and his associates at the McDonnell-Douglas Aircraft Company. Several comprehensive publications (6,7) of this theory exist, and therefore it will not be repeated. Although Smith's theory is applicable to two and three dimensional flows, this analysis is limited to a two dimensional, incompressible, inviscid and irrotational flow field.

7.2 Formulation of the Problem

The airfoil without a flap is positioned in the z-plane as described in section (3.2). This configuration is shown pictorially in figure (30). In this problem there is a wake extending to infinity. The wake is bounded by free streamlines,one springing from the spoiler tip and one from the trailing edge. Experimentally the base pressure on the airfoil in this wake region takes a constant value. Since no satisfactory theory for predicting the base pressure correctly has been devised, all such theories require at least one empirical parameter. There is no advantage in correctly modelling the constant value of this base pressure over the wake region. If the theory correctly predicts the separation pressure coefficients on the free streamlines detaching from the spoiler tip and the trailing edge, the pressure on the airfoil between the streamlines inside the wake can be assumed constant, and equal to the separation pressure, regardless of what type of flow is in this region. This approach was used effectively by Jandali (1) and Parkinson (11). Their method of using sources on the body in the wake region to create the wake

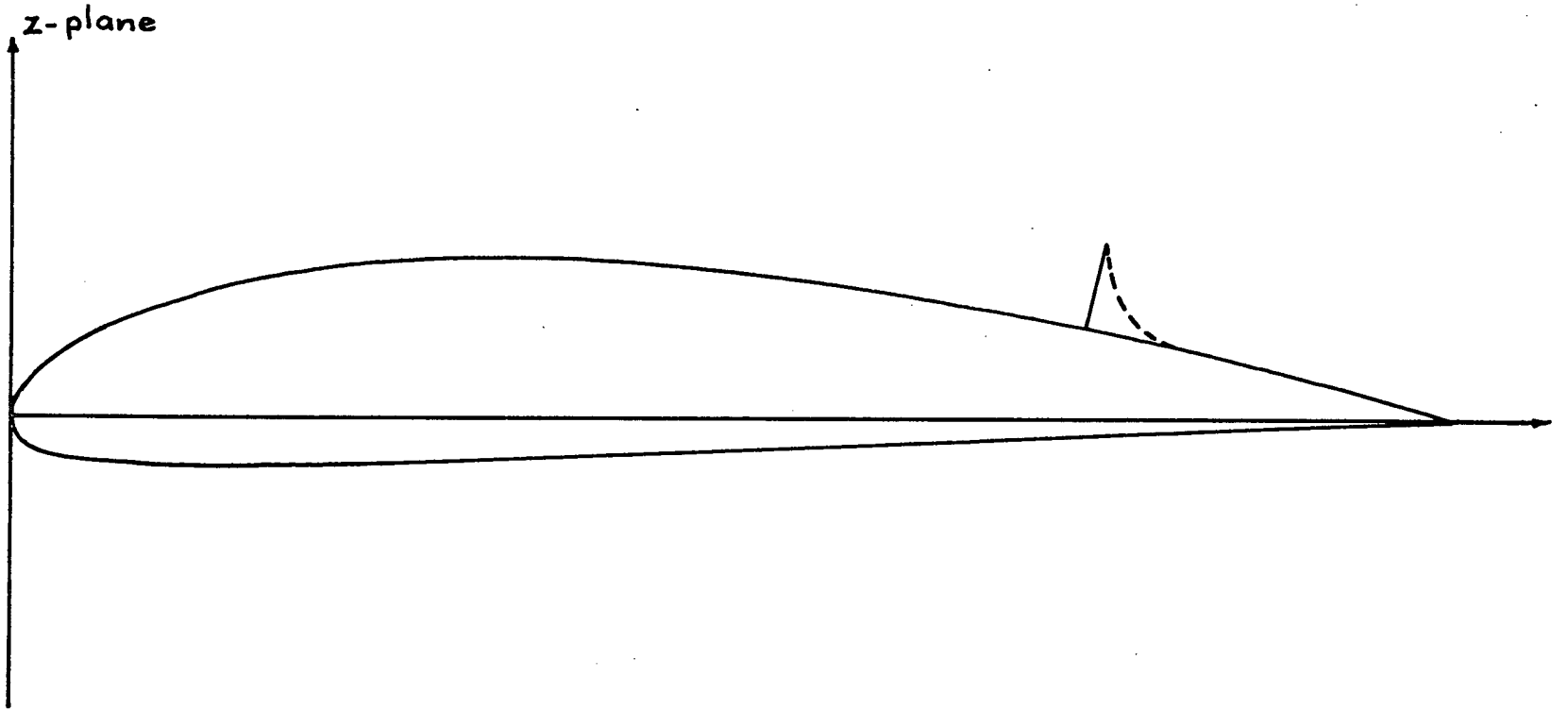

FIGURE (30): AIRFOIL IN THE Z-PLANE

is also pursued here. Jandali considers both 1 and 2-source models for a solid airfoil with a normal spoiler. The current theory is not limited to a normal spoiler. Use of the 2-source model allows the pressure to be stipulated on both separating free streamlines. The 1-source model allows the pressure to be stipulated on only one of the separating free streamlines. The other value floats freely, but was shown by Jandali to be finite. The iterative method of positioning the source in the numerical technique employed in the current theory makes it extremely difficult to consider the 2-source problem. In the 2-source model there are five unknowns; the two source strengths, two source positions and one unknown circulation. There are however only four conditions; the two Kutta conditions, and the stipulation of the base pressure at the spoiler tip and at the trailing edge of the airfoil. This problem will be discussed further when the 2-source model is treated in detail.

7.3 Boundary Conditions

The boundary conditions for the 1-source problem, itemized in detail, are as follows:

(i) Kutta condition at the trailing edge and spoiler tip.

(ii) Pressure stipulated on the separation free streamline at the spoiler tip.

(iii) Surface normal velocity condition of no flow through the surface.

Although Smith's theory is an exact analytical theory, numerical approximations are necessary in obtaining a solution. The airfoil is divided into straight line elements the centres of which are the control points. The Kutta condition at the trailing edge is then satisfied by matching the tangential velocity at the last control point

on the upper surface to the tangential velocity at the last control point on the lower surface. This matching technique applies identically in satisfying the Kutta condition at the spoiler tip. It must be realized that these conditions are not applied right at the separation point, but at the last control points before the separation point. This is inherent in the method and cannot be avoided. Hence in satisfying condition (ii), the pressure is actually stipulated at the last control point before the spoiler tip. There are then three conditions to be satisfied by three unknowns. The unknowns are; the source position, the source strength and the circulation about the airfoil. Condition (iii) also can only be satisfied at the control points and this is done in the usual way of putting a distribution of sources over the elements. For the 2-source model conditions (i) and (iii) remain unchanged and condition (ii) becomes:

(ii) Pressure stipulated on the separation free streamline at the spoiler tip and at the trailing edge.

7.4 1-Source Model

First the method of solving this problem for the 1-source model will be described. Suppose that a source is positioned somewhere on the airfoil between the spoiler and the trailing edge. The solution can then be determined directly by satisfying the Kutta condition at the spoiler tip of the airfoil, and by stipulating the pressure on the last element before the spoiler tip. The trailing edge is then observed to see if the Kutta condition there is satisfied. If it is not satisfied the source can be moved along the surface of the airfoil, and the solution determined again. This procedure is repeated until it is observed that the Kutta condition is satisfied at the trailing edge. When this occurs the correct solution has been determined.

In order to effect a solution a large circular fillet is placed behind the airfoil spoiler. This is necessary since the spoiler otherwise is infinitely thin and not adaptable to Smith's method. Such a modification to the airfoil and spoiler in the wake region has no effect on the problem solution. Modification to the airfoil surface in this region was also employed by Jandali. In positioning the source onset flow care must be taken to ensure that as the source moves along the surface, it passes smoothly through the control points.

It now remains to adopt the above arguments into a mathematical formulation of the problem. In this configuration there are three onset flows to the airfoil, namely the free stream, the concentrated source flow and the circulatory flow. Following Smith's technique the circulatory flow is created by distributing vorticity over the elements of the airfoil. Suppose A_{ij}, an element of matrix A, is the normal velocity at control point i due to a unit source distribution over element j, and B_{ij}, an element of matrix B, is the tangential velocity. Then $-B_{ij}$ is the normal velocity at control point i due to a unit vorticity distribution over element j, and A_{ij} is the tangential velocity. The normal velocity is defined as positive outwards from the airfoil and the tangential velocity is defined as positive in a clockwise direction starting from the leading edge.

If V_{n_i} and V_{t_i} are the normal and tangential velocities respectively, due to the concentrated source of unit strength and $\frac{\partial \phi}{\partial n_i}$ and $\frac{\partial \phi}{\partial t_i}$ those due to a unit free stream, the normal velocity boundary condition (iii) can be written as

$$A_{ij}\sigma_j = -\frac{\partial \phi}{\partial n_i} + B_{ij}\delta_j\gamma - V_{n_i}\lambda ,$$

where γ is the uniform vorticity strength, λ the concentrated source strength and σ_j the strength of the source distribution on the jth

element. Suppose that starting from the leading edge in a clockwise manner N_1 is the number of the last element before the spoiler tip and N_2 the first element after the spoiler tip. Suppose also that N_3 and N_4 are respectively the last element before and the first element after the trailing edge. The Kutta condition at the spoiler tip then gives the equation:

$$\frac{\partial \phi}{\partial t_{N_1}} + B_{N_1 j}\sigma_j + A_{N_1 j}\delta_j \gamma + V_{t_{N_1}}\lambda = -\frac{\partial \phi}{\partial t_{N_2}} - B_{N_2 j}\sigma_j - A_{N_2 j}\delta_j \gamma - V_{t_{N_2}}\lambda .$$

Application of boundary condition (ii) gives the final equation:

$$\frac{\partial \phi}{\partial t_{N_1}} + B_{N_1 j}\sigma_j + A_{N_1 j}\delta_j \gamma + V_{t_{N_1}}\lambda = \sqrt{1 - C_{p_b}} ,$$

where C_{p_b} is the base pressure, obtained experimentally, and empirically entered into the solution. These equations can be combined to give the equation:

$$\begin{bmatrix} A_{ij} & -B_{ij}\delta_j & V_{n_i} \\ B_{N_1 j} + B_{N_2 j} & (A_{N_1 j} + A_{N_2 j})\delta_j & V_{t_{N_1}} + V_{t_{N_2}} \\ B_{N_1 j} & A_{N_1 j}\delta_j & V_{t_{N_1}} \end{bmatrix} \begin{bmatrix} \sigma_j \\ \gamma \\ \lambda \end{bmatrix} = \begin{bmatrix} -\frac{\partial \phi}{\partial n_i} \\ -\left(\frac{\partial \phi}{\partial t_{N_1}} + \frac{\partial \phi}{\partial t_{N_2}}\right) \\ -\frac{\partial \phi}{\partial t_{N_1}} + \sqrt{1 - C_{p_b}} \end{bmatrix} .$$

This essentially raises the order of the matrix A by two and can be solved directly. The Kutta condition at the trailing edge can then be expressed mathematically as

$$\frac{\partial \phi}{\partial t_{N_3}} + B_{N_3 j}\sigma_j + A_{N_3 j}\delta_j \gamma + V_{t_{N_3}}\lambda = -\frac{\partial \phi}{\partial t_{N_4}} - B_{N_4 j}\sigma_j - A_{N_4 j}\delta_j \gamma - V_{t_{N_4}}\lambda .$$

The concentrated source must be iteratively moved and the solution

recalculated until this equation is satisfied. Once this equation is satisfied the tangential velocity at the ith control point, T_i, is given by

$$T_i = \frac{\partial \phi}{\partial t_i} + B_{ij}\sigma_j + A_{ij}\delta_j\gamma + V_{t_i}\lambda.$$

The pressure coefficient at the ith control point denoted by C_{P_i}, is

$$C_{P_i} = 1 - T_i^2.$$

7.5 2-Source Model

The 2-source model is solved in an identical manner. It was pointed out in section (7.2) that in this problem there are five unknowns with only four conditions. Jandali (1) used the zero lift incidence as the extra condition. That condition is not adaptable to this theory and some other condition is necessary. Jandali found that the second source fell on the airfoil between the first source and the trailing edge and was weaker in strength than the first source. He found that if the second source was moved towards the trailing edge its strength approached zero, and the 2-source model approached the 1-source model. In the current work it is not proposed to search for another condition suitable for this theory, but merely to demonstrate how the boundary conditions can be satisfied, and how the numerical technique shows consistency with Jandali's results. The second source in the 2-source model is therefore merely fixed on the airfoil surface in a position that makes the present theory agree with Jandali's 2-source model. This conveniently positions the second source between the first source and the trailing edge of the airfoil as in Jandali's theory.

Suppose V_{2n_i} and V_{2t_i} are the normal and tangential velocities respectively due to the second source of unit strength. If λ_2 is the strength of the second source, and the first source strength and velocities are given the subscript 1, then development of this problem as in the 1-source problem gives the equation:

$$\begin{bmatrix} A_{ij} & -B_{ij}\delta_j & V_{1n_i} & V_{2n_i} \\ B_{N_1 j}+B_{N_2 j} & (A_{N_1 j}+A_{N_2 j})\delta_j & V_{1t_{N_1}}+V_{1t_{N_2}} & V_{2t_{N_1}}+V_{2t_{N_2}} \\ B_{N_1 j} & A_{N_1 j}\delta_j & V_{1t_{N_1}} & V_{2t_{N_1}} \\ B_{N_3 j} & A_{N_3 j}\delta_j & V_{1t_{N_3}} & V_{2t_{N_3}} \end{bmatrix} \begin{bmatrix} \sigma_j \\ \gamma \\ \lambda_1 \\ \lambda_2 \end{bmatrix} = \begin{bmatrix} -\frac{\partial \phi}{\partial n_i} \\ -\left(\frac{\partial \phi}{\partial t_{N_1}}+\frac{\partial \phi}{\partial t_{N_2}}\right) \\ -\frac{\partial \phi}{\partial t_{N_1}}+\sqrt{1-C_{p_0}} \\ -\frac{\partial \phi}{\partial t_{N_3}}+\sqrt{1-C_{p_0}} \end{bmatrix}.$$

Once again this equation must be solved and the Kutta condition at the trailing edge observed. The first source, as in the 1-source model must be iteratively relocated until the Kutta condition at the trailing edge is satisfied. Since the pressure, and hence the velocity, has been stipulated on the last control point before the trailing edge on the upper surface of the airfoil, this Kutta condition can be expressed mathematically as

$$\frac{\partial \phi}{\partial t_{N_4}} + B_{N_4 j}\sigma_j + A_{N_4 j}\delta_j \gamma + V_{1t_{N_4}}\lambda_1 + V_{2t_{N_4}}\lambda_2 = -\sqrt{1-C_{p_0}}\,.$$

Once this equation is satisfied the pressure coefficient at the ith control point is

$$C_{p_i} = 1 - T_i^2$$

where

$$T_i = \frac{\partial \phi}{\partial t_i} + B_{ij}\sigma_j + A_{ij}\delta_j \gamma + V_{1t_i}\lambda_1 + V_{2t_i}\lambda_2\,.$$

The pressure coefficient can be numerically integrated to determine the lift coefficient for any case desired. This completes the solution to the steady state airfoil spoiler problem for both 1 and 2-source models. Results from the above theory for the 1 and 2-source models are presented in section (9).

Some comment is warranted on the numerical procedures. Generally when grading the elements and determining element size, the guidelines given by Smith (6) are satisfactory. It has been found necessary in this problem to reduce the element size on the underside of the airfoil in that region opposite the concentrated sources which are situated on the upper surface. Relatively speaking these sources are quite strong and the element size should be much less than the distance between the elements and the source. A value of 110 elements was found to give good accuracy. On an I.B.M. 360/67 computer the iterative solution to this problem for 110 elements has a typical execution time of 60 seconds for both 1 and 2-source models. This time quoted includes six iterations of relocating the source position.

SECTION 8

AIRFOIL WITH A SLOTTED FLAP AND A SPOILER

8.1 Formulation of the Problem

The airfoil is positioned in the z-plane as described in section (3.2). The configuration is shown pictorially in figure (31). In this case of a slotted flap, the problem is essentially a two body problem where one of the bodies is of the type described in section (7), and the other body, the flap, is a basic airfoil. There is one extra unknown, the circulation about the flap, and one extra boundary condition, the Kutta condition at the flap trailing edge. The choices of an iterative or a direct solution, as presented by Smith (6) are open to such a multiple body problem. Both methods were tried and the direct method was chosen as simpler and shorter in computation time.

8.2 Boundary Conditions

The boundary conditions for the 1-source problem are:

(i) Kutta conditions at the main foil trailing edge, flap trailing edge and the spoiler tip.

(ii) Pressure stipulated on the separation free streamline at the spoiler tip.

(iii) Surface normal velocity condition of no flow through the surface.

For the 2-source model boundary condition (ii) becomes:

(ii) Pressure stipulated on the separation free streamlines at the spoiler tip and main foil trailing edge.

8.3 1-Source Model

The manner in which this problem is solved follows identically

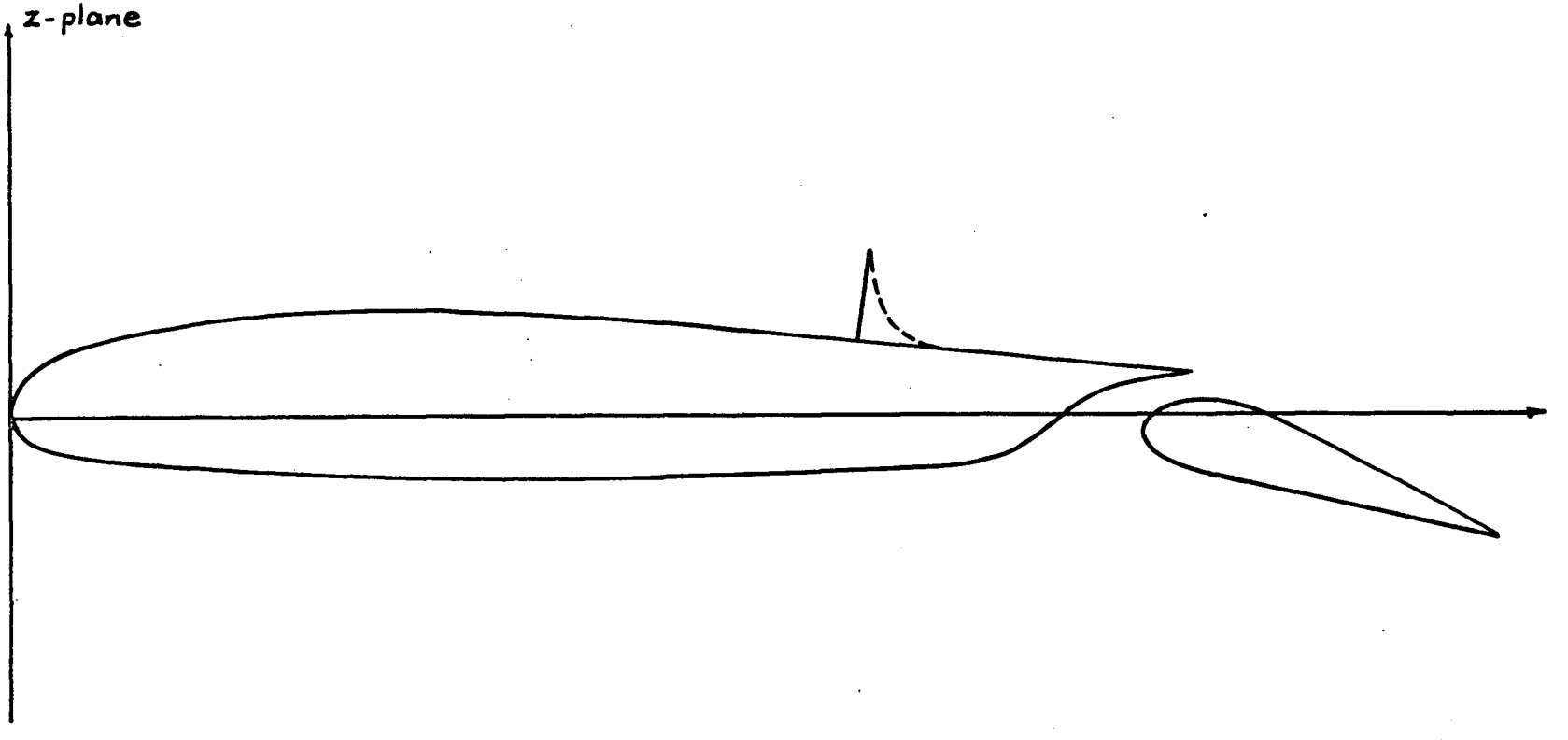

FIGURE (31): AIRFOIL IN THE Z-PLANE

the procedure described in sections (7.4) and (7.5). Suppose $-B^{T1}_{ik}$ is the normal velocity at control point i, on the main foil or flap, due to a unit vorticity distribution over element k, on the main foil, and A^{T1}_{ik} is the tangential velocity. Similarly $-B^{T2}_{il}$ and A^{T2}_{il} are the velocities due to a unit vorticity distribution over element l, on the flap. The normal velocity boundary condition (iii) becomes

$$A_{ij}\sigma_j = -\frac{\partial \phi}{\partial n_i} + B^{T1}_{ik}\delta_k\gamma_1 + B^{T2}_{il}\delta_l\gamma_2 - V_{n_i}\lambda \ ,$$

where γ_1, is the vorticity strength on the main foil and γ_2, the vorticity strength on the flap. Suppose that the elements are numbered from the leading edge of the main foil clockwise around the main foil, and then from the leading edge of the flap clockwise around the flap. All symbols and definitions given in section (7) apply directly to this solution. Suppose that N_5 is the number of the last element before the flap trailing edge and N_6 is the first element after the flap trailing edge. The Kutta condition at the trailing edge of the flap gives the equation:

$$\frac{\partial \phi}{\partial t_{N_5}} + B_{N_5 j}\sigma_j + A^{T1}_{N_5 k}\delta_k\gamma_1 + A^{T2}_{N_5 l}\delta_l\gamma_2 + V_{t_{N_5}}\lambda = -\frac{\partial \phi}{\partial t_{N_6}} - B_{N_6 j}\sigma_j - A^{T1}_{N_6 k}\delta_k\gamma_1 - A^{T2}_{N_6 l}\delta_l\gamma_2 - V_{t_{N_6}}\lambda \ .$$

The Kutta condition at the spoiler tip gives the equation:

$$\frac{\partial \phi}{\partial t_{N_1}} + B_{N_1 j}\sigma_j + A^{T1}_{N_1 k}\delta_k\gamma_1 + A^{T2}_{N_1 l}\delta_l\gamma_2 + V_{t_{N_1}}\lambda = -\frac{\partial \phi}{\partial t_{N_2}} - B_{N_2 j}\sigma_j - A^{T1}_{N_2 k}\delta_k\gamma_1 - A^{T2}_{N_2 l}\delta_l\gamma_2 - V_{t_{N_2}}\lambda \ .$$

Application of boundary condition (ii) gives the final equation:

$$\frac{\partial \phi}{\partial t_{N_1}} + B_{N_1 j}\sigma_j + A^{T1}_{N_1 k}\delta_k\gamma_1 + A^{T2}_{N_1 l}\delta_l\gamma_2 + V_{t_{N_1}}\lambda = \sqrt{1 - C_{p_b}} \ .$$

These equations can be combined to give the equation:

$$\begin{bmatrix} A_{ij} & -B^{T1}_{ik}\delta_k & -B^{T2}_{i\ell}\delta_\ell & V_{n_i} \\ B_{N_1 j}+B_{N_2 j} & (A^{T1}_{N_1 k}+A^{T1}_{N_2 k})\delta_k & (A^{T2}_{N_1 \ell}+A^{T2}_{N_2 \ell})\delta_\ell & V_{t_{N_1}}+V_{t_{N_2}} \\ B_{N_5 j}+B_{N_6 j} & (A^{T1}_{N_5 k}+A^{T1}_{N_6 k})\delta_k & (A^{T2}_{N_5 \ell}+A^{T2}_{N_6 \ell})\delta_\ell & V_{t_{N_5}}+V_{t_{N_6}} \\ B_{N_1 j} & A^{T1}_{N_1 k}\delta_k & A^{T2}_{N_1 \ell}\delta_\ell & V_{t_{N_1}} \end{bmatrix} \begin{bmatrix} \sigma_j \\ \gamma_1 \\ \gamma_2 \\ \lambda \end{bmatrix} = \begin{bmatrix} -\frac{\partial \phi}{\partial n_i} \\ -\left(\frac{\partial \phi}{\partial t_{N_1}}+\frac{\partial \phi}{\partial t_{N_2}}\right) \\ -\left(\frac{\partial \phi}{\partial t_{N_5}}+\frac{\partial \phi}{\partial t_{N_6}}\right) \\ -\frac{\partial \phi}{\partial t_{N_1}}+\sqrt{1-C_{p_0}} \end{bmatrix}.$$

This equation can be solved directly. The Kutta condition at the trailing edge of the main can be expressed as

$$\frac{\partial \phi}{\partial t_{N_3}} + B_{N_3 j}\sigma_j + A^{T1}_{N_3 k}\delta_k\gamma_1 + A^{T2}_{N_3 \ell}\delta_\ell\gamma_2 + V_{t_{N_3}}\lambda = -\frac{\partial \phi}{\partial t_{N_4}} - B_{N_4 j}\sigma_j - A^{T1}_{N_4 k}\delta_k\gamma_1 - A^{T2}_{N_4 \ell}\delta_\ell\gamma_2 - V_{t_{N_4}}\lambda .$$

Once this equation has been satisfied the tangential velocity at the ith control point is

$$T_i = \frac{\partial \phi}{\partial t_i} + B_{ij}\sigma_j + A^{T1}_{ik}\delta_k\gamma_1 + A^{T2}_{i\ell}\delta_\ell\gamma_2 + V_{t_i}\lambda ,$$

and the pressure coefficient is

$$C_{p_i} = 1 - T_i^2 .$$

8.4 2-Source Model

The discussion of the 2-source model given in section (7.5) is fully applicable to this solution. Development of the problem as given in section (7.5) and (8.3) leads to the equation

$$\begin{bmatrix} A_{ij} & -B^{T1}_{ik}\delta_k & -B^{T2}_{il}\delta_l & V_{1n_i} & V_{2n_i} \\ B_{N_1 j}+B_{N_2 j} & (A^{T1}_{N_1 k}+A^{T1}_{N_2 k})\delta_k & (A^{T2}_{N_1 l}+A^{T2}_{N_2 l})\delta_l & V_{1t_{N_1}}+V_{1t_{N_2}} & V_{2t_{N_1}}+V_{2t_{N_2}} \\ B_{N_5 j}+B_{N_6 j} & (A^{T1}_{N_5 k}+A^{T1}_{N_6 k})\delta_k & (A^{T2}_{N_5 l}+A^{T2}_{N_6 l})\delta_l & V_{1t_{N_5}}+V_{1t_{N_6}} & V_{2t_{N_5}}+V_{2t_{N_6}} \\ B_{N_1 j} & A^{T1}_{N_1 k}\delta_k & A^{T2}_{N_1 l}\delta_l & V_{1t_{N_1}} & V_{2t_{N_1}} \\ B_{N_3 j} & A^{T1}_{N_3 k}\delta_k & A^{T2}_{N_3 l}\delta_l & V_{1t_{N_3}} & V_{2t_{N_3}} \end{bmatrix} \begin{bmatrix} \sigma_j \\ \gamma_1 \\ \gamma_2 \\ \lambda_1 \\ \lambda_2 \end{bmatrix} = \begin{bmatrix} -\frac{\partial\phi}{\partial n_i} \\ -\left(\frac{\partial\phi}{\partial t_{N_1}}+\frac{\partial\phi}{\partial t_{N_2}}\right) \\ -\left(\frac{\partial\phi}{\partial t_{N_5}}+\frac{\partial\phi}{\partial t_{N_6}}\right) \\ -\frac{\partial\phi}{\partial t_{N_1}}+\sqrt{1-C_{p_b}} \\ -\frac{\partial\phi}{\partial t_{N_3}}+\sqrt{1-C_{p_b}} \end{bmatrix}$$

The Kutta condition becomes

$$\frac{\partial\phi}{\partial t_{N_4}} + B_{N_4 j}\sigma_j + A^{T1}_{N_4 k}\delta_k\gamma_1 + A^{T2}_{N_4 l}\delta_l\gamma_2 + V_{1t_{N_4}}\lambda_1 + V_{2t_{N_4}}\lambda_2 = -\sqrt{1-C_{p_b}}\,.$$

Once this equation is satisfied the pressure coefficient at the ith control point is

$$C_{p_i} = 1 - T_i^2,$$

where

$$T_i = \frac{\partial\phi}{\partial t_i} + B_{ij}\sigma_j + A^{T1}_{ik}\delta_k\gamma_1 + A^{T2}_{il}\delta_l\gamma_2 + V_{1t_i}\lambda_1 + V_{2t_i}\lambda_2\,.$$

Once again this pressure coefficient can be numerically integrated to determine the lift coefficient. This solves the problem of the steady state airfoil with a slotted flap and a spoiler.

In solving this problem care should be taken to follow the guidelines given at the end of section (7). The number of elements needed is approximately 100 for the main foil and 80 for the flap. With such a number of elements the execution time for this solution is approximately 4 minutes for both 1 and 2-source models. This time

includes six iterative changes in the source position.

SECTION 9

RESULTS AND COMPARISONS

In the first part of this section the theoretical results for a solid airfoil with a spoiler are presented. These results are compared with theoretical results obtained by Jandali (1). The latter part of this section shows the solution to the problem of an airfoil with a spoiler and a slotted flap. Experimental or other theoretical results are not available for this case, and hence only the theoretical change in the pressure distribution over the basic foil and flap is given.

The second source in the theories developed in sections (7.5) and (8.4) was arbitrarily located between the first source and the trailing edge. It was discussed in section (7.5) that some further condition is necessary to fix the position of this second source. If the circulation about the airfoil is neglected, one of the existing conditions could be used for a mathematical solution to the problem. However, such neglect of the circulation gives an erroneous result, varying widely from experiment. It is therefore necessary to include the circulation, and look for another condition. It will be recalled from section (7.5) that this second source is much weaker than the first source, and approaches zero strength as its location approaches the trailing edge. The 2-source model then approaches the 1-source model. The 2-source model agrees more closely with experiment and satisfies all the boundary conditions. The theoretical results presented here are intended to demonstrate this point and to show consistency with Jandali's results.

9.1 Solid Airfoil with a Spoiler

The results given in this section were determined by Jandali (1)

for a 14% Clark Y airfoil shown in figure (30). The spoiler is located at the 70% chord point. Since the theory presented by Jandali is limited to normal spoilers, theoretical comparisons can only be presented for this case. First figures are presented comparing the current results for normal spoilers with those obtained theoretically by Jandali. Some results for spoilers of varying angles for the 1-source model then follow. All angles of incidence presented for the Clark Y are measured from the lower surface. Spoiler heights are given as a percentage of the airfoil chord.

Figure (32) shows a comparison between the pressure distributions for the Jandali 1-source model and the present 1-source model for a 10% normal spoiler at an airfoil incidence of 12 degrees. Figure (33) shows the corresponding comparison for the 2-source model. In these results the chord is 4.043 as given by Jandali. The agreement between theories is seen to be very good. The agreement between theory and experiment was shown by Jandali to be quite good except in the region in front of the spoiler, where there is actually a region of separated flow. Potential theory is not able to model such a flow. Analytically any such sharp concave corner will produce a stagnation point, and hence in this region the theory diverges from experiment. In the surface singularity theory employed it will be recalled that the flow properties are considered at control points that are slightly removed from such sharp corners, and theoretically the stagnation point will never be reached. The trend towards a stagnation point however, is strongly evident. Figure (34) shows a comparison between the Jandali 1-source model and the present 1-source model for a 5% normal spoiler at an airfoil incidence of 10 degrees. The corresponding comparison for the 2-source model is presented in figure (35). Although only representative results have

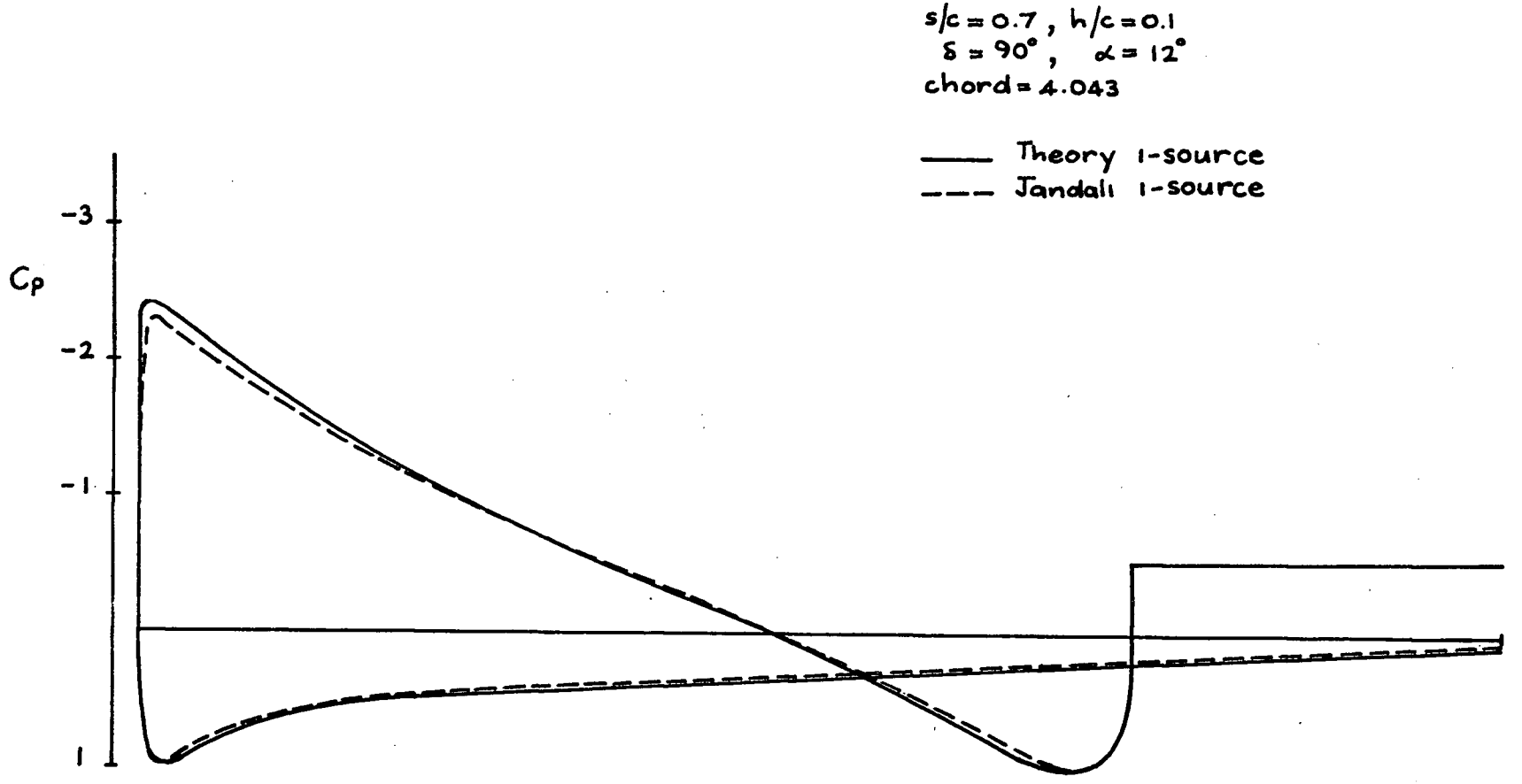

FIGURE (32): PRESSURE DISTRIBUTION FOR CLARK Y AIRFOIL WITH SPOILER

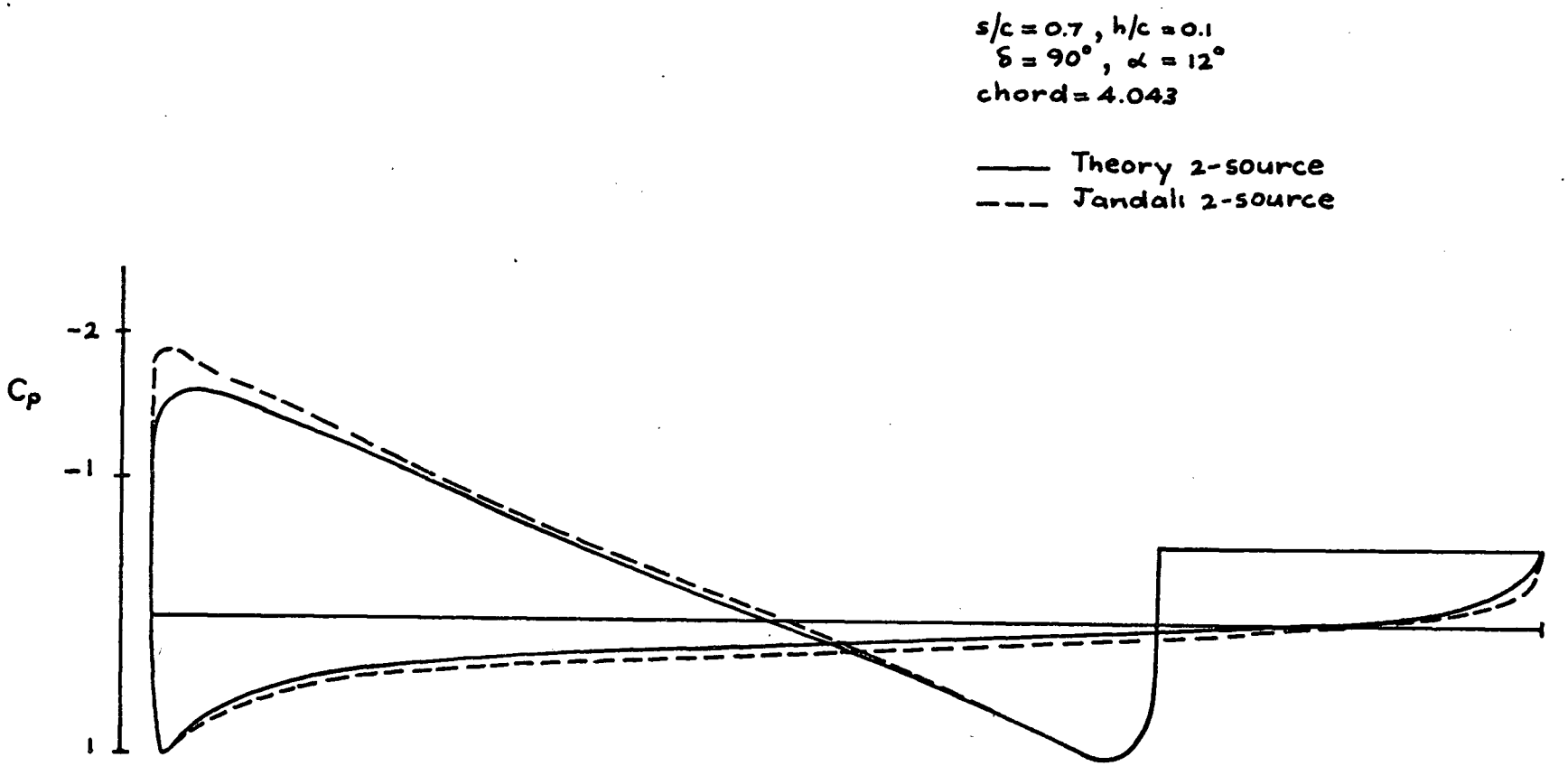

FIGURE (33): PRESSURE DISTRIBUTION FOR CLARK Y AIRFOIL WITH SPOILER

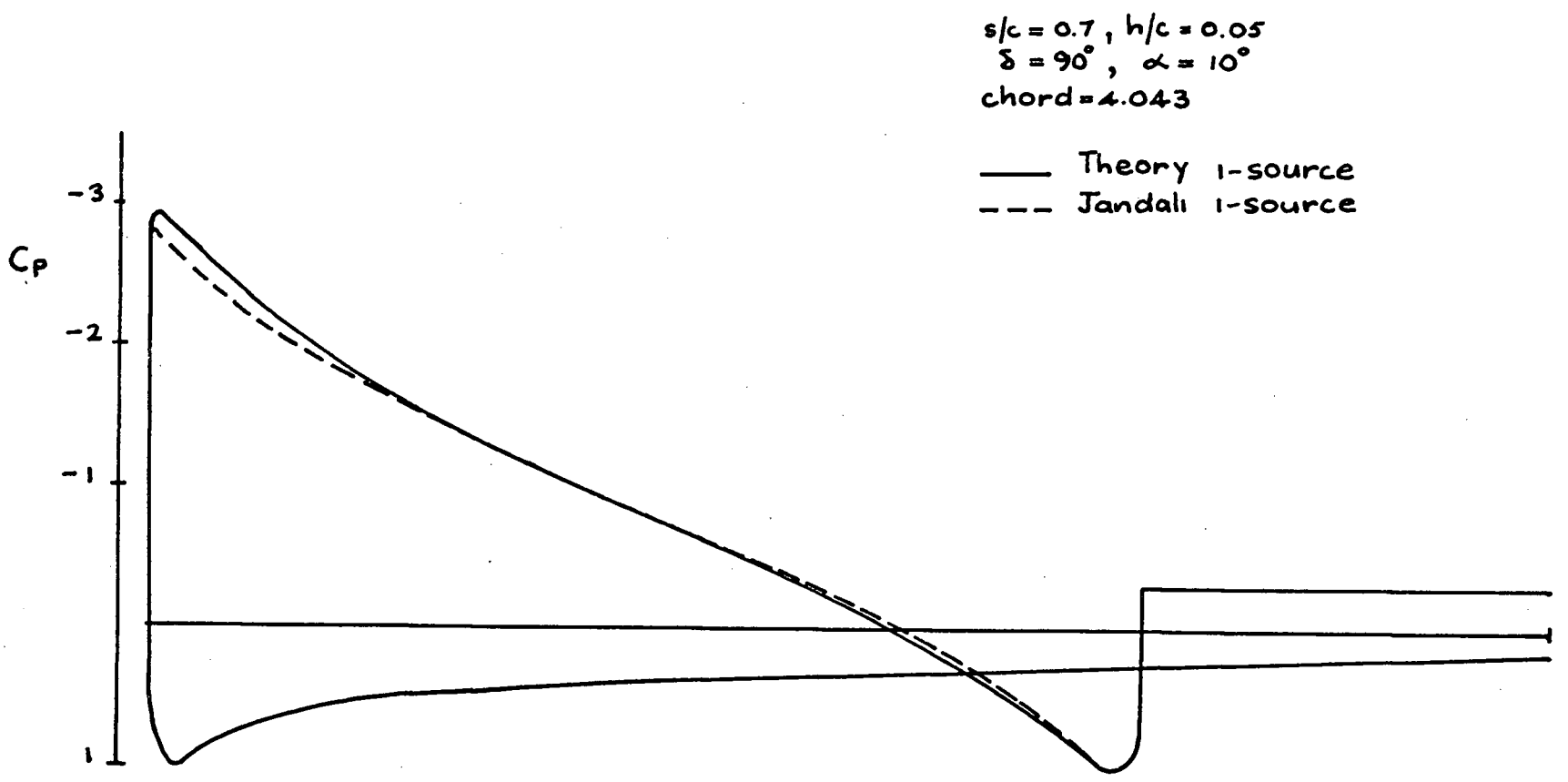

FIGURE (34): PRESSURE DISTRIBUTION FOR CLARK Y AIRFOIL WITH SPOILER

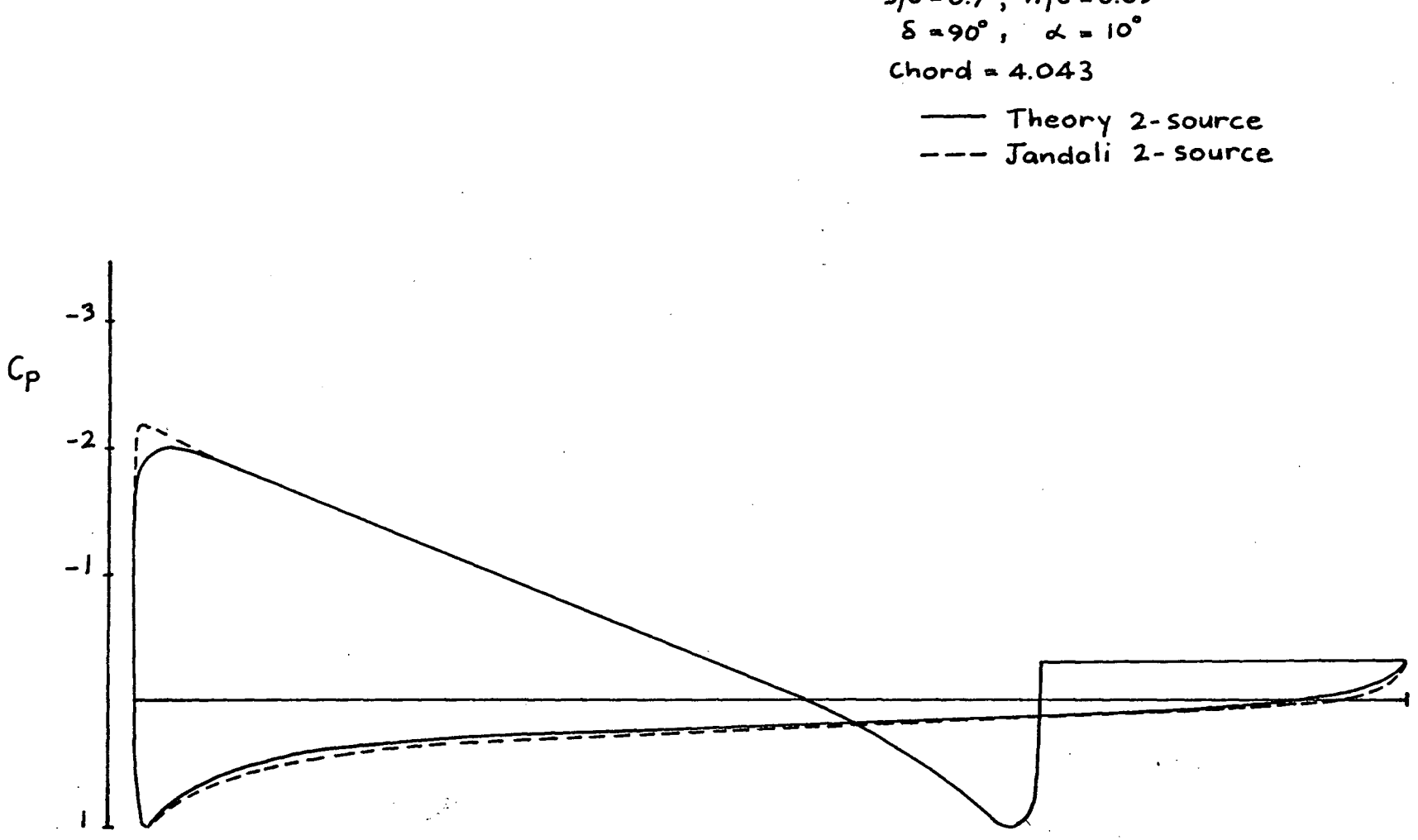

FIGURE (35): PRESSURE DISTRIBUTION FOR CLARK Y AIRFOIL WITH SPOILER

been presented it can be seen that the agreement is excellent, and that the two theories are consistent.

Next it is demonstrated how the theoretical pressure distribution changes as the spoiler angle is progressively increased to 90 degrees. In figure (36) the pressure distributions for the 1-source model are presented for the Clark Y airfoil with a 10% spoiler at the 70% chord point with angles of 30, 60, and 90 degrees, and these are compared to the theoretical distribution for the case of no spoiler. The airfoil incidence in all cases is 12 degrees. It can be seen how the pressure peak and the area between the curve and the chord line progressively decrease as the spoiler angle increases. Such decreases signify a progressive loss in lift. The basic airfoil pressure distribution was calculated using Smith's theory (6), and it can be once again seen that the theory is unable to predict a stagnation point at the finite angle trailing edge. It is more noticeable for the cases with inclined spoilers that, although the pressure distribution in front of the spoiler tends towards a stagnation point, it does not actually reach it. The consideration of control points around such a concave corner as the spoiler base has the affect of rounding the corner and the theory is not expected to model the stagnation point correctly.

9.2 Airfoil with a Slotted Flap and a Spoiler

The results presented in this section are for the NACA 23012 airfoil with a 25.66% slotted flap shown in figure (31). The basic theoretical and experimental pressure distributions are shown in figure (37) for this airfoil at 8 degrees incidence and 20 degrees flap angle. The experimental results were obtained from reference (12). Since no experimental results are available for the spoiler

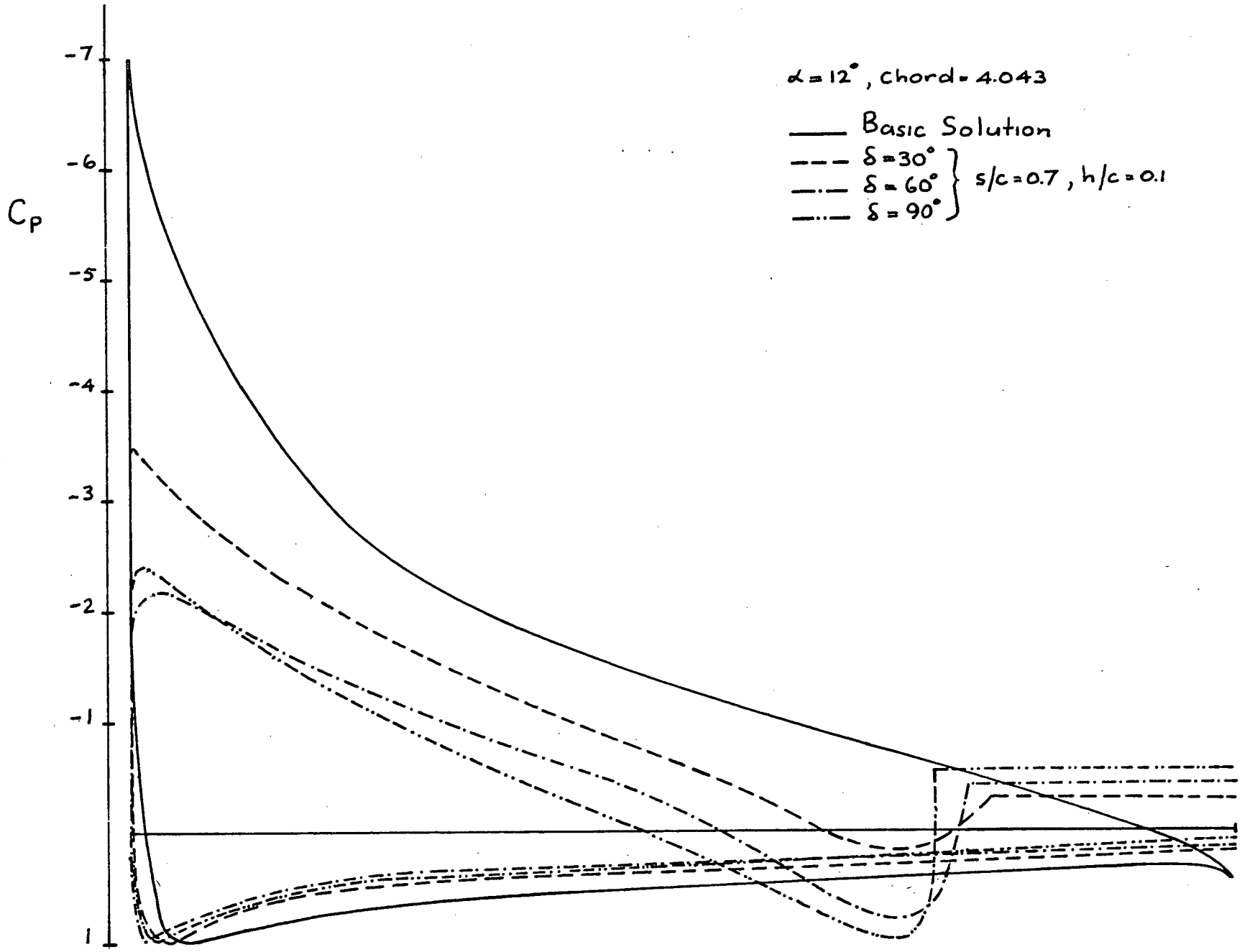

FIGURE (36): PRESSURE DISTRIBUTION FOR CLARK Y AIRFOIL WITH AND WITHOUT SPOILER

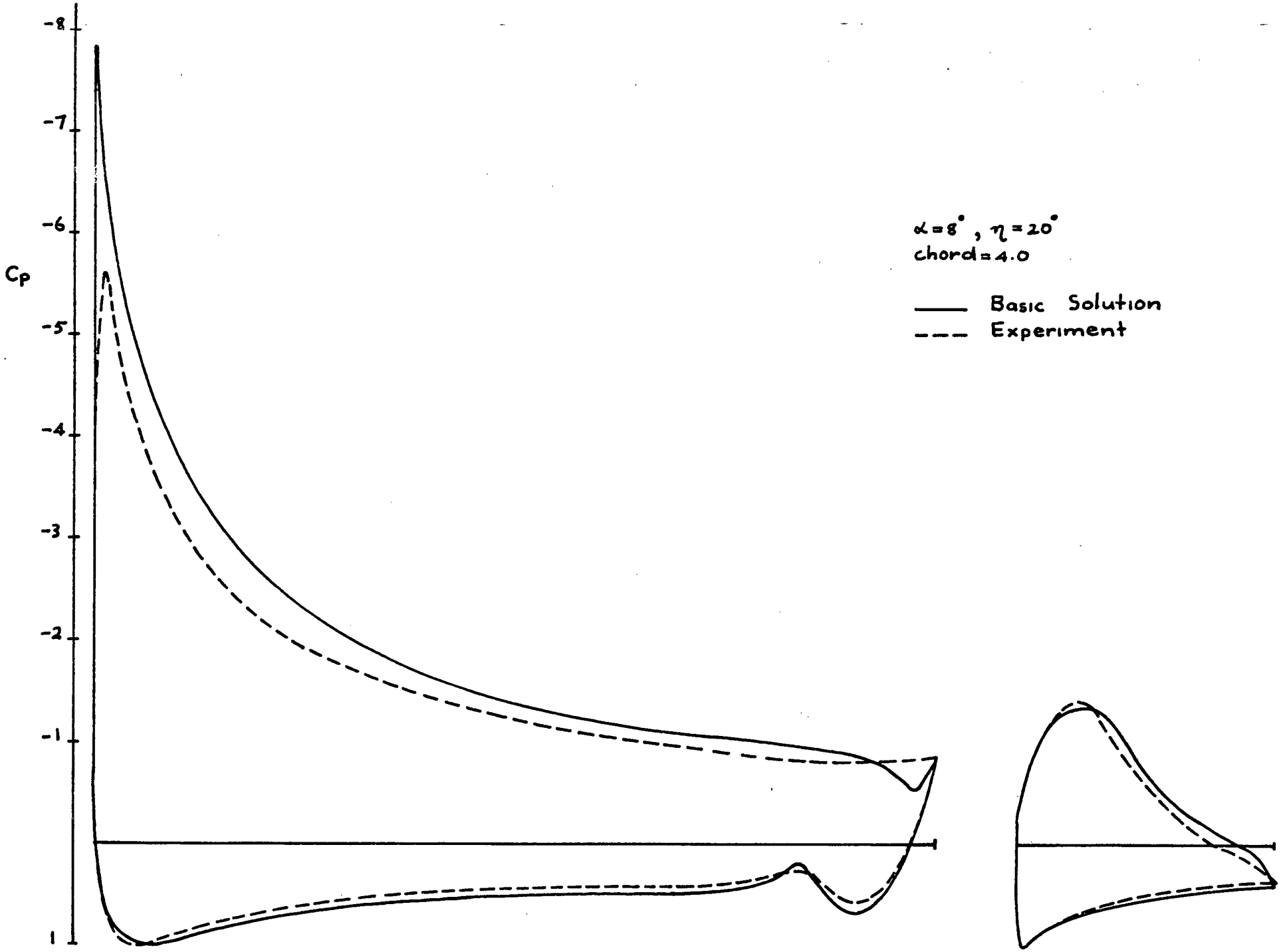

FIGURE (37): PRESSURE DISTRIBUTION FOR NACA 23012 AIRFOIL AND SLOTTED FLAP WITHOUT SPOILER

case only representative examples of the theoretical results are shown. It will be demonstrated how the present 2-source model is superior to the 1-source model. The pressure distributions for the airfoil with a spoiler at varying angles will be compared to the basic distribution calculated using Smith's theory (6). In the following results the spoiler is positioned at the 60% chord point. The airfoil incidence is 8 degrees and the airfoil chord is 4.0. The flap angle is 20 degrees. The empirical input of base pressure coefficient is set at -1.0 in the absence of experimental results. Figure (38) is a comparison between the present 1-and 2-source models for a 10% normal spoiler. This comparison shows the 1-source model giving an unrealistically high pressure peak on the flap. It will be recalled that in the 1-source model only the Kutta condition is stipulated at the main foil trailing edge, and the separation pressure coefficient, although finite, determines its own value. In this case it determines a very negative value of less than -2. The main foil trailing edge is so close to the flap that this high negative value directly affects the negative pressure peak on the flap, making it unrealistically high. It would be expected then that if the separation pressure was stipulated at the main foil trailing edge, as in the 2-source model, a direct effect would be noticed on the flap. This point is indeed demonstrated in figure (38), where it can be seen that the 2-source model gives a much better result than the 1-source model. The second source in this case has been arbitrarily located between the first source and the trailing edge of the main foil. For this reason the solution for the 2-source model will not be pursued further.

The effect of spoiler angle is shown in figure (39). In this figure the theoretical result for a basic airfoil with a slotted

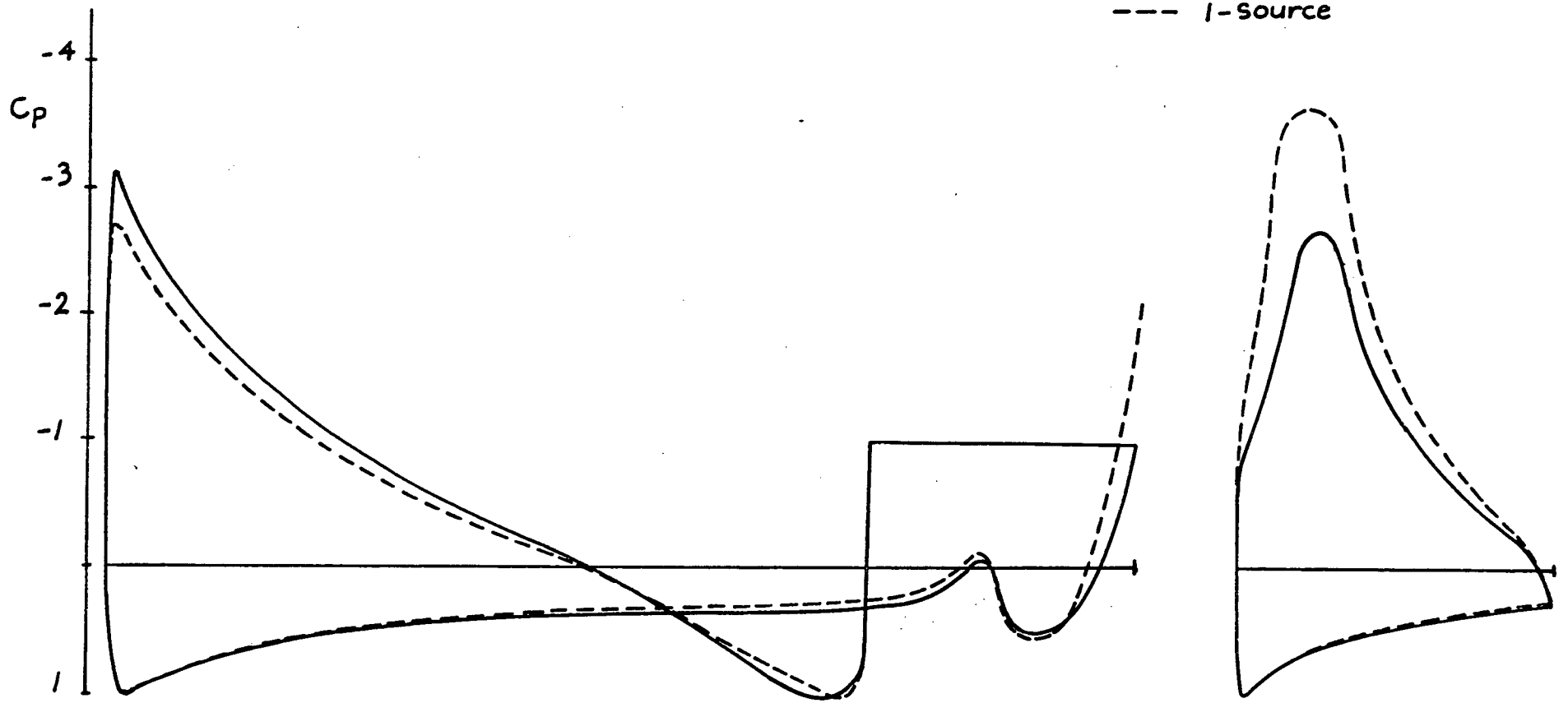

FIGURE (38): PRESSURE DISTRIBUTION FOR NACA 23012 AIRFOIL AND SLOTTED FLAP WITH SPOILER

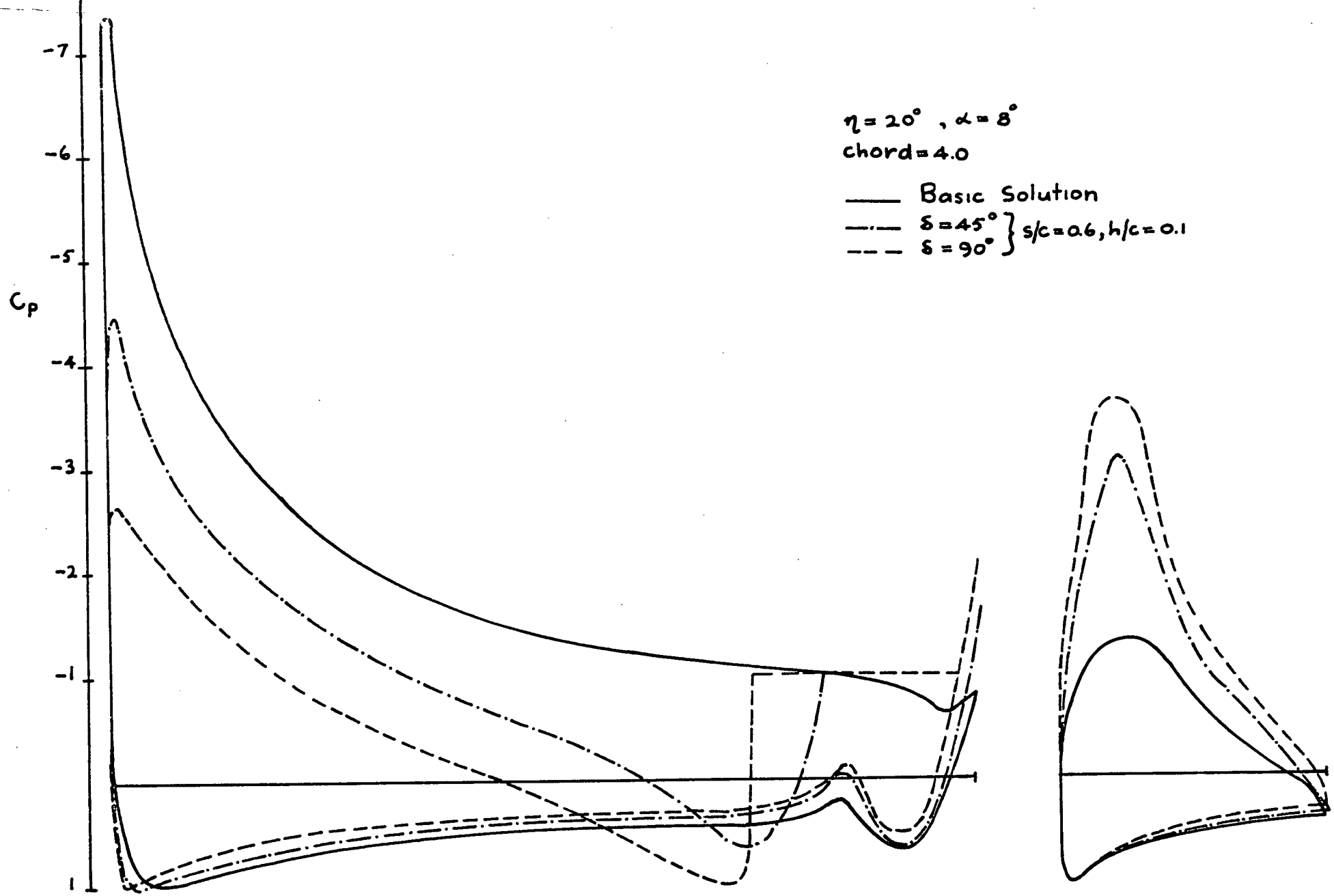

FIGURE (39): PRESSURE DISTRIBUTION FOR NACA 23012 AIRFOIL AND SLOTTED FLAP WITH AND WITHOUT SPOILER

flap is presented with the 1-source model for a 10% spoiler at angles of 45 and 90 degrees. Once again the characteristic losses in pressure coefficient can be observed as the spoiler angle increases.

SECTION 10

CONCLUSION

The lift given by the linearized cavity potential theory developed in part I shows good agreement with experiment. The pressure predicted by the theory gives only qualitative information about the pressure distribution on the airfoil. Such singularities in the pressure distribution as given by the theory are inherent in linearized techniques. Only theoretical results for the spoiler actuation problem have been presented. Experimental measurement is currently being done in an attempt to verify these results.

In part II the theory was shown to give pressure distributions consistent with Jandali's theory (1) for the solid airfoil with a normal spoiler. Jandali showed that this result was in good agreement with experiment except for a small region in front of the spoiler. In this region the actual flow separates and the theoretical prediction of a stagnation point is not in agreement with experiment. Although no experimental or other theoretical results are available for the case of angular spoilers, the good agreement for the normal spoiler case is an indication that these results most likely agree closely with experiment.

For the case of an airfoil with a spoiler and a slotted flap, experimental results are not available. The 2-source model, which gives much better results for this case than the 1-source model, is probably in quite good agreement with experiment. Investigation is necessary for a further condition to fix the position of the second source. It should also be verified that the theory does in fact agree with experiment.

REFERENCES

1. Jandali, T. 1970 "A Potential Flow Theory for Airfoil Spoilers" Ph.D. Thesis, University of British Columbia.

2. Woods, L.C. 1953 "Theory for Airfoil Spoilers" A.R.C. R&M 2969.

3. Barnes, C.S. 1965 "A Developed Theory of Spoilers on Airfoils" A.R.C. C.P. 887.

4. Parkin, B.R. 1959 "Linearized Theory of Cavity Flow in Two-Dimensions" RAND P-1745.

5. Fabula, A.G. 1962 "Thin-Airfoil Theory Applied to Hydrofoils with a Single Finite Cavity and Arbitrary Free Streamline Detachment" J.F.M. pp. 227-240.

6. Hess, J.L.&Smith A.M.O. 1966 "Calculation of Potential Flow about Arbitrary Bodies" Prog. in Aero. Sciences Vol. 8, Pergamon Press, Oxford.

7. Giesing, J.P. 1965 "Potential Flow about Two-Dimensional Airfoils" Rept. LB 31946, Douglas Aircraft Co.

8. Bisplinghoff, R.L., Ashley, H.& Halfman, R.L. 1955 "Aeroelasticity" Addison-Wesley Publishing Co. pp. 284-285.

9. Pope, A.& Harper, J.J. 1966 "Low-Speed Wind Tunnel Testing" John Wiley & Sons.

10. Maskell, E.C. 1963 "A Theory of Blockage Effects on Bluff Bodies and Stalled Wings in a Closed Wind Tunnel" R&M 3400.

11. Parkinson, G.V.& Jandali, T. 1970 "A Wake Source Model for Bluff Body Potential Flow" J.F.M. Vol. 40, pp. 577-594.

12. Wenzinger, C.J.& Delano, J.B. 1938 "Pressure Distribution over an NACA 23012 Airfoil with a Slotted and a Plain Flap" T.R. No. 633, NACA.